Technische Universität München

TUM School of Natural Sciences

Influence of stress and nutrients on the production of high-value oleochemicals in *Rhodococcus erythropolis*

Selina Alexandra Engelhart-Straub

Vollständiger Abdruck der von der TUM School of Natural Sciences der Technischen Universität München zur Erlangung des akademischen Grades einer

Doktorin der Naturwissenschaften (Dr. rer. nat.)

genehmigten Dissertation.

Vorsitz:	Prof. Dr. Tom Nilges
Prüfer der Dissertation:	1. Priv.-Doz. Dr. Norbert Mehlmer
	2. apl. Prof. Dr. Wolfgang Eisenreich

Die Dissertation wurde am 18.12.2023 bei der Technischen Universität München eingereicht und durch die TUM School of Natural Sciences am 26.02.2024 angenommen.

Contents

I Abstract

Bacteria belonging to the genus of *Rhodococcus* have the ability to accumulate lipids, which enables the production of a sustainable alternative to traditional petrochemical resources. This work investigates the capabilities of the oleaginous and carotenogenic bacterium *Rhodococcus erythropolis* JCM3201^{T}, which offers unique metabolic capacities and has a high potential as a source of valuable lipids, including triacylglycerols and carotenoids.

To enable effective use for industrial purposes, exploring the nutritional requirements of this bacterium is critical. The first chapter investigates nine nitrogen sources and eight carbon sources at a fixed carbon-to-nitrogen ratio of 100:1 (16 g L^{-1} carbon, 0.16 g L^{-1} nitrogen). While the best growth was achieved using glucose and ammonium acetate, the highest lipid production occurred when glucose und yeast extract were used. To optimize biomass, lipid, and carotenoid production, a Central Composite Design was employed to determine the ideal concentrations of nitrogen and carbon. The highest biomass was attained at a carbon-to-nitrogen ratio of 18.87 (11 g L^{-1} carbon, 0.583 g L^{-1} nitrogen), whereas the highest lipid production resulted from a medium containing 11 g L^{-1} carbon and only 0.017 g L^{-1} nitrogen. The top carotenoid production occurred at a carbon-to-nitrogen ratio of 12 (6 g L^{-1} carbon, 0.5 g L^{-1} nitrogen). This work enhances our understanding of *R. erythropolis* physiology under diverse nutritional conditions, thereby facilitating the development of refined media formulations to produce valuable oleochemicals and pigments like rare odd-chain fatty acids and monocyclic carotenoids.

Furthermore, *R. erythropolis* has shown resilience against different stressors, although its response to light was still unexplored. The second chapter of this thesis examines how *R. erythropolis* reacts to various wavelengths of light. Notably, carotenoid levels were significantly boosted in cultures exposed to white, green, and blue light compared to non-illuminated controls. Blue light, in particular, demonstrated antimicrobial effects. Intriguingly, light stress induced shifts in cellular lipid composition. Warm white and green light led to increased levels of odd-chain fatty acids (C15:0, C17:1), while exposure to blue light caused a shift toward more saturated fatty acids (from C16:1 to C16:0). In-depth proteomics analysis identified the upregulation of oxidative stress-related proteins when exposed to light.

II Zusammenfassung

Bakterien, die zur Gattung *Rhodococcus* gehören, haben die Fähigkeit Lipide zu akkumulieren, die eine nachhaltige Alternative zu herkömmlichen petrochemischen Ressourcen darstellen können. In dieser Arbeit werden die Fähigkeiten des ölhaltigen und carotinogenen Bakteriums *Rhodococcus erythropolis* JCM3201^T untersucht, welches über einzigartige metabolische Kapazitäten verfügt und ein hohes Potenzial als Produzent wertvoller Lipide, darunter Triacylglycerine und Carotinoide, hat.

Um eine effektive Nutzung für industrielle Zwecke zu ermöglichen, ist die Erforschung des Nährstoffbedarfs dieses Bakteriums von entscheidender Bedeutung. Im ersten Kapitel werden neun Stickstoff- und acht Kohlenstoffquellen bei einem konstanten Kohlenstoff-Stickstoff-Verhältnis von 100:1 untersucht (Kohlenstoffgehalt 16 g L^{-1}, Stickstoffgehalt 0,16 g L^{-1}). Während das beste Wachstum mit Glukose und Ammoniumacetat erzielt wurde, war die Lipidproduktion bei Verwendung von Glukose und Hefeextrakt am höchsten. Zur Optimierung der Biomasse-, Lipid- und Carotinoidproduktion wurde ein Central Composite Design verwendet, um die idealen Stickstoff- und Kohlenstoffkonzentrationen zu ermitteln. Die höchste Biomasse wurde bei einem Kohlenstoff-Stickstoff-Verhältnis von 18,87 (11 g L^{-1} Kohlenstoff, 0,583 g L^{-1} Stickstoff) erreicht, während die höchste Lipidproduktion bei einem Medium mit 11 g L^{-1} Kohlenstoff und nur 0,017 g L^{-1} Stickstoff erzielt wurde. Die höchste Carotinoid-Produktion trat bei einem Kohlenstoff-Stickstoff-Verhältnis von 12 auf (6 g L^{-1} Kohlenstoff, 0,5 g L^{-1} Stickstoff). Diese Arbeit verbessert unser Verständnis der Physiologie von *R. erythropolis* unter verschiedenen Nährstoffbedingungen und fördert so die Entwicklung optimierter Medienzusammensetzungen zur Produktion von wertvollen Oleochemikalien und Pigmenten, wie seltene ungeradkettige Fettsäuren und monozyklische Carotinoide.

Darüber hinaus hat sich *R. erythropolis* als widerstandsfähig gegenüber verschiedenen Stressfaktoren erwiesen, doch seine Reaktion auf Licht war noch unerforscht. Im zweiten Kapitel dieser Arbeit wird untersucht, wie *R. erythropolis* auf verschiedene Wellenlängen an Licht reagiert. Dabei wurde festgestellt, dass die Carotinoidkonzentration in Kulturen, die weißem, grünem und blauem Licht ausgesetzt waren, im Vergleich zu nicht-beleuchteten Kontrollen deutlich erhöht war. Vor allem blaues Licht zeigte eine antimikrobielle Wirkung. Interessanterweise führte Lichtstress zu Verschiebungen in der zellulären Lipidzusammensetzung. Warmes weißes und grünes Licht führte zu einem erhöhten Gehalt an ungeradkettigen Fettsäuren (C15:0, C17:1), während die Exposition gegenüber blauem Licht eine Verschiebung hin zu mehr gesättigten Fettsäuren (von C16:1 zu C16:0) bewirkte. Tiefgehende Proteomanalysen zeigten das Proteine, die mit oxidativem Stress zusammenhängen, unter Lichteinwirkung hochreguliert werden.

III Acknowledgements

I would like to express my sincere gratitude to **Prof. Dr. Thomas Brück** for granting me the opportunity to pursue my doctoral degree at his chair. I would like to thank **PD Dr. Norbert Mehlmer** for his supervision and support during my dissertation. I am deeply grateful for his valuable ideas, insights and advice during my time at the chair. His broad expertise and critical evaluation has been instrumental in my research work and improved my scientific skills.

Further, I would like to thank **Prof. Dr. Wolfgang Eisenreich** for his examination and evaluation of my dissertation work.

I would like to extend my thanks to the entire research group for their support and their friendship. Their diverse expertise, insightful feedback and willingness to help created a positive work environment which made my research progress possible. The evenings spent together playing volleyball or barbecuing made this time very special. I extend my thank you to my project partner **Philipp Cavelius** and **Dr. Dania Awad** for offering their valuable feedback and advice regarding my research. I especially want to thank **Martina Haack** for her invaluable support in the analytical work and the great amount of work she puts into our projects. I would like to thank **Felix, Manfred, Nadim, Nate** and **Sophia** for their friendship and mutual support in the lab.

I would like to express my deep felt thank you to **Nicolai Flach** for his unparalleled support, understanding and love. Your belief in me and your encouragement were invaluable!

A big thank you to my family and friends! I especially appreciate my parents **Christine** and **Roman** for their advice, love and trust during this time. I am deeply grateful to my twin sister, **Julia**. Thank you for always being there for me!

IV List of abbreviations

AGPAT	1-acylglycerol–3-phosphate O-acyltransferase
ANOVA	analysis of variance
BMBF	German Federal Ministry of Education and Research
BO	bayesian optimisation
C. oleaginosus	*Cutaneotrichosporon oleaginosus*
CCC	circumscribed Central Composite Design
CCD	Central Composite Design
CCF	face centered Central Composite Design
CCI	inscribed Central Composite Design
CrtB	phytoene synthase
CrtE	geranylgeranyl pyrophosphate synthase
CrtI	phytoene dehydrogenase
CrtLm	lycopene β-cyclase
CrtO	β-carotene ketolase
DAG	diacylglycerol
DGAT	DAG *O*-acyltransferase
DMAPP	dimethylallyl pyrophosphate
DOE	Design of Experiment
DTT	dithiothreitol
DXP	1-deoxyxylulose-5-phosphate
DXR	DXP reductoisomerase
DXS	DXP synthase
E. coli	*Escherichia coli*
FAME	fatty acid methyl ester
FID	flame ionization detector
FPP	farnesyl pyrophosphate

GAP	glyceraldehyde-3-phosphate
GGPP	geranylgeranyl diphosphate
GPAT	glycerol-3-phosphate O-acyltransferase
GPP	geranyl diphosphate
IDI	isopentenyl-diphosphate delta-isomerase
IPP	isopentenyl pyrophosphate
MEP	2-C-methyl-D-erythritol-4-phosphate
OCFA	odd chain fatty acid
OFAT	one-factor-at-a-time
PAP	phosphatidic acid phosphatase
R. erythropolis	*Rhodococcus erythropolis*
R. jostii	*Rhodococcus jostii*
R. opacus	*Rhodococcus opacus*
R. toruloides	*Rhodosporidium toruloides*
ROS	reactive oxygen species
RSM	Response Surface Methodology
SCO	single cell oils
SRM	selected-reaction monitoring
SWW	standard warm white
TAG	triacylglycerols
TIMS	timsTOF Pro mass spectrometer
WE	wax ester
Y. lipolytica	*Yarrowia lipolytica*

1 Introduction

1.1 Sustainable Production of Oleochemicals

As fossil fuels are a limited, non-renewable, and polluting resource [1], alternative energy sources such as sustainably generated bioproducts need to be explored [2]. One subgroup, which could replace petroleum derivatives in several sectors, are oleochemicals, a class of aliphatic compounds industrially derived from plant and animal lipids [3]. Fatty acids and fatty alcohols account for 75 % of the basic oleochemicals followed by fatty methyl esters and fatty amines [4]. These compounds are used in various industries such as cosmetics, lubricants, bioplastic, food additives and polymers depending on their chemical structure [5,6]. Vegetable and animal-derived oils and fats constitute the main renewable source for the production of oleochemicals [4,7]. These compounds often have limited availability, are subjected to environmental concerns and are in competition with food supply [2,8,9].

In contrast, oleaginous microorganisms are able to produce high amounts of lipids, also termed single cell oils (SCO), from waste streams under sustainable production conditions [2,10]. As these SCO often have a similar fatty acid profile as plant oils, they can be considered as a suitable substitute [10,11]. Despite significant effort and progress, the current cost of SCO production and the conversion into low-value fuel chemicals continues to be too high to compete with plant oil based alternatives [12]. The selling price for a large percentage of oleochemicals is comparable with the cost of the sugar feedstock needed for production [3]. In contrast, the commercial production of special products of a high value such as very long polyunsaturated fatty acids is economically competitive [9,13]. Oleaginous microorganisms are also promising hosts for hydrophobic terpene compounds, as lipid bodies might serve as storage capacity and precursors, such as acetyl-CoA, are available [14].

When choosing the correct microbial strain for oleochemical production, a number of different possibilities is available depending on the application, ranging from bacteria, yeast, algae to fungi. They either can be used as natural producers like the oleaginous yeast *Cutaneotrichosporon oleaginosus* for microbial oil production [15] or as recombinant producers like *Escherichia coli* for the production of long chain fatty acids [16].

Well-established microbes such as *E. coli* and *Saccharomyces cerevisiae* are convenient and industrially robust hosts. A broad knowledge and wide tool-set is available, in order to obtain high titres of a wide range of both natural and non-natural products [17-20]. However, the production of lipids including fatty acids was found challenging in these model organisms, resulting in low production titres. To circumvent this problem, non-common oleaginous hosts can be used as producers [21]. The ability of novel microorganisms to grow on a simple

medium utilizing inexpensive carbon sources is essential for cost competitiveness of a product [22]. Novel organisms offer a wide metabolic diversity, including a wide range of feedstocks or the native production of target compounds, but the research of a new microorganism involves various challenges, with the major ones being the lack of knowledge, the need for a complete and assembled genome and available genetic tools [20,23]. Furthermore, the capacity to modify the genome is crucial for a platform organism, a range of approaches can be used such as random or targeted editing, gene deletion, CRISPR-based genome editing and recombineering [20,23].

In order to move toward a more carbon-neutral world, a multi-tiered approach is necessary, which includes the use of sustainable, bio-based alternatives to fuel and chemicals [24]. To achieve this goal, a bioeconomy derived of low-carbon emission technologies has to be developed. A variety of expression systems have to be developed in order to evaluate the optimal expression conditions and host strain. For different applications, different organism will be advantageous. This thesis is investigating *Rhodococcus erythropolis* as potential producer of lipids and carotenoids and its development as a robust platform organism for a variety of products.

1.1.1 Oleaginous Microorganisms

While all microorganisms produce a minimal amount of lipids (mostly fatty acids) in the membrane for vital functions, some oleaginous microorganisms are able to accumulate over 20 % lipids per dry biomass under nutrient-limited conditions, especially nitrogen or phosphate limitation. These lipids are mainly consisting of triacylglycerols (TAG), which are stored in so called lipid bodies [13,25,26]. Oleaginous microorganisms have an inherent advantage as production platform for oleochemicals as natural producers of TAG combined with the ability to genetically modify these synthesis pathways [8]. This group includes a variety of microorganisms, including microalgae, yeast, fungi and bacteria, with a varying fatty acids profile depending on producer and growth environment [9]. This provides an advantage, as the nutrient source or metabolic engineering strategies can be utilized to modify the composition to a certain extend [1].

Some extensively studied oleaginous microorganisms are yeasts such as *Yarrowia lipolytica*, *Rhodosporidium toruloides* and *C. oleaginosus* and bacteria such as *Rhodococcus opacus* and *Arthrobacter* species, all able to accumulate high amounts of lipids up to 80 % of their dry cell weight [1,15,25,27].

R. toruloides is a natural producer of carotenoids, lipids and industrially relevant enzymes [28]. Fast screening techniques allow for the selection of the optimal strain and culture conditions for each specific application, for examples an at-line flow cytometric protocol with which

carotenoid content and cell viability can be determined [28-30]. Furthermore, metabolic engineering allows for increased product titers. The production of high-value lipids was achieved through genetic engineering, such as oils with increased levels of oleic acids as biolubricants and hydraulic fluids [31], linoleic acid, which is important for human health [32], very long chain fatty acids as important feedstocks for plastics and cosmetics [33] or fatty alcohols, which find use as lubricants, surfactants and solvents [34].

The most studied oleaginous bacteria belong to the genus of *Rhodococcus* [1]. Their potential for the synthesis of valuable oleochemicals was demonstrated with the production of wax esters (WE), which are industrially used in lubricants and cosmetics [12,35]. Compared to saturated WEs, unsaturated WEs are of higher value and much more difficult to obtain. Currently, the majority of unsaturated WEs is harvested from jojoba desert shrub *Simmondsia chinensis* with limited availability [12,36-38]. *Rhodococcus jostii* RHA1 has been engineered to produce WEs in fed-batch fermentations, with a yield of up to 75 % unsaturated WEs [12].

On top of lipid yield and rapid growth, utilization of sustainably produced growth substrates is an essential factor in the evaluation of an oleaginous microorganism. Hydrolysates, gained from vast and inexpensive waste streams, can be used as substrates for the respective microorganism reducing the overall cost of the process. In this context the most abundant raw material worldwide, lignocellulosic biomass, is a promising source. Examples include agro-industrial residues such as wheat straw, sugarcane bagasse [39] or waste from industrial paper mills [40]. For a cost-efficient process, all carbon sources found have to be used by the organism, as well as the organism being able to tolerate growth and lipid production inhibitors often occurring in hydrolysates [41,42]. In hydrolysates extracted from lignocellulosic biomass, glucose, xylose and arabinose are the main carbohydrate components, from which the second two cannot be naturally utilized by *Rhodococcus* [43-45]. Therefore, the genetic modification of the organism to utilize all carbon sources efficiently is important to economically produce oleochemicals. During the depolymerization of lignin, aromatic mixtures that inhibit growth are generated. As *R. opacus* is able to tolerate these compounds, the aromatic bioconversion of *R. opacus* was elucidated in a multi-omic approach. This improved understanding allows to identify novel targets to generate improved strains for lignin valorisation [46]. With genetic engineering, the utilization of novel substrates as well as the production of recombinant products can be established. Oleaginous microorganisms represent a new platform technology with potential for storage of lipophilic compounds in their lipid bodies [47]. While genetic engineering is still challenging in non-model oleaginous microorganisms, the methods are constantly improving [48].

1.1.2 OleoBuild

The OleoBuild project, funded by the German Federal Ministry of Education and Research (BMBF, grant number: 031B0853A), investigated the potential of the oleogenic und carotenogenic bacterium *R. erythropolis* [49] and yeast *R. toruloides* [50] as versatile, standardized and robust platform organisms for the production of hydrophobic building blocks.

The here presented work focuses on *R. erythropolis* as a production organism. To this end, a detailed scientific understanding of the native production of carotenoids and lipids in these organisms was required in order to enhance their yield. Systems biology, synthetic, structural biology and bioinformatics methods were employed to develop targeted molecular genetic engineering strategies for the manipulation of *R. erythropolis*. Sustainable fermentation strategies were used to enable the utilization of the lignocellulosic by-product wheat bran as a sustainable carbon source in *R. erythropolis*. To this end, key enzymes of carbohydrate metabolism were identified and genetically introduced. In addition, intricate recombinant metabolic pathways were engineered in the bacterium to produce the hydrophobic model compounds ß-ionone and cembratrienol, which are used in the areas of fragrances and novel biodegradable crop protection applications [51-53]. In order to achieve efficient biocatalytic production of these products, a targeted engineering of the recombinant and endogenous metabolic pathways was required. For this purpose, precursors as well as the corresponding metabolic enzymes were analyzed. Intracellular lipid vesicles were harnessed to serve as an endogenous sink for hydrophobic compounds. This approach was aimed at reducing end-product toxicities and facilitating the subsequent product recovery process [47,54,55]. In order to demonstrate the production of commercially relevant levels of ß-ionone and cembratrienol, cultivation parameters were established to achieve high cell densities for all production strains. Schematic overview of this project is given in Figure 1.

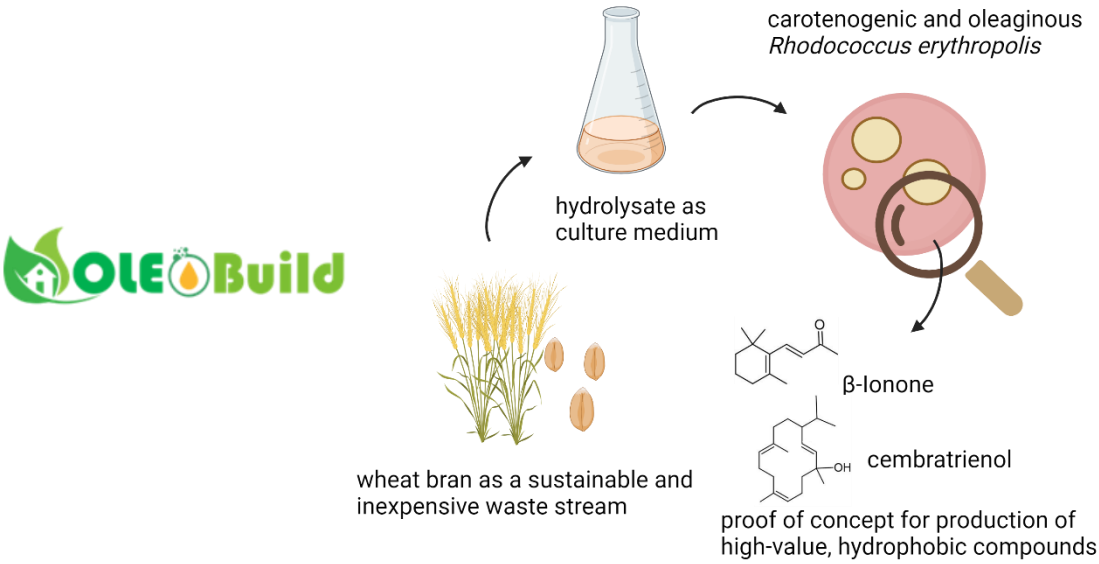

Figure 1: Schematic description of the BMBF funded project "OleoBuild". Structures drawn with ChemSketch, version 2023.1.2, Advanced Chemistry Development, Inc. (ACD/Labs) and figure created with BioRender.com.

1.2 *Rhodococcus* as a Platform Organism for Oleochemicals

1.2.1 Choosing *Rhodococcus erythropolis* as Producer

Rhodococcus is a very diverse genus of gram-positive, non-sporulating, aerobic and non-motile nocardioform actinomycetes [56]. Their genome has a high G+C content, with a genome size of around 6 - 7 Mb, the presence of plasmids, both linear and circular can increase the size by an additional one to two Mb. Due to a large genome size, they can accommodate non-essential genes which make the genus highly variable [57].

They are ideal candidates for biotechnological applications as they are metabolically versatile and can degrade many difficult organic compounds in respect to their recalcitrance and toxicity, such as short- and long chain alkanes and aromatic compounds [58,59]. They are reported as natural producers of a wide range of products such as glycolipid surfactants, carotenoids, TAGs and polyhydroxyalkanoates [58]. Lipid yields up to 80 % (g_{Lipid} g^{-1}_{DCW}) have been achieved in *R. erythropolis* DCL14 [60]. Production of new antibiotics and novel siderophores have also been reported [58,61]. Compared to other actinomycetes, *Rhodococcus* has a high growth rate, can grow on conventional nutrient medium and can be handled in a similar manner to *E. coli*. Due to the high G+C content it is suitable for expression of genes from other actinomycetes such as *Streptomyces*, which have the disadvantage of a life cycle with differentiation such as sporulation [57].

Within the genus *Rhodococcus*, seven distantly related species-groups were identified with Group A (*R. equi* cluster), Group B (*Rhodococcus sensu stricto* cluster), Group C (*R. opacus*

cluster), Group D (*R. erythropolis* cluster), Group E (*R. fascians* cluster) and two minor cluster F and G. Group D encompasses environmental samples classified as *R. erythropolis, R. qingshengii, R. rhodochrous* as well as unclassified strains. A high genetic and metabolic heterogeneity between the groups was found, making their application in various industrial processes highly appealing. The capacity for the accumulation of high amounts of TAG appears to be confined to group C [62,63]. Oleagenicity, a conservative metabolic approach, could provide an advantage in nutrient-limited ecosystems such as deserts or arid habitats [63].

R. erythropolis is able to perform a wide range of enzymatic reactions including oxidations, dehydrogenations, epoxidations, hydroxylations, hydrolysis and desulfurisations [49]. *R. erythropolis* is further recognized as one of the best flocculating bacteria [64]. In their genome, a large number of enzymes is encoded for a plethora of bioconversions and degradations. The growth and production of recombinant proteins has been proven in a wide range of temperature from 4 to 35 °C [65,66]. The production of recombinant proteins that damage the host cell at low temperature is advantageous as enzymatic activity can be suppressed [17]. The intracellular milieu is different to, for example, *E. coli* as gram-negative bacterium or *Bacillus subtilis* as gram-positive bacterium with a moderate G+C content. *R. erythropolis* can produce recombinant proteins such as bacterial lipoglycoproteins from *Mycobacterium tuberculosis,* which are difficult to express in *E. coli* [67,68]. The cell wall of *R. erythropolis* is difficult to disrupt due to the mycolic acid composition, therefore protein extraction is hindered. A lysozyme-sensitive mutant could solve this [69].

1.2.2 Stress Adaptation of *Rhodococcus*

In nature, bacteria encounter various challenges compared to the controlled conditions in biotechnological processes, such as harsh competition, nutritional limitations, changes in physical conditions or the exposure to various chemical compounds. Through evolution, surviving organisms adapted to their specific niche by developing complex regulatory networks enabling a response at global level to overcome adverse conditions and maintain their integrity [70]. It is necessary to recognize an environmental condition in order to cope with it, since a cellular response without a stimulus is unfavorable, as this energy could be used for growth instead. Thus, for efficient growth and development a careful regulation of the stress response is necessary [71,72].

Rhodococci can survive under various extreme stress conditions, as can be seen in their wide range of natural habitats [73]. They can be found as a part of microbial communities [63] in habitats from soil to seawater including Alpine soils, deep sea, coastal sediments and Arctic as well as Antarctic samples [49]. Furthermore, *Rhodococci* have been found in contaminated

areas such as oilfields in India [74], phenol-polluted sludge in China [75] or in textile effluent-contaminated soil in India [76]. These bacteria are metabolically active over a wide range of pH levels (3-11) and temperatures (-2 to +40°C) [73]. The existence of this bacteria genus in such diverse environments can to a part be explained by their extraordinary metabolic versatility and high resistance to stress conditions [58]. A wide range of stress factors that *Rhodococci* are able to withstand, such as desiccation, starvation, cold and heat stress, toxic metal and organic compounds are often combined and associated with oxidative stress in the cell [73]. Partially reduced reactive oxygen species (ROS), including superoxide anions, hydrogen peroxide and hydroxyl radicals, have the potential to harm cells and even cause cell death. In exposed cells, DNA, membrane, lipids and proteins are impaired. To prevent this, most organisms produce catalases, peroxiredoxins and superoxide dismutases, which are able to react with oxidants and neutralize them [70]. Further, the cell wall of *Rhodococcus* includes mycolic acids, either attached to an arabinogalactan complex or a trehalose disaccharide, which enables the transport of hydrophobic substrates into the cell and the resistance against many toxic compounds [77,78]. A further reason for the high resistance of *Rhodococcus* is the ability to alter the fatty acids composition of its membrane lipids, affecting the fluidity. The cell envelope protects the cell from the outside environment as a multilayered outer barrier. The dynamic cell membrane consists of a lipid bilayer and associated proteins. As a response to stress, the cell envelope can be modified by altering length, branching and saturation of fatty acid acyl chains. Additionally, lipid composition can change as well as the production of various proteins, which protect the membrane [77]. Further, a relative large genome provides a redundancy of catabolic pathways [56].

Various physiological adaptations to stress have been detected in *Rhodococci* cells, including increased production of lipids [79], carotenoids or surfactants. Protection can also be achieved by aggregation and biofilm formation. Genome-wide techniques, such as proteomics and transcriptomics, showed the up- and downregulation of hundreds of genes in reaction to stress situations, elucidating complicated and global regulation responses. There is a knowledge gap in the understanding of the adaptation of bacteria to extreme conditions, which is essential in the development of biotechnological processes and to harness this adaptation into enhanced product formation [73].

1.2.3 Genetic Engineering and Toolbox of *R. erythropolis*

As a non-model bacterium, the genetic engineering tools and techniques for *Rhodococcus* strains were limited. The engineering of *R. erythropolis* is challenging due to its high genome G+C content and low transformation and recombination efficiencies [19]. A method for codon optimization method was developed with statistical analysis of 204 genes, which were recombinantly expressed in the same vector. As most important characteristic, the mRNA

folding energy at 5' regions as well as the codon frequency have been identified. Interestingly a species-specific influence on the repetition rate of codons and amino acids has been detected [68]. Further, multiple *E. coli – R. erythropolis* shuttle vectors have been constructed, which utilize two different replication origins and different antibiotic resistance marker genes such as chloramphenicol and tetracycline. Constitutive and inducible expression vectors are available, with an expression yield of up to 10 mg recombinant protein per liter of culture [65,66,80]. As inducers methanol [81] and thiostrepton [66] have been established. Plasmids can be introduced using effective electrotransformation protocols [80]. Furthermore, random mutagenesis with a adapted transposon system [82] has been developed. Unmarked gene deletion is possible due to the use of sacB as counter-selectable marker via homologous recombination [83].

In this thesis, the type strain JCM3201 has been used for all experiments, originally isolated from soil [84]. While the genome of *R. erythropolis* JCM3201^T has been sequenced before (GenBank accession number BCRM00000000), an improved genome assembly level has been presented in 2019 by Yoshida et al. [85] utilizing Illumina and PacBio sequencing.

1.2.4 Lipid Biosynthesis in *Rhodococcus*

1.2.4.1 Triacylglycerols

In general, SCO consist of lipids with 4 to 28 unbranched carbon chain lengths, either saturated or unsaturated [27]. TAG have a wide range of application in food additives, cosmetics, lubricants, oleochemicals and biofuels [9,58]. As long as there is an excess of nutrients, the oleaginous microorganisms will grow and accumulate biomass. When a nutrient, often nitrogen or phosphate, is depleted from the medium and carbon is still available in excess, lipid biosynthesis is stimulated [86,87]. Lipids function as reserve storage material [9,13] and are stored in so called lipid bodies surrounded by a phospholipid monolayer [88].

The amount and profile of the produced lipids depends on the microorganism as well as the mode of cultivation, carbon and nitrogen source, pH, oxygen availability and temperature. Further, the ratio of carbon to nitrogen influences the lipid accumulation [9]. While a high C:N boosts lipogenesis, a too high carbon concentration may inhibit growth and lipogenesis [89]. Therefore, the form of carbon as well as its concentration has to be chosen carefully [89]. As high amounts of carbon are necessary to trigger lipid accumulation, a low-cost substrate is necessary for an economic process [9,89]. Besides the selected carbon source, the nitrogen source also influences lipid accumulation and profile. In literature, organic and inorganic sources are used as well as a combination of both. These sources include yeast extract, peptone/tryptone, urea, ammonium sulfate, ammonium chloride and many more [9].

Gram-positive actinobacteria can accumulate high amounts of bacterial TAG [63], whereby bacterial fatty acids are generally shorter than their eukaryotic counterparts and do not display polysaturation [1]. While TAG serve as energy reserve in eukaryotic organisms, the occurrence in bacteria has not been described much [79,90]. Their primary function is to serve as energy and carbon storage. Additionally, they have been suggested to regulate cellular membrane fluidity and act as a sink for reducing equivalents. Furthermore, fatty acids and their derivates serve as precursors for the synthesis of cell envelopes [91]. Lipid accumulation has been observed in certain genera of gram-positive bacteria like *Streptomyces*, *Rhodococcus* and *Nocardia*, with *Rhodococcus* as the most extensively investigated species with reported yields of more than 70 % lipid per dry cell weight [1,58].

In *Rhodococci* and other actinobacteria, the Kennedy pathway [92] serves as the primary route for TAG synthesis (Figure 2). This metabolic process involves the sequential acylation of glycerol-3-phosphate with fatty acyl-CoAs. Glycerol-3-phosphate O-acyltransferase (GPAT) and 1-acylglycerol–3-phosphate O-acyltransferase (AGPAT) catalyse these acylation steps, leading to the production of phosphatidic acid. The subsequent transformation of phosphatidic acid into diacylglycerol (DAG) is achieved through dephosphorylation, facilitated by the action of phosphatidic acid phosphatase (PAP). The final stage involves the sn-3 acylation of DAG by the enzyme DAG *O*-acyltransferase (DGAT). Intriguingly, *Rhodococci* exhibit a multitude of homologous enzymes associated with the Kennedy pathway within their genomic makeup. However, it's noteworthy that a lack of both biochemical and molecular genetic characterization currently hampers a comprehensive understanding of these enzymes' functional properties [93,94].

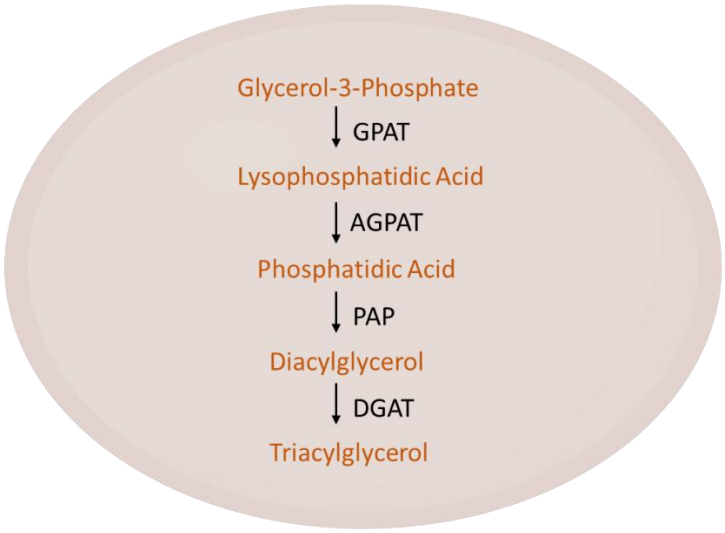

Figure 2: The Kennedy pathway of triacylglycerol biosynthesis as proposed in Rhodococcus*. GPAT: glycerol-3-phosphate acyl transferase; AGPAT: acylglycerol-3-phosphate acyl transferase; PAP: phosphatidic acid phosphatase; DGAT: diacylglycerol acyl transferase. Adapted from Amara et al. (2016) [93]. Created with BioRender.com.*

1.2.4.2 Carotenoids

Carotenoids comprise a diverse group of lipid-soluble pigments that alter the color of their producer, ranging from yellow to orange to deep red [95,96]. From a chemical background, they are typically tetraterpenoids, grouped in carotenes, which only contain a hydrocarbon backbone, and xanthophylls, which are oxidation products of carotenes. The presence of conjugated double bonds in their structure is responsible for their antioxidant activity [95-98]. Due to this, they play an important role in the protection of cell membranes against light damage, oxidation and free radicals. As ROS and oxidative damage are postulated to be involved in causing and progression of various chronic diseases, carotenoids can serve as dietary nutrients by reducing the risk of several degenerative diseases including cancer and cardiovascular disease while also stimulating the immune response [99-101]. Further, they play a role as precursors for vitamins [58], for example ß-carotene is a precursor of vitamin A [47]. Naturally, they are produced by a wide range of organisms, including plants, microalgae, bacteria and especially fungi and yeasts. Animals and humans are unable to produce carotenoids and supplement carotenoids with their diet [100,102]. Although there are over 1204 known naturally occurring carotenoids from 722 organisms (324 bacterial carotenoids) [103], only a few are commercially available such as ß-carotene, astaxanthin and lutein, which are often produced chemically. Industrially, they are used as food and feed additives, as well as in pharmaceutical and cosmetic products. Recently, there has been an increasing preference for naturally produced microbial carotenoids over their chemically synthesized counterparts, leading to an increase in market value [95,104]. Natural carotenoids are regarded to have higher biological properties due to more favorable cis/trans isomer mixtures [96]. Compared to extraction from plants, microbial production offers advantages such as higher process control, higher yield and scalability. While carotenoids form crystals in aqueous environment [105,106], they can be stored in the lipid bodies of *Y. lipolytica* [47]. The production of carotenoids in oleaginous organisms could enable the storage of high titers of product. Numerous factors, including carbon source, light exposure, temperature, aeration and the presence of metal ions and salts, affect both the yield and composition of carotenoids [99]. There are also attempts to increase yield through genetic engineering [107-109].

Carotenoid-producing bacteria can be divided into the subgroups anoxygenic phototrophic, oxygenic phototrophic and non-phototrophic [110]. Anoxygenic photosynthetic bacteria possess a photosystem to harvest light. This process is facilitated by the accessory pigments of bacteriochlorophyll and additional carotenoids, carotenoid biosynthesis is regulated by oxygen and light [95]. The group of oxygenic phototrophic bacteria consist of cyanobacteria, which produce phycobiliproteins and chlorophyll *a* instead. It is hypothesized that carotenoids in non-phototrophic bacteria serve as protection against photo-oxidative damage [110].

Carotenoid synthesis in most bacteria occurs through the 2-C-methyl-D-erythritol-4-phosphate (MEP) pathway, also named 1-deoxyxylulose-5-phosphate (DXP) pathway [104,111,112], utilizing glyceraldehyde-3-phosphate (GAP) and pyruvate from the central carbon pathway as substrates. To generate isopentenyl pyrophosphate (IPP), a key building block, the process requires three molecules of ATP and two molecules of NADPH as cofactors [113]. Within the MEP pathway, IPP biosynthesis commences with the condensation of GAP and pyruvate. This is followed by a reductive isomerization step, coupling with cytidine triphosphate, and ultimately a phosphorylation and cyclization reaction. After the formation of isoprene precursors, namely one molecule of dimethylallyl pyrophosphate (DMAPP) and three molecules of IPP, these units combine through three prenyl-transferase reactions to yield geranylgeranyl diphosphate (GGPP). Further, two GGPP molecules can be combined to create phytoene (C40). This phytoene undergoes four double-bond additions to give rise to lycopene, a precursor for various carotenoids like β-carotene, zeaxanthin, and astaxanthin [111]. In Figure 3, the pathway to carotenoid production as proposed in *Rhodococcus* is shown.

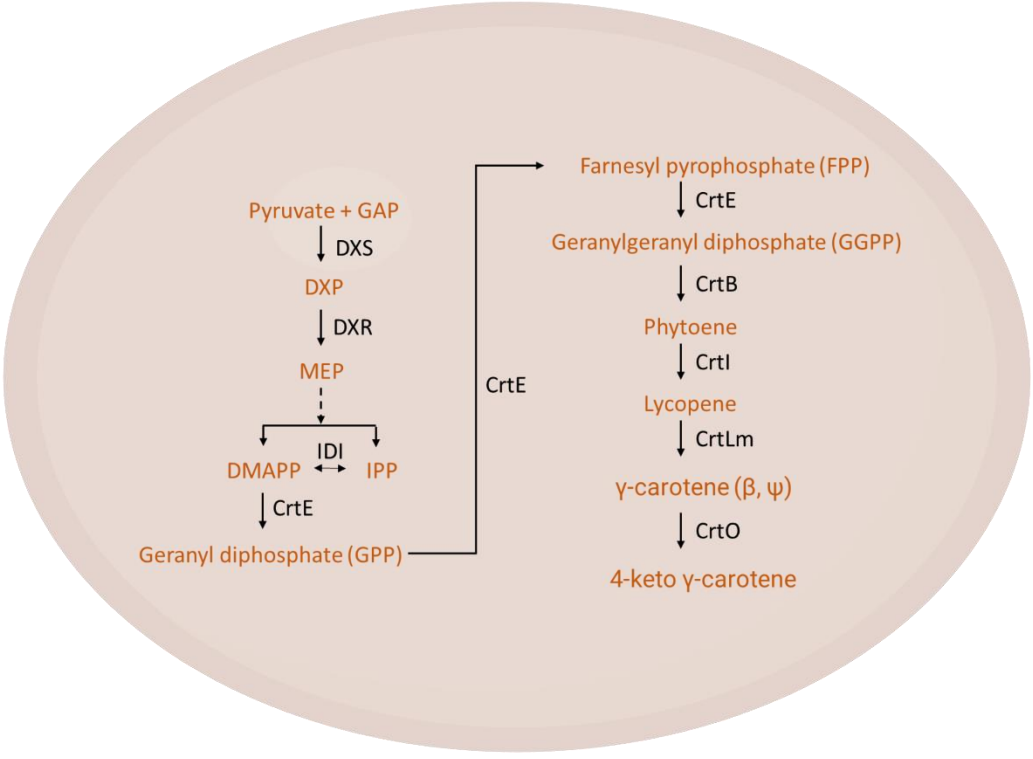

Figure 3: Pathway of carotenoid production in Rhodococcus*. GAP: Glyceraldehyde-3-phosphate; DXS: DXP Synthase; DXP: 1-deoxyxylulose-5-phosphate; DXR: DXP reductoisomerase; MEP: 2-C-methyl-D-erythritol-4-phosphate; DMAPP: dimethylallyl pyrophosphate; IPP: isopentenyl pyrophosphate; IDI: isopentenyl-diphosphate delta-isomerase; CrtE: geranylgeranyl pyrophosphate synthase; CrtB: phytoene synthase; CrtI: phytoene dehydrogenase; CrtLm: lycopene β-cyclase; CrtO: β-carotene ketolase. Adapted from Li et al. (2020) [111] and Tao et al. (2006) [114]. Created with BioRender.com.*

In *Rhodococcus* strains, many different carotenoid pigments are produced, located either intracellularly in the lipid droplet, in the plasma membrane or in the cell wall [58]. In

R. erythropolis AN12 4-keto-γ-carotene and γ-carotene were identified as main compounds, additional carotenoids, including β-carotene, lycopene, and phytoene have been identified in different *R. erythropolis* strains [114,115]. Carotenoids are one specific type of terpenoids, for which IPP and DMAPP are the universal precursors [116]. Bottlenecks and regulation checkpoints of terpenoid and carotenoid production have to be identified in order to utilize genetic modification in a targeted way. For this, omics-techniques can be used to allow an in-depth understanding of the organism. Proteomics can be used to identify novel functional genes and pathways and to identify changes in protein expression due to changed substrates or process conditions [117]. Therefore, a better understanding of the carotenoid biosynthesis can be used to modify its regulation and establish the recombinant production of various terpenoids.

1.2.5 Process Optimisation of *Rhodococcus* by Response Surface Methodology

To transform a strain into an effective production platform, it is crucial to analyse the nutritional requirements and substrate adaptability of the strain. If the organism is flexible in the use of its substrate, various waste streams and inexpensive carbon sources can be utilized. A robust organism is advantageous due to its ability to survive fluctuations in the process conditions like pH, temperature and medium composition as waste streams often have a varying composition.

Every bacteria has essential requirements of nutrients consisting of water, a carbon and nitrogen source and some mineral salts [118,119], which have to be supplied in the culture medium. Synthetic media are composed of clearly defined, minimal ingredients, while for complex media the exact chemical composition is not known [120]. Hydrolysates generated from waste streams vary in composition. For simplified and increased reproducibility of experiments, synthetic media simulating the waste stream hydrolysate is preferred at a laboratory scale. Here, the discrete impact of certain nutrients can be better investigated [121].

Processes involving microbial systems are often improved by one-factor-at-a-time (OFAT)-optimization approach, which is time intensive and only allows conclusions regarding the influence of one variable, not the interactions between them [122,123]. However, statistics-based response surface methodology (RSM) facilitates the rapid screening of parameters at decreased cost. The mathematical modelling algorithm was originally developed by Box and Wilson [124] and is used to describe the relationship between a response of interest and a number of associated input variables in a low-degree polynomial model [125]. Therefore, this allows to identify optimum conditions in a multivariable system. At a reduced number of runs, it enables to identify optimal cultivation conditions. Additionally, this method allows the

determination of the impact of independent variables on the process both individually and in combination [126,127].

Central Composite Design (CCD), the most popular of all second-order designs, consist of three portions: First, complete 2^k factorial design, where the level of factors are coded -1 and 1 in form of extract points. Next, an axial portion of 2*k* points, with two points on the axis of each variable in a distance of alpha from the center, called star points. Further n_0 center points are applied [125,128]. CCD has been utilized before for media optimization in *Rhodococcus,* such as in the production of biosurfactant by *Rhodococcus* spp. MTCC2574 [129] and odd chain fatty acid (OCFA) by *Rhodococcus* sp. YHY01 [130].

Depending on the alpha value, three types of CCD are distinguished. A Central Composite Circumscribed design (CCC) is the original form. Here the star points set new extremes for the minimum and maximum values of the variables. The Central Composite inscribed design (CCI) is used when the limits of the factors are truly limiting, therefore using the factor levels as star points. In a Central Composite Face-centered design (CCF) alpha equals ±1 therefore the star points are positioned at the center of each face of the design space [131,132]. Pictorial representation of each design is shown in Figure 4.

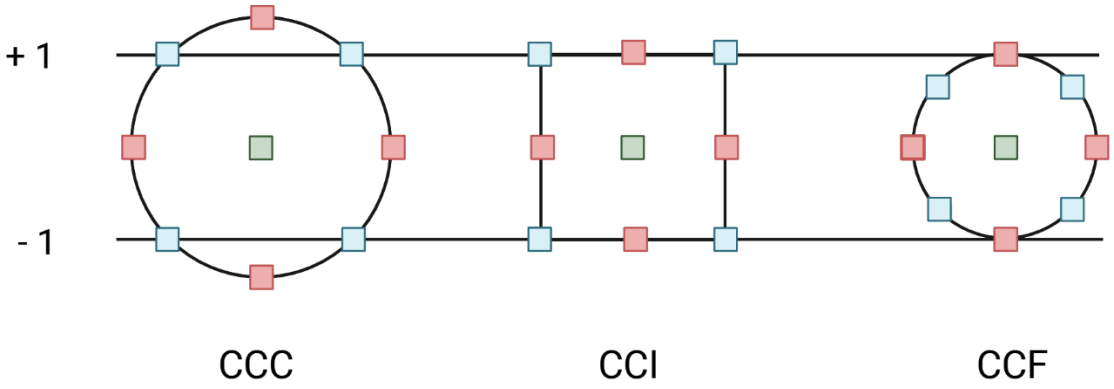

Figure 4: Different types of Central Composite Design with center point in green, extract points in blue and star points in red. CCC: Central Composite Circumscribed design, CCI: Central Composite inscribed design, CCF: Central Composite Face-centred design. Adapted from Natrella [133]. Created with BioRender.com.

2 Materials and Methods

The following paragraph contains an overview of the key methods, procedures, and tools utilized in this thesis. Detailed information can be found in the materials and methods sections of the respective publications included in this thesis.

2.1 Media Composition

Prior to autoclaving, pH of the media was adjusted using the appropriate acid or base. Trace elements, sugars or media components that are not heat-stable were either sterilized via filtration or separate autoclaving. Afterwards, they were added to the autoclaved, final media.

Table 1. Luria-Bertani Broth / Agar

Yeast extract	5 g L^{-1}
NaCl	10 g L^{-1}
Tryptone / Peptone	10 g L^{-1}
Agar-Agar (if needed)	15 g L^{-1}
ddH_2O	Up to 1 L

Table 2. Modified 457. Mineral Medium (Brunner, DSMZ), pH 6.9 [134] without nitrogen source

Main Medium		Trace element solution SL-4		Trace element solution SL-6	
Na_2HPO_4	2.44 g L^{-1}	EDTA	0.5 g L^{-1}	$ZnSO_4$ x 7 H_20	0.10 g L^{-1}
KH_2PO_4	1.52 g L^{-1}	$FeSO_4$ x 7 H_2O	0.20 g L^{-1}	$MnCl_2$ x 4 H_2O	0.03 g L^{-1}
$MgSO_4$ x 7 H_20	0.2 g L^{-1}	SL-6	100 mL	H_3BO_3	0.30 g L^{-1}
$CaCl_2$ x 2 H_2O	0.05 g L^{-1}	ddH_2O	900 mL	$CoCl_2$ x 6 H_2O	0.20 g L^{-1}
SL-4	10 mL			$CuCl_2$ x 2 H_2O	0.01 g L^{-1}
ddH_2O	Up to 1 L			$NiCl_2$ x 6 H_2O	0.02 g L^{-1}
				Na_2MoO_4 x 2 H_2O	0.03 g L^{-1}
				ddH_2O	Up to 1 L

2.2 Bacterial Strain and Culture Conditions

The bacterium *R. erythropolis* JCM3201^T (DSM No. 43066, German Collection of Microorganisms and Cell Cultures GmbH) was used in all experiments. Cultivations were

performed in a rotary incubator (New Brunswick InnovaTM 44 and 42, Eppendorf, Hamburg, Germany) and incubated at 28 °C and 120 rpm.

The strain was preserved on LB agar plates and replated from cryostocks at least every four weeks. To prepare seed cultures, single colonies were first cultivated in 100 mL of LB liquid medium in 500 mL baffled shaking flasks for 48 h.

2.2.1 Screening of Different Nitrogen and Carbon Sources

100 mL '457. Mineral Medium' (Brunner, DSMZ) in 500 mL baffled shake flasks were inoculated to OD_{600} 0.2 and cultivated for 192 h. Nitrogen and carbon sources, listed in Table 3, were selected individually for each experiment. Nitrogen content of yeast extract (10.8 % w/w) and tryptone/peptone (12.3 % w/w) was defined based on supplier's information (Carl Roth, Germany). All cultivation were performed in biological triplicates with 16 g L^{-1} elemental carbon and 0.16 g L^{-1} elemental nitrogen. When testing nitrogen sources, glucose was used as carbon source. When testing carbon sources, ammonium acetate was used as nitrogen source.

Table 3. Matrix of nitrogen and carbon sources tested with their chemical composition. Adapted from Engelhart-Straub et al. (2023) [135].

Nitrogen Source	Chemical Composition	Carbon Source	Chemical Composition
Ammonium chloride		Glucose	
Diammonium hydrogen phosphate		Galactose	Monosaccharides
Ammonium sulfate	Defined inorganic	Fructose	
Potassium nitrate		Lactose	
Ammonium nitrate		Sucrose	Disaccharides
Yeast extract	Complex organic	Maltose	
Tryptone/Peptone		Sorbitol	Sugar alcohol
Urea	Defined organic	Glycerol	
Ammonium acetate			

2.2.2 Response Surface Methodology: Screening of Different Carbon-to-Nitrogen Concentrations and Ratios

A full CCD consisting of 21 runs with different carbon (3.93 to 18.07 g L^{-1} elemental carbon) and nitrogen (0.02 to 0.58 g L^{-1} elemental nitrogen) concentrations was performed, covering a C:N of 12:1 to 647:1 (Table 4). Glucose was used as carbon source and ammonium acetate as nitrogen source. While the center point was replicated five times, all other ratios were performed in biological duplicates. Every analysis was performed in two technical replicates. With a start OD_{600} of 0.2, cultivations were run for 192 h.

Table 4. Range of values used in Central Composite Design. Adapted from Engelhart-Straub et al. (2023) [135].

Variable	Factor Level				
	−1.414	**−1**	**0**	**+1**	**+1.414**
Nitrogen concentration (g L^{-1})	0.017	0.1	0.3	0.5	0.583
Carbon concentration(g L^{-1})	3.929	6	11	16	18.071

2.2.3 Cultivation under Light of Different Wavelengths

In biological triplicates, cultures were exposed to different wavelengths of light (LED), including blue (425, 455 and 470 nm), green (510 nm), red (680 nm), standard warm white (SWW) light. LEDs were set at an equal energy output of 236 W m^{-2}. Experiments were performed in a customized shaker unit, illuminated with bottom-up LEDs [136], each flask shaded to avoid cross-illumination. In a separate shaker, dark control samples were cultivated in a light-free environment. 500 mL baffled shaking flasks with Duran GL32 Membrane Vented Screw caps (DWK Life Science, Wertheim, Germany) holding 100 mL LB were used. Cultures were inoculated to OD_{600} 0.5.

2.2.4 Cultivation under LED Light for Proteomic Analysis

For proteomics analysis, cultures were illuminated with white LEDs. For this purpose, LED Mini-Matrices (Spectral color of 6500 K, max. 750 µmol m^{-2} s^{-1}, 504 LEDs, 27 × 42 cm, 24V; LUMITRONIX® LED-Technik GmbH, Hechingen, Germany) were installed at a height of 30 cm in a rotary shaker. Samples grown in the dark were used as control.

2.3 Analysis

2.3.1 Growth Analysis

Optical density was determined at 600 nm in a photometer (Nano Photometer NP80, IMPLEN, Munich, Germany). The sample volume of 1 mL was contained in standard semi-micro cuvettes.

A defined volume of culture was sampled into pre-weighed falcon tube, followed by centrifugation (3500× *g*, 10 min). Subsequently, cells were washed and lyophilized (−80 °C, ≥ 72 h). Subsequently, the weight of the empty vessel was deducted from the weight of the tube holding the lyophilized biomass.

Cell morphology and contamination was assessed with a light microscope (Motic BA310E) equipped with a Moticam 5.0 MP (both Moticeurope, Barcelona, Spain).

2.3.2 Pigment Extraction

For pigment extraction, a defined amount of lyophilized biomass was mixed with either 0.5 or 2 mm glass beads along with 1 mL of HPLC-grade acetone. The resulting mixture was vortexed for 10 min and then subjected to centrifugation (8000× *g*, 5 min). Subsequently, 700 µL of the supernatant was transferred into a glass tube. To prevent light exposure, all vessels were wrapped in aluminium. Carotenoid levels were determined at an absorbance of 454 nm (Nano Photometer NP80, IMPLEN, Munich, Germany), measured in a solvent-stable cuvette.

In case of wet biomass, utilized for proteomic analysis, 7.5 mL cell suspension was centrifuged and subsequently washed with ddH_2O for pigment extraction. The cell pellet was mixed with 0.5 mm glass beads and 1.5 mL hexane: acetone: ethanol (2:1:1 - *v*/*v*/*v*). To achieve cell lyses, the suspension was vortexed horizontally for 30 min, followed by centrifugation (20,000× *g*,10 min). Carotenoids levels of the hexane phase were directly measured at an absorbance of 454 nm (UV/Vis spectrophotometer Hewlett Packard 8453, HP, Palo Alto, CA, USA) in a solvent-stable cuvette.

2.3.3 Fatty Acid Analysis

Lipids contained in lyophilized biomass were extracted and converted into fatty acid methyl ester (FAME) and subsequently analysed using gas chromatography. For this, a defined amount of lyophilized biomass was weighed into a 10 mL glass vial, which was sealed with a bimetallic lid containing a septum (Macherey-Nagel, Düren, Germany). For methyl esterification of intracellular TAGs, the MultiPurposeSampler MPS robotic (Gerstel, Linthicum Heights, MD, USA), including QuickMix, CF200 and Agitator/Stirrer was utilized. For quantification, a stock solution of the internal standard of 10 g L^{-1} glyceryl tridodecanoate (C12:0; Sigma-Aldrich, St. Louis, MO, USA) was prepared in toluol. Than 490 µL toluol and 10 µL internal standard were added to the biomass and mixed (1000 rpm, 1 min). Next, 1 mL of 0.5 M sodium methoxide in methanol was transferred to the vial and subsequently vortexed at 80 °C (750 rpm, 20 min). After a cooling step at 5 °C for 5 min, 1 mL of 5 % HCl in methanol (Supleco 17935 solution, Merck AG, Darmstadt, Germany) was added. The mixture was vortexed at 80 °C (750 rpm, 20 min), followed by cooling at 5 °C for 5 min. Next, 400 µL ddH_2O was added to the vial, which was then vortexed (1000 rpm, 30 s). After that, 1 mL hexane was added. To extract FAMEs, three intervals of intermittent shaking (2000 rpm, 12 s) were performed. The vial was then centrifuged (1000 rpm, 3 min). After another cooling step at 5 °C for 1 min, a defined volume of 200 µL of the organic phase was transferred to micro vials (Macherey-Nagel, Düren, Germany).

Analysis and quantification of the FAMEs were conducted using a GC-2025 coupled to AOC-20i Auto injector and AOC-20s Auto sampler (Shimadzu, Duisburg, Germany) with a flame

ionization detector (FID) [137,138]. The injection temperature was set at 240 °C with a split ratio of 10 and a helium purge flow of 3 mL min^{-1}. All samples were injected at a volume of 1 µL. To achieve separation, a Zebron ZB-wax column (Phenomenex, Aschaffenburg, Germany) (30 m × 0.32 mm, film thickness 0.25 µm) was used. The initial oven temperature was 150 °C, held for 1 min before ramping up at a rate of 5 °C min^{-1} up to a final temperature of 240 °C for 6 min. Hydrogen as carrier gas had a constant flow rate of 3 mL min^{-1}. The FID measurements were performed at 245 °C with 40 mL min^{-1} flow of hydrogen, 400 mL min^{-1} flow of synthetic air and 30 mL min^{-1} flow of nitrogen as makeup gas. For identification, the standards Marine Oil FAME mix (20 components from C14:0 to C24:1; Restek GmbH, Bad Homburg, Germany) and FAME #12 mix (C13:0, C15:0, C17:0, C19:0, C21:0; Restek GmbH, Bad Homburg, Germany) were used. Measurements were normalized based on the internal standard methyl laurate (C12; Restek GmbH, Bad Homburg, Germany). For calibration measurements, runs with concentrations of 20, 5, 1, 0.5, 0.1 mg mL^{-1} Marine Oil FAME Mix were performed. Further, FAME #12 concentrations of 5, 2.5, 1.25, 0.5, 0.25, 0.05, 0.01 mg mL^{-1} and methyl laurate concentrations of 2, 1, 0.2, 0.05, 0.01, 0.002 mg mL^{-1} were used. The calibration enabled comparative quantitation. Fatty acid profiles were analysed as a percentage of the total fatty acid content (*w*/*w*).

To identify branched fatty acid, GC–MS analysis was conducted using the Thermo Scientific™ TRACE™ Ultra Gas Chromatograph coupled with a Thermo DSQ™ II mass spectrometer and Triplus™ Autosampler injector. For the analysis, a BPX5 column (30 m × 0.25 mm, film thickness of 0.25 µm; Trajan Scientific Australia Pty Ltd, Victoria, Australia) was employed. An initial column temperature of 50 °C was used for separation, this was increased at a rate of 4 °C min^{-1} until reaching a final temperature of 250 °C. Hydrogen, as carrier gas, was used at a constant flow rate of 0.8 mL min^{-1}.

2.4 Proteomics

2.4.1 Protein Extraction and Precipitation

To protect the proteins, harvested cells were strictly kept on ice or at 4 °C during centrifugation steps. After centrifugation of 25 mL culture (8000× *g*, 10 min), the bacterial cell pellet was washed twice with ddH_2O. For lysis and protein extraction, the cell pellets were mixed with Protein Extraction Reagent Type 4 (Sigma-Aldrich, St. Louis, MO, USA) (1:3, *v*/*v*) and glass beads. Next, samples were vortexed for 30 min, followed by an ultrasonic bath for 60 min (Ultrasonic Cleaner UCD—THD, VWR, Radnor US). After centrifugation (13,750× *g*, 30 min), the supernatant was mixed 1:1 (*v*/*v*) with 20 % trichloric acid (*v*/*v*) in HPLC-grade acetone (*v*/*v*) supplemented with 10 mM dithiothreitol (DTT) for protein precipitation. Subsequently, the mixture was vortexed and incubated for 1 h and −20 °C. After a centrifugation step (13,750× *g*,

10 min), 1 mL of acetone with 10 mM DTT was used to wash the protein pellet twice. The air-dried pellet was dissolved in 8 M urea solution containing 10 mM DTT. Each condition was analysed in three biological and two technical replicates.

2.4.2 Protein Quantification and SDS-PAGE

Protein concentration was measured at 280 nm absorbance (NanoPhotometer NP80, Implen GmbH, Munich, Germany). The protein extracts were visually detected on a 12 % SDS polyacrylamide gel to assess the quality [139].

2.4.3 In-Gel Digestion of Protein Samples and LC-MS/MS Analysis

Protein extract were further subjected to in-gel digestion [140-142]. Proteins were run shortly into the resolving gel of a 12 % SDS polyacrylamide gel und afterwards stained with Coomassie Brilliant Blue (SERVA Electrophoresis GmbH, Heidelberg, Germany). Stained protein bands were cut from the gel and into small pieces (around 1 mm^3). Those pieces were washed with acetonitrile to remove the Coomassie Brilliant Blue completely. Next, samples were dried under vacuum for 15 min (GeneVac Evaporator, GeneVac HiTechTrader, Ipswich, United Kingdom). Gel pieces were reduced (10 mM DTT and 50 mM ammonium bicarbonate) at 56 °C for 30 min, than washed with acetonitrile, followed by alkylation (55 mM iodoacetamide and 50 mM ammonium bicarbonate) at room temperature for 20 min. Next samples were again washed with acetonitrile and dried under vacuum for 15 min. Samples were rehydrated in digest solution with Trypsin Gold (V5280, Promega, Madison, WI, USA). The enzymatic digestion was performed overnight at 37 °C, with moderate shaking. For peptide extraction, gel pieces were incubated in different solutions, each for 15 min, using 50 mM ammonium bicarbonate, 100 % acetonitrile, and 5 % formic acid solution. Under vacuum, the collected solution was dried, before peptides were dissolved in 1 % formic acid and filtered through a 13.3 kDa spin-filter. This sample was measured via LC-MS/MS analysis.

Protein analysis was performed on a timsTOF Pro mass spectrometer (TIMS) combined with a NanoElute LC System (Bruker Daltonik GmbH, Bremen, Germany), containing an Aurora column (250 × 0.075 mm, 1.6 µm; IonOpticks, Hanover St., Australia) [140]. Two mixtures were used as mobile phase for reverse-phase separation: 0.1 % (*v*/*v*) formic acid—2 % (*v*/*v*) acetonitrile—water mixture (A) and 0.1 % (*v*/*v*) formic acid—acetonitrile mixture (B). The mobile phase was added as a binary gradient with a flow rate of 0.4 µL min^{-1}. A separation cycle lasted 120 min (linearly: 2–17 % B in 60 min, 17–2 5 % B in 30 min, 25–37 % B in 10 min, 37–95 % B in 10 min, maintaining B at 95 % for 10 min) with an oven temperature of 50 °C. TIMS was set in PASEF Mode using these settings: mass range, 100–1700 mass: charge [m/z] ratio; ion mobility ramp, 0.6–1.6 V·s/cm^2; 10 MS/MS scans per ion mobility ramp (total cycle time 1.16 s); charge range 0–5; active exclusion for 0.4 min; target intensity of 20000 counts;

intensity threshold of 1000 counts. Appropriate to the ion-mobility ramp, collision energy was ramped stepwise, starting at 20 eV up to 59 eV. As electrospray ionisation source parameters 1600 V were used for the capillary voltage and at a dry gas temperature of 180 °C, 3 L min^{-1} nitrogen, measurements were conducted in a positive ion mode. For mass calibration sodium formate cluster was used, for calibration of the TIMS Hexais (2,2-difuoroethoxy) phosphazene, Hexakis (2,2,3,3-tetrafuoropropoxy) phosphazene, and Chip cube high mass references (m/z ratios of 622, 922, and 1222, respectively) were used [143,144]. To facilitate normalization of the measurements, three quality control samples, each consisting of an equal volume of each sample, were analysed at regular intervals between samples (first, mid and last sample).

2.5 Bioinformatic Analysis

2.5.1 Response Surface Methodology and Further Statistical Analysis

For set-up and analysis of the design, Design-Expert Software, Version 22.0.2 (Stat-Ease, Inc. Minneapolis, USA) was used. For media optimization of different carbon and nitrogen concentrations, a full Central Composite Design with five center points and eight non-center points in duplicates was applied. For star points, an alpha value of 1.41421 was set. To evaluate suitability of the design, the analysis of variance (ANOVA) was used. The model analysed the effect of carbon and nitrogen levels on biomass (g L^{-1}), lipid content (mg $g\text{-}^{1}_{DCW}$) and carotenoid titres (Abs_{454nm} mg^{-1}_{DCW}) as dependent variables. Non-significant terms not essential for hierarchy were removed from the model.

2.5.2 Bioinformatic analysis of proteomics

For peptide and protein identification, PEAKS Studio software 10.6 (Bioinformatics Solutions Inc., Waterloo, ON, Canada) [145-147] was applied. Based on a genome assembly, *R. erythropolis* JCM3201^{T} protein (fasta) database was downloaded from NCBI (https://www.ncbi.nlm.nih.gov/genome/?term=txid1833[orgn], 10 May 2022, 5954 proteins). Search parameters were set at precursor mass of 25 ppm using monoisotopic mass, fragment ion of 0.05 Da, trypsin as digestion enzyme, maximum of two missed cleavages per peptide, FDR of 1.0 % and at least 1 unique peptide per identified protein has to be found. The Quantification tool PEAKSQ compared different groups, with a mass error tolerance of 20.0 ppm, Ion Mobility Tolerance of 0.05 Da, a Retention Time Shift Tolerance of 6 min (Auto Detect), and a minimum of 2 for fold change and significance. All proteins detected with these settings were exported and subjected to functional characterization with KOALA (KEGG Orthology And Links Annotation, https://www.kegg.jp/blastkoala/, accessed on 4 July 2022) [148]. In addition, the annotations were validated manually using NCBI and Uniprot databases.

3 Research

3.1 Summaries of included publications

Chapter I Optimization of *Rhodococcus erythropolis* JCM3201^T Nutrient Media to Improve Biomass, Lipid, and Carotenoid Yield Using Response Surface Methodology

The article "Optimization of Rhodococcus erythropolis JCM3201^T Nutrient Media to Improve Biomass, Lipid, and Carotenoid Yield Using Response Surface Methodology" has been published in Microorganisms in August 2023 (DOI: 10.3390/microorganisms11092147). The author of this thesis, Selina Engelhart-Straub, designed and carried out the experimental work, evaluated the experimental data and wrote the manuscript.

R. erythropolis JCM3201^T is a carotenogenic and oleaginous bacteria which offers industrial value due to its unique enzyme capabilities in bioconversion and degradation. Further, it is a potential producer for a range of products such as carotenoids, triacylglycerols and biosurfactants [58,149]. In order to use this strain as an efficient production platform and explore its potential, the strain's nutritional requirements have to be characterized. Determination of the most favorable fermentation conditions is crucial for an economically efficient process, as the medium composition directly affects both yield and productivity [123]. Carbon and nitrogen source and concentration as well as the ratio of them both influence biomass, lipid and carotenoid production [9,99].

The presented study investigated the substrate adaptability of *R. erythropolis*. With an OFAT method, the strain was cultivated on nine nitrogen and eight carbon sources at an elemental carbon (16 g L^{-1}) and nitrogen (0.16 g L^{-1}) weight ratio of 100:1. The nitrogen sources included the defined inorganic sources ammonium chloride, diammonium hydrogen phosphate, ammonium sulfate, potassium nitrate and ammonium nitrate. As complex organic sources yeast extract and tryptone/peptone were included as well as defined organic sources urea and ammonium acetate. As carbon sources the monosaccharides glucose, galactose and fructose, the disaccharides lactose, sucrose and maltose and the sugar alcohol sorbitol and glycerol were investigated. Maximum biomass acquisition (2.84 g L^{-1}) was obtained with the nitrogen source ammonium acetate, whereas the complex nitrogen sources yeast extract (156.7 mg g^{-1}_{DCW}) followed by tryptone/peptone (132.3 mg g^{-1}_{DCW}) achieved the highest lipid yields. Defined inorganic carbon sources induced a prolonged lag phase. With regard to differing carbon sources, the highest biomasses were observed with glucose (3.10 g L^{-1}), followed by sucrose (2.47 g L^{-1}). Notably, sugar alcohols, sorbitol (93.8 mg g^{-1}_{DCW}) and glycerol (86.1 mg g^{-1}_{DCW}) induced elevated lipid titres.

A response surface methodology was employed to investigate different carbon and nitrogen concentrations and ratios and determined conditions for enhances biomass, lipid and carotenoid formation after 192 h. For this purpose, a full Central Composite Design (CCD) was performed. The highest biomass (8.00 g L^{-1}) was obtained in a medium with 11 g L^{-1} carbon and 0.583 g L^{-1} nitrogen, while the highest amount of lipids (100.5 mg g^{-1}_{DCW}) was produced by cultures grown in a medium with 11 g L^{-1} carbon and only 0.017 g L^{-1} nitrogen, which was the minimum concentration tested. *R. erythropolis* cultivated in a medium with 6 g L^{-1} carbon and 0.5 g L^{-1} nitrogen produced the highest amount of carotenoids (0.021 Abs_{454nm} mg^{-1}_{DCW}). While biomass production increased with increasing carbon and nitrogen concentration, lipid production decreased. The carotenoid production increased with increasing nitrogen and decreasing carbon concentration. These results could be a foundation for further research, offering novel insights into the physiology of *R. erythropolis* under variable nutritional conditions.

Chapter II Effects of Light on Growth and Metabolism of *Rhodococcus erythropolis*

The article "Effects of Light on Growth and Metabolism of Rhodococcus erythropolis" has been published in Microorganisms in August 2022 (DOI: 10.3390/microorganisms10081680). The author of this thesis, Selina Engelhart-Straub, and Philipp Cavelius contributed equally to the work and writing of this manuscript. They designed and carried out the experimental work, evaluated the experimental data and wrote the manuscript.

The aerobic, gram-positive and resilient bacteria of the genus *Rhodococcus* are promising producers of a range of compounds including biosurfactants, carotenoids and triacylglycerols [58,149]. Like all aerobic organisms, the bacteria is exposed to oxidative stress in the form of reactive oxygen species (ROS), which may trigger the damage of cellular components [150]. Oxidoreductases, specifically catalases and peroxidases, are responsible to perform cellular detoxification from ROS. Organisms are also able to withstand stress through modifications of the fatty acid structure of the membrane [151-153]. Additionally, carotenoids are able to deactivate these highly reactive radicals. Carotenoids are found in in almost all photosynthetic and some non-photosynthetic organisms such as *R. erythropolis* [154]. Little is known about the function of carotenoids in *R. erythropolis* and its response to light. The presented study investigated the adaptation mechanisms of *R. erythropolis* exposed to different wavelengths of light including blue (425, 455 and 470 nm), green (510 nm), red (680 nm) as well as standard warm white (SWW) light. When exposed to red light (680 nm), no significant difference in growth, carotenoid and lipid production compared to dark controls could be detected. In contrast, carotenoid levels were significantly elevated in cultures illuminated with white (standard warm white), green (510 nm) and blue light (470 nm), with significantly decreased biomass accumulation after 94 h and 122 h in cultures illuminated with green (510 nm) and blue light (470 nm). Interestingly, blue light (455, 425 nm) demonstrated anti-microbial effects with significantly decreased dry cell weights. Microscopy revealed agglomerations for cultures exposed to blue light (455 nm) and even dense cellular aggregates for cultures illuminated with 425 nm light, further validating studies which investigate the antimicrobial properties of blue light [155,156]. The cellular lipid composition increased in its amount of OCFAs (C15:0, C17:1) when cultivated under white (standard warm white) and green (510 nm) light. Propanoyl-CoA was proposed as primer for the OCFA synthesis [130,157], several enzymes involved in the synthesis of it were found to be upregulated under white (standard warm white) light. Exposure to blue light (470, 455, 425 nm), shifted the fatty acid profiles to more saturated fatty acids (C16:1 to C16:0), which is hypothesized to render the membrane less permeable [73]. Detected by time-resolved proteomics analysis, a number of oxidative stress-related proteins including stress-related sigma factors and peroxidases where identified to be upregulated under white light illumination.

3.2 Full length publications

Optimization of *Rhodococcus erythropolis* JCM3201^T Nutrient Media to Improve Biomass, Lipid, and Carotenoid Yield Using Response Surface Methodology

microorganisms

MDPI

Article

Optimization of *Rhodococcus erythropolis* JCM3201^T Nutrient Media to Improve Biomass, Lipid, and Carotenoid Yield Using Response Surface Methodology

Selina Engelhart-Straub, Martina Haack, Dania Awad, Thomas Brueck * and Norbert Mehlmer *

Werner Siemens-Chair of Synthetic Biotechnology, Department of Chemistry, TUM School of Natural Sciences, Technical University of Munich, 85748 Garching, Germany

* Correspondence: brueck@tum.de (T.B.); norbert.mehlmer@tum.de (N.M.)

Abstract: The oleaginous bacterium *Rhodococcus erythropolis* JCM3201^T offers various unique enzyme capabilities, and it is a potential producer of industrially relevant compounds, such as triacylglycerol and carotenoids. To develop this strain into an efficient production platform, the characterization of the strain's nutritional requirement is necessary. In this work, we investigate its substrate adaptability. Therefore, the strain was cultivated using nine nitrogen and eight carbon sources at a carbon (16 g L^{-1}) and nitrogen (0.16 g L^{-1}) weight ratio of 100:1. The highest biomass accumulation (3.1 ± 0.14 g L^{-1}) was achieved using glucose and ammonium acetate. The highest lipid yield (156.7 ± 23.0 mg g^{-1}_{DCW}) was achieved using glucose and yeast extract after 192 h. In order to enhance the dependent variables: biomass, lipid and carotenoid accumulation after 192 h, for the first time, a central composite design was employed to determine optimal nitrogen and carbon concentrations. Nine different concentrations were tested. The center point was tested in five biological replicates, while all other concentrations were tested in duplicates. While the highest biomass (8.00 ± 0.27 g L^{-1}) was reached at C:N of 18.87 (11 g L^{-1} carbon, 0.583 g L^{-1} nitrogen), the highest lipid yield (100.5 ± 4.3 mg g^{-1}_{DCW}) was determined using a medium with 11 g L^{-1} of carbon and only 0.017 g L^{-1} of nitrogen. The highest carotenoid yield (0.021 ± 0.001 Abs_{454nm} mg^{-1}_{DCW}) was achieved at a C:N of 12 (6 g L^{-1} carbon, 0.5 g L^{-1} nitrogen). The presented results provide new insights into the physiology of *R. erythropolis* under variable nutritional states, enabling the selection of an optimized media composition for the production of valuable oleochemicals or pigments, such as rare odd-chain fatty acids and monocyclic carotenoids.

Keywords: *Rhodococcus*; response surface methodology; central composite design; media optimization; FAMEs; lipids; carotenoids

Citation: Engelhart-Straub, S.; Haack, M.; Awad, D.; Brueck, T.; Mehlmer, N. Optimization of *Rhodococcus erythropolis* JCM3201^T Nutrient Media to Improve Biomass, Lipid, and Carotenoid Yield Using Response Surface Methodology. *Microorganisms* **2023**, *11*, 2147. https://doi.org/10.3390/microorganisms11092147

Academic Editor: Hitoshi Miyasaka

Received: 3 August 2023
Revised: 17 August 2023
Accepted: 21 August 2023
Published: 24 August 2023

1. Introduction

A number of bacteria, some of which belong to the actinomycetes group, such as *Streptomyces*, *Rhodococcus*, and *Mycobacterium*, can accumulate lipids and triacylglycerols (TAG) when grown under nitrogen limitation [1]. These single-cell oils (SCOs) have the potential to serve as sustainable alternatives to fossil fuels [2]. Some bacteria can also inherently produce carotenoids. These isoprenoids range in color from yellow to red. Due to their antioxidant nature, carotenoids, which are stored in the cell membrane, play a crucial role in photo quenching and protection of the cell from photodamage. Photo-oxidative damage is dangerous for vital cellular machinery, such as DNA, lipids, and proteins. Therefore, biotic and abiotic stress triggers many organisms to accumulate carotenoids [3,4]. Carotenoids are utilized in a wide range of commercial industries, including the pharmaceutical, food, feed, and cosmetics industries [5]. The Gram-positive and aerobic bacteria of the diverse genus *Rhodococcus* offer a wide range of catabolic diversity and unique enzymatic capabilities [6,7]. Furthermore, the members of this genus can typically withstand various stress conditions, including metal toxicity and desiccation [8]. Due to this adaptability, *Rhodococcus* is a

potential producer of various products, such as biosurfactants, bioflocculants, carotenoids, triacylglycerols, and antimicrobial compounds [8]. A range of micro-organisms, including microalgae, yeast and fungi, are able to produce lipids and carotenoids in higher quantities [9,10], with each species having specific advantages and disadvantages as producers. Microalgae or cyanobacteria can use carbon dioxide as their carbon source and produce photoautotrophic lipids and carotenoids, but they also have disadvantages, such as low lipid productivity and long fermentation duration for microalgae [11], as well as low carotenoid content for cyanobacteria [12]. *Rhodococcus* strains are of high interest as robust producers, as they can be genetically modified and harbor a large set of enzyme genes. As one of the few bacterial genera, *Rhodococcus* is only able to produce monocyclic carotenoids [8]. Further, the fatty acid profile revealed the production of rare odd-chain fatty acids [13]. The heterogeneous taxon *Rhodococcus* can be grouped into seven distantly related species-groups, i.e., A–G. All *R. erythropolis* strains belong to the species group D, which further includes *R. qingshengii* and several unclassified strains [14]. To enable the industrial application of *R. erythropolis*, an efficient genome-reduction tool was recently developed to produce a genome-structure-stabilized host strain. This strain allows the removal of unfavorable genes/functions [15]. Interestingly, *R. erythropolis* was initially classified as a non-oleaginous species due to its low lipid content when grown on glucose. However, recent studies have reported that this strain can exhibit an oleaginous and robust phenotype when grown on glycerol [16,17]. The carotenoids 4-keto-γ-carotene and γ-carotene were produced by *R. erythropolis* AN12, and in other *R. erythropolis* strains additional carotenoids, such as β-carotene, lycopene, and phytoene, have been identified [18,19]. The scarce research demonstrating lipid accumulation in this bacterium, as well as the limited studies investigating its carotenoid production under different nutrient sources, underscore the pressing need for further characterization to comprehensively elucidate its biology and explore its potential for the production of vital compounds. In this work, a wide range of nitrogen and carbon sources are tested in parallel to derive direct conclusions on their influence on yield of biomass, lipids, and carotenoids. Further, changes in the fatty acid profile are analyzed, thereby allowing the identification of the most promising application.

Identifying the optimal fermentation conditions is crucial to developing cost-efficient processes, as the medium composition directly correlates to product yield and productivity. The carbon source is considered to be the most essential medium component. It serves as an energy source and, therefore, plays a vital role in regulating the growth and production of primary and secondary metabolites. However, the selection and concentration of the nitrogen source cannot be neglected [20]. Nitrogen is an essential nutrient used in the synthesis of many cell components and metabolites. In yeast, inorganic nitrogen sources are better suited to biomass accumulation, while organic nitrogen sources have been shown to improve lipid production [21,22]. The precise ratio of carbon to nitrogen in the cultivation medium is crucial to improve lipid accumulation, as it typically occurs when micro-organisms are grown in excess of carbon, while other nutrients, particularly nitrogen, are limited [23]. Since growth is restricted under limited conditions, TAG accumulation mainly occurs in the stationary phase, as TAG are efficient storage compounds [1]. The one-factor-at-a-time (OFAT) optimization approach, which is commonly used in microbial systems, is very time consuming, consisting of iterative removal, supplementation, and replacement experiments. It is also unable to consider interactions between variables [20,24]. Statistics-based response surface methodology (RSM), on the other hand, allows rapid parameter screening at a reduced cost. RSM, which is a mathematical modeling algorithm developed by Box and Wilson [25], can be used as an experimental strategy to identify optimum conditions in a multivariable system. It is an efficient optimization technique, as it reduces the cost and time required to identify optimal cultivation conditions by reducing the number of examined conditions in an experimental design. Furthermore, this method enables defining the standalone effects of independent variables on the process, as well as their interactions [26,27]. Central composite design (CCD) has previously been utilized for the media optimization of *Rhodococcus* in various contexts, such as diesel oil [28]

and aflatoxin B1 degradation [26] by *R. erythropolis*, the production of biosurfactant by *Rhodococcus* spp. MTCC2574 [29], and odd-chain fatty acid (FA) production by *Rhodococcus* sp. YHY01 [13]. CCD has not previously been used to optimize the production of lipids and carotenoids in *R. erythropolis*.

In the presented data, media optimization to increase biomass, lipid, and carotenoid accumulation of *R. erythropolis* JCM3201^T was performed via a threefold method: sequential investigation of nine distinct nitrogen sources and eight selected carbon sources was followed by the optimization of the carbon-to-nitrogen ratio via a circumscribed and rotatable CCD. The results shed light on the growth characteristics and FA profile of *R. erythropolis*, with the aim being to facilitate future studies of its use as a secondary metabolite producer.

2. Materials and Methods

2.1. Bacterial Strain and Inoculum Preparation

R. erythropolis JCM3201^T (DSM No. 43066, German Collection of Micro-Organisms and Cell Cultures GmbH, Braunschweig, Germany) was maintained using Luria–Bertani (LB) agar plates (10 g L^{-1} of peptone, 5 g L^{-1} of yeast extract, 10 g L^{-1} of sodium chloride, and 14 g L^{-1} of agar). For inoculum, single colonies were cultured in 500-milliliter baffled shake flasks holding 100 mL of LB medium at 120 rpm (New Brunswick InnovaTM 44, Eppendorf, Hamburg, Germany) for 48 h. Afterward, the inoculum was transferred to prospective optimization media.

2.2. Cultivation Medium

All cultures were cultivated in 500-milliliter baffled shake flasks holding 100 mL of '457. Mineral Medium' (Brunner, DSMZ, Braunschweig, Germany). As a cultivation medium, '457. Mineral Medium' (Brunner, DSMZ)) [30] (pH 6.9) was used, which contained 2.44 g L^{-1} of Na_2HPO_4, 1.52 g L^{-1} of KH_2PO_4, 0.20 g L^{-1} of $MgSO_4 \times 7\ H_2O$, 0.05 g L^{-1} of $CaCl_2 \times 2\ H_2O$, and 10 mL of trace element solution SL-4. Trace element solution SL-4 contained 0.50 g L^{-1} of EDTA, 0.20 g L^{-1} of $FeSO_4 \times 7\ H_2O$, and 100 mL of trace element solution SL-6. Trace element solution SL-6 contained 0.10 g L^{-1} of $ZnSO_4 \times 7\ H_2O$, 0.03 g L^{-1} of $MnCl_2 \times 4\ H_2O$, 0.30 g L^{-1} of H_3BO_3, 0.20 g L^{-1} of $CoCl_2 \times 6\ H_2O$, 0.01 g L^{-1} of $CuCl_2 \times 2\ H_2O$, 0.02 g L^{-1} of $NiCl_2 \times 6\ H_2O$, and 0.03 g L^{-1} of $Na_2MoO_4 \times 2\ H_2O$. Carbon and nitrogen sources were individually selected for each experiment.

2.3. Experimental Design

Media optimization was divided into three stages, with the first and second stages investigating various nitrogen and carbon sources using an OFAT strategy. Nitrogen sources encompassed ammonium chloride, diammonium hydrogen phosphate, ammonium sulfate, potassium nitrate, ammonium nitrate, yeast extract, tryptone/peptone, urea and ammonium acetate (Table 1). Based on the supplier's information (Carl Roth, Karlsruhe, Germany), yeast extract and tryptone/peptone contained 10.8% (*w*/*w*) and 12.3% (*w*/*w*) nitrogen, respectively. To examine the effect of the nitrogen source on growth, a medium, which contained 40 g L^{-1} of glucose (16 g L^{-1} carbon) and 0.16 g L^{-1} of nitrogen, was used. Carbon sources encompassed glucose, galactose, fructose, lactose, sucrose, maltose, sorbitol, and glycerol (Table 1). For the screening of carbon sources, cultivation was carried out in media using the optimal nitrogen source, as observed in the previous stage of optimization, which was ammonium acetate. For each nitrogen and carbon source, biological triplicates were prepared. Each culture was inoculated to OD_{600nm} 0.2 and cultivated at 28 °C and 120 rpm for 192 h.

Following the RSM strategy, different carbon-to-nitrogen concentrations and ratios were assessed. Subsequently, the effect of varying carbon-to-nitrogen sources on the growth, as well as lipid and carotenoid production of *R. erythropolis*, was compared. A total of 9 different carbon-to-nitrogen ratios were tested using a CCD. Concentrations ranged from 3.93 to 18.07 g L^{-1} elemental carbon and 0.02 to 0.58 g L^{-1} elemental nitrogen, with

glucose and ammonium acetate used the as carbon and nitrogen sources, respectively. Carbon-to nitrogen ratios ranged from 12:1 to 647:1. For the center point (11 g L^{-1} of carbon and 0.3 g L^{-1} of nitrogen), five biological replicates were prepared; all other ratios were prepared in biological duplicates. Each culture was analyzed in two technical replicates. Cultures were inoculated to OD_{600} 0.2 and then cultivated for 192 h (28 °C, 120 rpm).

Table 1. Matrix of tested nitrogen and carbon sources, as well as their chemical nature.

Number	Nitrogen Source	Chemical Nature	Carbon Source	Chemical Nature
1	Ammonium chloride	Defined inorganic	Glucose	Monosaccharides
2	Diammonium hydrogen phosphate		Galactose	
3	Ammonium sulfate		Fructose	
4	Potassium nitrate		Lactose	Disaccharides
5	Ammonium nitrate		Sucrose	
6	Yeast extract	Complex organic	Maltose	
7	Tryptone/peptone		Sorbitol	Sugar alcohol
8	Urea	Defined organic	Glycerol	
9	Ammonium acetate			

2.4. Growth Analysis

Optical density was measured at 600 nm using a photometer (Nano Photometer NP80, IMPLEN, Munich, Germany). Standard semi-micro cuvettes made of polystyrene were used, and each cuvette had a path length of 10 mm.

For dry cell weight (DCW) analysis, 30 mL of culture was sampled after 140 and 192 h. For the CCD, 30 mL of culture was divided into two pre-weighed falcon tubes. Cultures were centrifuged (3500× *g*, 5 min), and the cells were washed using bidistilled water and lyophilized (−80 °C, ≥72 h). After gravimetric measurements, the weight of the empty vessels was subtracted from that of vessels containing lyophilized biomass.

2.5. Carotenoid Extraction

Carotenoid extraction from dry biomass was carried out as previously shown [31]. Depending on availability, between 2 and 10 mg biomass was weighed into 1.5-milliliter Eppendorf tubes. In brief, pigments were extracted using acetone after cell disruption via glass beads (2 mm). The absorbance at 454 nm was measured using a Nano Photometer NP80 (IMPLEN, Munich, Germany), and the titer calculated according to Formula (1).

$$\text{Carotenoid titer } (Abs_{454nm}\ mg^{-1}{}_{DCW}) = \text{Absorbance } (Abs_{454nm})/\text{Dry Biomass (mg)} \quad (1)$$

2.6. Fatty Acid Profile

FA analysis was carried out according to the method described by Engelhart-Straub et al. [31]. In brief, lipids extracted from biomass were converted into fatty acid methyl ester (FAME) via MultiPurposeSampler MPS robotic (Gerstel, Linthicum Heights, MD, USA). FAMEs were measured via gas chromatography (GC-2025 coupled to an AOC-20i auto-injector and an AOC-20s auto-sampler, Shimadzu, Duisburg, Germany) and equipped with a flame ionization detector. For separation, a Zebron ZB-wax column (30 m × 0.32 mm, film thickness 0.25 µm, Phenomenex, Aschaffenburg, Germany) was used. The external standards, namely Marine Oil FAME mix (20 components from C14:0 to C24:1; Restek GmbH, Bad Homburg, Germany) and FAME #12 mix (C13:0, C15:0, C17:0, C19:0, and C21:0; Restek GmbH, Bad Homburg, Germany), were utilized for the identification and quantification of FAMEs. Normalization was based on the internal methyl laurate standard (C12; Restek GmbH, Bad Homburg, Germany).

For the identification of branched FA, GC–MS was performed using a Thermo Scientific™ TRACE™ Ultra Gas Chromatograph instrument coupled with a Thermo DSQ™ II

mass spectrometer and a Triplus™ Autosampler injector. For this analysis, a BPX5 column (30 m × 0.25 mm, film thickness of 0.25 µm) acquired from von Trajan Scientific Australia Pty Ltd. (Ringwood, Victoria, Australia) was used. The separation was performed at an initial column temperature of 50 °C, which increased at a rate of 4 °C min^{-1} up to a final temperature of 250 °C. The used carrier gas was hydrogen at a constant flow rate of 0.8 mL min^{-1}.

2.7. Response Surface Methodology and Further Statistical Analysis

Design-Expert Software, Version 22.0.2 (Stat-Ease, Inc., Minneapolis, MN, USA) was adopted for the design and analysis of the media optimization. A full central composite design with eight non-center points in duplicates and five center points, as well as an alpha value of 1.41421, was performed. The range of values is listed in Table 2. The analysis of variance (ANOVA) was used to estimate the appropriate statistical parameter and evaluate the suitability of the design. The effects of carbon and nitrogen levels on the level of the dependent variables—biomass (g L^{-1}), lipid content (mg g^{-1}_{DCW}) and carotenoid titers (Abs_{454nm} mg^{-1}_{DCW})—were analyzed. Non-significant terms not needed for hierarchy were excluded from the model.

Table 2. Range of values for central composite design.

Variable	Level				
	−1.414	**−1**	**0**	**+1**	**+1.414**
Carbon (g L^{-1})	3.929	6	11	16	18.071
Nitrogen (g L^{-1})	0.017	0.1	0.3	0.5	0.583

3. Results and Discussion

3.1. Effect of Different Nitrogen Sources on Biomass, Lipid, and Carotenoid Formation of R. erythropolis

To determine the appropriate carbon and nitrogen concentrations and assess the effects of different carbon and nitrogen sources on *R. erythropolis*, a full central composite design-based DOE (design of experiment) analysis was performed. Glucose was selected as the carbon source, and ammonium sulfate was used as the nitrogen source. While increasing the carbon and nitrogen concentrations resulted in increased biomass formation, a low nitrogen concentration induced increased lipid production. To produce a significant amount of biomass while retaining nitrogen limitation at a later point in the cultivation, a C:N of 100:1, with 16 g L^{-1} of carbon and 0.16 g L^{-1} of nitrogen, was used for the following experiments, in which the effects of different nitrogen and carbon sources on *R. erythropolis* were examined.

This study examined nine distinct nitrogen sources, including ammonium chloride, diammonium hydrogen phosphate, ammonium sulfate, potassium nitrate, and ammonium nitrate, as defined inorganic sources. Yeast extract and tryptone/peptone were used as complex organic sources, in addition to urea and ammonium acetate, which were used as defined organic sources (Figure 1).

The cultivation proceeded for eight days under identical conditions, which allowed direct comparison. Yields of biomass, lipids, and carotenoids were determined after 140 and 192 h, as two timepoints enable a more detailed assessment of the differences between the cultures. Cultures containing any of the five defined inorganic sources exhibited slow growth at the beginning (Figure 1a). When inorganic nitrogen was used as nitrogen source, compared to complex sources, the micro-organism needed additional energy to perform amino acid synthesis [27]. The lowest biomass accumulation was achieved for potassium nitrate as the nitrogen source, with a DCW of 0.36 ± 0.08 g L^{-1} after 192 h. In contrast, a strain identified as *Rhodococcus* sp. BCH2 showed the highest growth on potassium nitrate, which was comparable to that of ammonium acetate [32]. The complex nitrogen sources' yeast extract and tryptone/peptone showed the fasted growth from the start of the cultiva-

tion with no detectable lag phase. Complex nitrogen sources provide additional nutrients, including amino acids, polypeptides, vitamins, and trace elements. Increased yield of biomass with complex nitrogen sources was achieved for a variety of micro-organisms, including *C. oleaginosus* and *A. oryzae* [27,33]. When cultivating the *R. erythropolis* strains MTCC1548, 2794, and 3951 using different nitrogen sources, inorganic nitrogen sources (ammonium sulfate and ammonium phosphate), as well as urea, resulted in very low biomass compared to complex organic nitrogen sources (yeast extract and meat peptone) [29]. In this study, *R. erythropolis* cultures, which contained the two aforementioned complex nitrogen sources, entered the stationary phase after approximately 115 h (Table S5). After 140 h, a DCW of 2.13 ± 0.07 g L^{-1} for yeast extract and 1.88 ± 0.03 g L^{-1} for tryptone/peptone was determined, with a decreased DCW after 192 h. The higher yield of the biomass when using yeast extract could be related to its high vitamin content relative to tryptone/peptone [34]. The final group of assessed nitrogen sources comprised defined organic sources in the form of urea and ammonium acetate. While urea induced an extended lag phase within the first 120 h, cultures with ammonium acetate exhibited a steady growth over 192 h and no lag phase. The highest biomass was achieved when ammonium acetate was used as the nitrogen source with a DCW of 2.84 ± 0.02 g L^{-1} after 192 h.

Since biomass productivity was the primary goal of these cultivations, an increased nitrogen content of 0.16 g L^{-1} was selected, leading to a lipid content of 5 to 16% in *R. erythropolis* after 192 h. The lipid content for all distinct nitrogen sources, except for potassium nitrate, increased between 140 and 192 h (Figure 1c). The highest lipid yield was determined for cultures grown using the complex nitrogen sources yeast extract and tryptone/peptone, which registered 156.7 ± 23.0 mg g^{-1}_{DCW} and 132.3 ± 15.4 mg g^{-1}_{DCW} after 192 h, respectively. As TAG accumulation primarily occurs in the stationary phase [1] and cultures grown on complex nitrogen sources entered the stationary phase after 115 h, a sufficient time period for lipid accumulation was allowed. In contrast, *R. erythropolis* exhibited a longer lag phase when grown using the five defined inorganic nitrogen sources, having a lipid content of 5–5.5% (g g^{-1}_{DCW}) after 192 h. Cultures grown on potassium nitrate showed a higher lipid content after 140 h, i.e., 10.5% (g g^{-1}_{DCW}). Inefficient utilization of this compound could potentially induce nitrogen limitation in these cultures during the early cultivation phase, which could explain the elevated lipid yield after 140 h. Cultures grown using ammonium acetate showed the highest DCW, having a lipid content of 68.3 ± 5.0 mg g^{-1}_{DCW} after 192 h. In *R. toruloides*, organic nitrogen sources also led to increased lipid contents compared to inorganic nitrogen sources [35].

When *R. opacus* PD630 was grown using waste paper hydrolysate, the inorganic nitrogen sources ammonium chloride, followed by ammonium sulfate, gave the highest biomass and lipid yield, having a lipid content of around 25% after 120 h. When grown using the complex nitrogen sources urea, yeast extract, and peptone, biomass and lipid accumulation was lower. The lipid content of cultures grown using urea (15.24%) was reported to be three-fold higher than that of cultures grown using yeast extract (5.69%) and peptone (4.34%) [2]. These results are in contrast to the presented data in this study. One reason for this outcome could be the utilization of the complex carbon source waste paper hydrolysate, which offers a wide range of readily metabolizable ammonia acids, polypeptides, nucleotides, various vitamins, and trace elements. Therefore, the advantage of a complex nitrogen source, like yeast extract or tryptone/peptone, could be masked, as these substances are already available. Furthermore, *R. opacus* generally produces higher amounts of TAGS than *R. erythropolis* while cultivated using sugars, organic acids, and hydrocarbons [8].

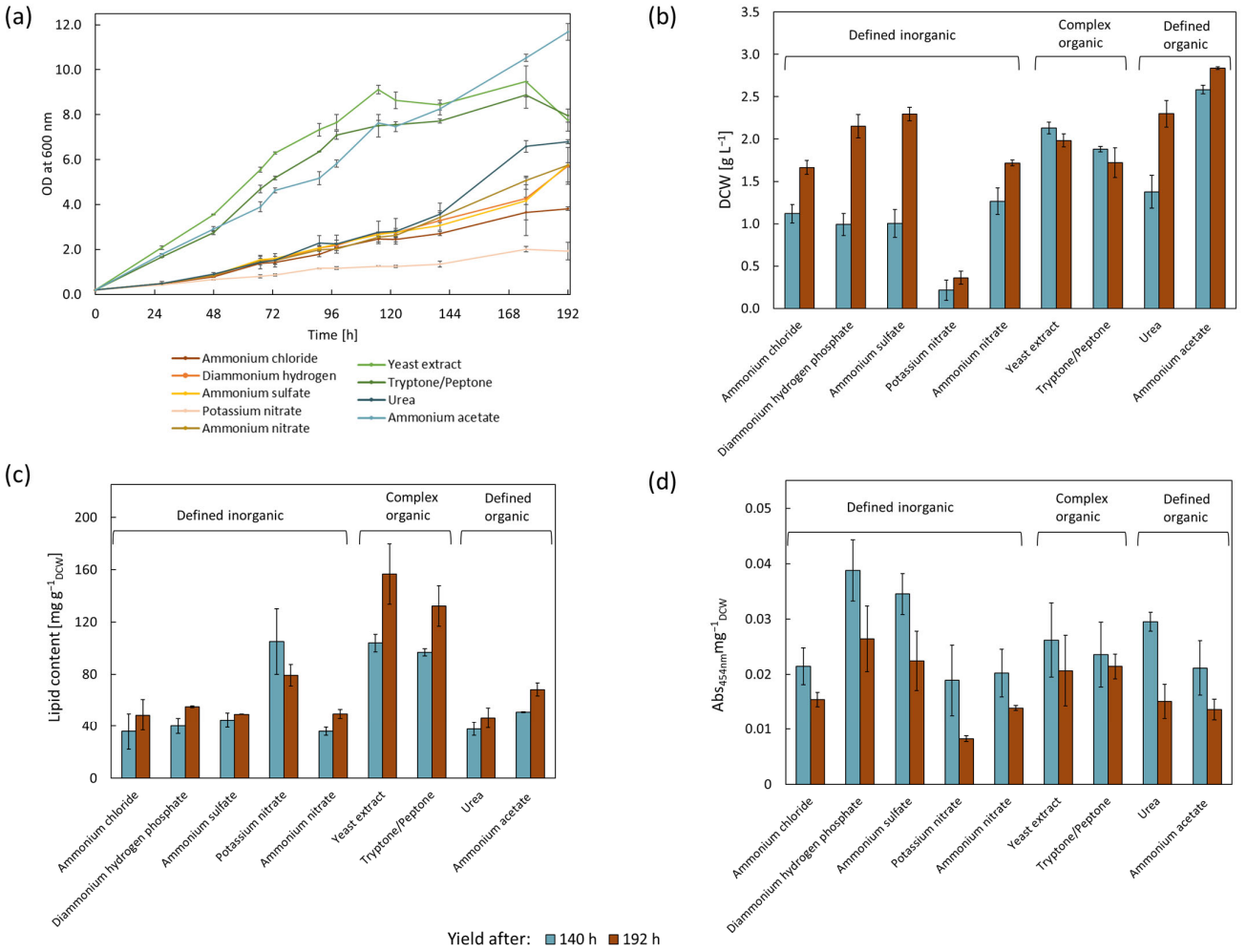

Figure 1. Effects of various nitrogen sources on growth curves, as well as biomass, lipid, and carotenoid accumulation of *R. erythropolis* after 140 and 192 h. Yield after 140 h is depicted in blue, and yield after 192 h is depicted in red. Samples were cultured using variable nitrogen sources at a nitrogen concentration of 0.16 g L^{-1} (C:N of 100, 16 g L^{-1} of carbon in the form of glucose), $n = 3$. (**a**) Cell growth measured as OD at 600 nm over 192 h. (**b**) Dry cell weight (DCW) at 140 and 192 h. (**c**) Lipid content (normalized to DCW) at 140 and 192 h. (**d**) Carotenoid accumulation (normalized to DCW) at 140 and 192 h.

The effect of different nitrogen and carbon sources on carotenoid accumulation in *R. erythropolis* has not previously been investigated. The carotenoid content of all cultures was assessed after 140 and 192 h (Figure 1d), with decreasing carotenoid contents recorded over this time period in all cultures. The highest carotenoid content was achieved when diammonium hydrogen phosphate (0.039 ± 0.006 $Abs_{454nm}mg^{-1}{}_{DCW}$) was used as a nitrogen source, followed by ammonium sulfate. Cultures grown using ammonium chloride, potassium nitrate, ammonium nitrate, and ammonium acetate produced similar amounts of carotenoids after 140 h, having an absorbance of between 0.019 and 0.021 $Abs_{454nm}mg^{-1}{}_{DCW}$. Temperature, pH, and carbon and nitrogen sources affect carotenoid production in micro-organisms [3,36,37]. *Rhodotorula glutinis* produced the highest amount of carotenoid using ammonium sulfate as nitrogen source, followed by yeast extract and peptone [34]. In contrast, for *Rhodotorula* sp. RY1801, the highest carotenoid production was achieved using yeast extract, followed by urea and ammonium sulfate. When ammonium nitrate was used as nitrogen source, the lowest carotenoid production was determined [36]. While the highest growth of the bacterium *Sphingobium* sp. was detected using diammonium hydrogen phosphate, complex nitrogen sources, like tryptone, soya

peptone, and okara, were found to be the best options for the production of the carotenoid nostoxanthin [38]. The fungi *Umbelopsis ramanniana* produces, using diammonium hydrogen phosphate and the carbon source maltose, the highest amount of carotenoids compared to other nitrogen sources, while using the carbon source glucose, the lowest amount of carotenoids is produced [39]. Urea increased the production of total carotenoids and, in particular, β-carotene in *Flavobacterium multivorum*, likely by inhibiting hydroxylase activity, thereby decreasing the production of zeaxanthin [40]. While some studies indicated higher carotenoid yields using organic nitrogen sources, this finding could not be observed in *Microbacterium paraoxydans* or in the presented data in this study [38,41].

3.2. Effect of Different Carbon Sources on Biomass, Lipid, and Carotenoid Formation by R. erythropolis

For the evaluation of different carbon sources, ammonium acetate was selected as the nitrogen source due to the resulting highest achieved biomass accumulation and relatively high lipid yields. A defined nitrogen source offers the advantage of a controlled medium composition; therefore, possible fluctuations can be directly traced to the carbon source. Eight carbon sources were examined in this work, including glucose, galactose, and fructose, as monosaccharides/hexose. Lactose, sucrose, and maltose were included as disaccharides. Moreover, the sugar alcohol sorbitol and glycerol were examined (Figure 2). The latter element represents an interesting carbon source; as the main by-product of biodiesel production, it has a low cost and is readily available [16,42].

The cultivation proceeded for eight days under identical conditions of 16 g L^{-1} of carbon and 0.16 g L^{-1} of nitrogen in the form of ammonium acetate, resulting in a C:N of 100. No growth in *R. erythropolis* was detected for arabinose and xylose, which is congruent with other *Rhodococcus* strains. However, xylose, as well as arabinose utilization, was achieved via genetic engineering in *R. opacus* PD630 and *R. jostii* [43–46]. Xylose assimilation capabilities enable the efficient utilization of cellulose and hemicellulose degradation products [47], such as wheat bran hydrolysate [48] or corn stover hydrolysate [49]. Very low growth with final biomasses of under 0.5 g L^{-1} were determined for cultures with galactose, lactose, and maltose. The inability to grow on galactose and lactose was reported in other *Rhodococcus* strains, such as *R. jostii*, *R. erythropolis*, *R. fascians*, and *R. equi* [50]. The only strain capable of growth on these carbon sources was *R. opacus* [50], which is also reported to grow on maltose [51]. Further, *R. erythropolis* ZJB-09149 could grow using maltose, as well as lactose [52]. When fructose was used as a carbon source in this study, the fastest growth was measured for the first 48 h, after which point the stationary phase was entered. When grown using the two sugar alcohols sorbitol and glycerol, the strain entered the stationary phase two days later at around 94 h. For cultures grown using the disaccharide sucrose, the stationary phase also started after 94 h, with a final DCW of 247; ±, 022; g, L^{-1}, noted after 192 h. The highest yield of biomass was achieved using glucose as a carbon source, with a DCW of 3.1 ± 0.14 g L^{-1} noted after 192 h. Interestingly, the stationary phase of cultures grown using glucose was not reached before 164 h, which was later than all other investigated carbon sources. When grown using different carbon sources, *R. erythropolis* strains MTCC1548, 2794, and 3951 showed distinct differences. While MTCC1548 grew best using glucose as carbon source, followed by glycerol, sucrose, and sorbitol, MTCC2794 and MTCC3951 showed the highest growth using sucrose, followed by sorbitol, glucose, and glycerol. Using glucose, MTCC2794 grew to around double the OD_{600} values of MTCC1548 and MTCC3951 [29]. When *R. erythropolis* LSSE8-1 was grown using different carbon sources, the highest OD_{600} was determined for glycerol, followed by sucrose and glucose, which is in reverse order to the growth investigated in this work [53]. The varying growth behaviors of *R. erythropolis* strains further emphasize the heterologous nature of these different strains.

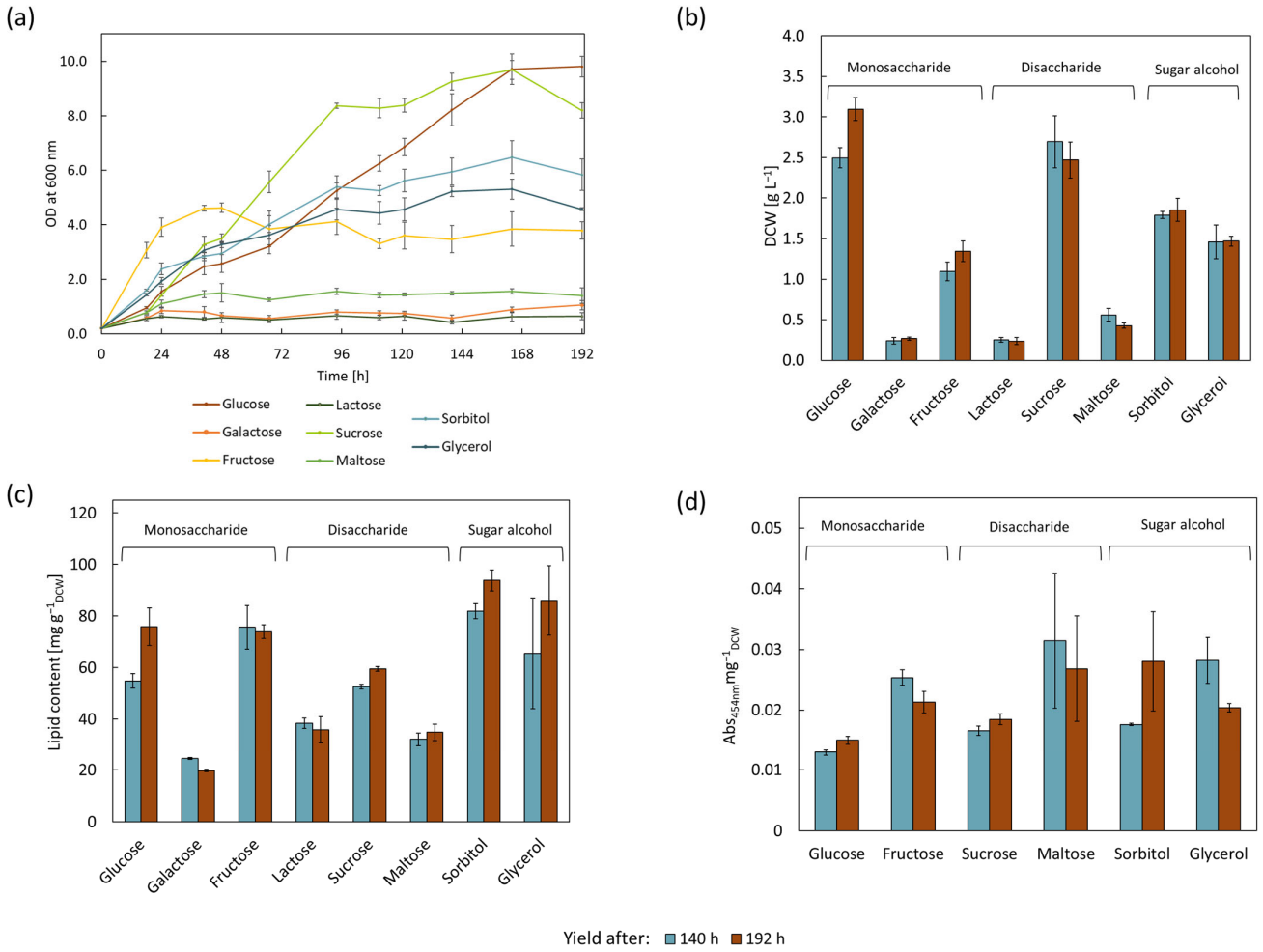

Figure 2. Effect of various carbon sources on growth, lipid, and carotenoid accumulation of *R. erythropolis* after 140 and 192 h of being cultured in parallel with carbon concentration of 16 g L^{-1}, holding all other conditions to be identical (C:N of 100, 0.16 g L^{-1} of nitrogen in the form of ammonium acetate), n = 3. Yield after 140 h is depicted in blue, and yield after 192 h is depicted in red. (**a**) Growth measured as OD at 600 nm over 192 h. (**b**) Dry cell weight (DCW) at 140 and 192 h. (**c**) Lipid content (normalized to DCW) at 140 and 192 h. (**d**) Carotenoid accumulation (normalized to DCW) at 140 and 192 h. No carotenoid extraction was performed for galactose and lactose due to a lack of sufficient biomass formation.

The lowest lipid contents ($\leq$3.6%) were measured for the cultures with galactose, lactose, and maltose, which also exhibited the lowest growth. Due to the low growth and, therefore, low consumption of nutrients, nitrogen limitation was presumably not reached. In comparison, fructose and glucose accumulated over double the amount of lipid. The highest lipid content was determined for the cultures grown using the sugar alcohols sorbitol and glycerol, which registered values of 93.8 $\pm$ 4.1 mg g^{-1}_{DCW} and 86.1 $\pm$ 13.4 mg g^{-1}_{DCW} after 192 h, respectively. Cortes et al. examined the effects of various carbon sources on the lipid accumulation in *R. erythropolis* DCL12 and *R. opacus* PWD14 cells. The experimental setup incorporated 0.01 g L^{-1} of nitrogen, and an excess of carbon (2 g L^{-1} of glucose) was used. *R. erythropolis* accumulated 78.71% (g g^{-1}_{DCW}) lipids in the stationary phase [54]. *R. erythropolis* IGTS8, when grown using 30 g L^{-1} of glycerol and 0.75 g L^{-1} of urea as carbon and nitrogen source, produced lipid content of 45.8% in 96 h [55].

Insufficient amounts of biomass were available to determine the carotenoid content of cultures grown using galactose and lactose. The highest carotenoid contents after 140 h

were measured in cultures grown using maltose and glycerol, followed by fructose. The lowest carotenoid content was determined for cultures using glucose, with only around half of the carotenoids compared to the former. While *R. mucilaginosa* grew the fastest in the glucose medium, the highest carotenoid concentration was measured in the sucrose molasses-containing medium. The highest product yield was obtained using whey lactose as the carbon source [37]. This result is in agreement with those of *Phaffia rhodozyma* strains, which showed increased carotenoid production when using xylose, followed by sucrose, rather than glucose, as the carbon source [56]. In contrast, glucose was determined to be the most suitable carbon source for the production of carotenoids in *Rhodotorula* sp. RY1801, followed by fructose. Sucrose, lactose, and maltose showed comparable levels of carotenoid production [36]. *Umbelopsis ramanniana* produced the highest carotenoid amount with maltose used as the carbon source, followed by lactose and glucose [39].

In previous studies, it was demonstrated that *Rhodococci* can grow on various waste stream hydrolysates, ranging from sugar cane molasse, orange waste, and olive mill waste to cellulosic feedstocks [42], rendering them potent organisms for use in sustainable industrial processes. The data presented here regarding the bacterium's behavior in a wide range of carbon and nitrogen sources offer a valuable resource for the identification of suitable and cost-effective growth media.

3.3. Effect of Nitrogen and Carbon Sources on the Fatty Acid Profile of R. erythropolis

The FA composition of *R. erythropolis* is heavily influenced by the cultivation conditions, including the carbon and nitrogen source, as well as the pH-value, temperature, and aeration [42]. FA represent an essential part of the phospholipid bilayer of the cellular membrane [57], which allows bacteria to adapt their lipid composition to maintain membrane fluidity and permeability in response to various stress conditions [58,59]. Bacteria of the actinomycetes group store large amounts of TAGs in lipid bodies. During lipid biosynthesis, an oleaginous layer is formed at the cytoplasm membrane, followed by the subsequent formation of lipid pre-bodies, which are finally released as mature lipid bodies in the cytoplasm [60].

The relative quantification of FAs is depicted as the percentage of total FAs (*w*/*w*) (Figure 3). Independent of the nitrogen or carbon source, the main components of the FA profile of *R. erythropolis* are palmitic acid (C16:0), 10-methyl octadecanoic acid (10-Me-18:0), myristic acid (C14:0), and oleic acid (C18:1). 10-Me-18:0 is a fully saturated and long-chain FA, which is characterized by a low melting temperature and high oxidative stability [61]. It occurs naturally in the membrane of a variety of actinobacteria [62]. In previous studies, 10-methyl octadecanoic acid was determined in *R. erythropolis* 3C-9 and DSM 43066 [63–65]. Tsitko et al. (1999) observed an increase of up to 34% of branched fatty acids (BFAs) of total FAs in *R. opacus* when cultivated using aromatic compounds. The role of 10-Me-18:0 in the protection of the membrane–cell wall structure against disruption was suggested [66].

The FA contents of all cultures grown using different nitrogen sources (Figure 1c), with the exception of cultures grown using potassium nitrate, increased between the samples taken after 6 (140 h) and 8 days (192 h). While the contents of palmitoleic acid (C16:1) decreased in all samples over time, the contents of palmitic acid (C16:0) increased in all samples, with exception of potassium nitrate, up to 34.1% in cultures grown using yeast extract and tryptone/peptone. Both nitrogen sources are associated with minimal differences between the two timepoints, i.e., 140 and 192 h. A distinct decrease in 10-methyl octadecanoic acid (10-Me-C18:0) was measured in samples grown using yeast extract (11.5%), tryptone/peptone (12.2%), and ammonium acetate (16.3%). In all other samples, contents of over 20% of this FA were determined. These three carbon sources also produced the highest contents of oleic acid (C18:1) and stearic acid (C18:0). Palmitic acid (C16:0) and oleic acid (C18:1) have been reported to be the main FAs in oleaginous *Rhodococci*, which produce high amounts of TAGs (50–75% $g_{lipid}\ g^{-1}{}_{DCW}$) [42].

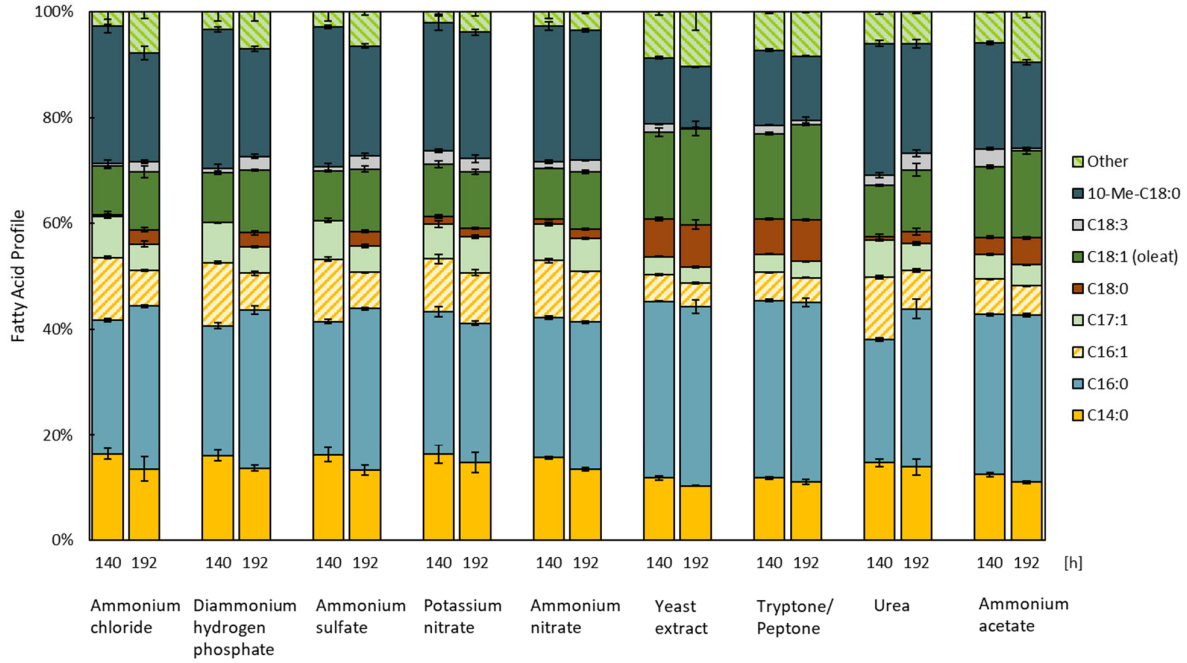

Figure 3. Fatty acid profiles of *R. erythropolis* grown using distinct nitrogen sources (n = 3). "Other" constitutes fatty acids with a total fatty acid content of representation below 3% (w/w) and includes C14:1, C15:0, C17:0, 14-Methyl-C16:0, C20:1, C20:3, C20:5, and C22:1. For each group, the two timepoints—140 h (left) and 192 h (right)—are depicted.

The FA profile of cultures grown using distinct carbon sources were also compared (Figure 4). Distinct FA profiles were determined for cultures grown on lactose and maltose. Between 33 and 38% of the profile was identified as 10-methyl octadecanoic acid (10-Met-C18:0), more than double the amounts compared to the cultures using glucose, fructose or glycerol. Galactose, lactose, and maltose not only sustained reduced biomass, but also resulted in low levels of oleic acid (C18:1) ($\leq$7.8%) and stearic acid (C18:0) ($\leq$2.2%).

When comparing the FA profiles of cultures grown using glucose and glycerol as carbon sources, cultures cultivated using glycerol exhibited an increased amount of oleic acid (C18:1; 15.1 compared to 20.6%) and a decreased amount of 10-methyl octadecanoic acid (10-Me-C18:0; 15.7 compared to 11.9%). These findings are in line with those of Bhatia et al. (2019), who identified distinct FA profiles of three different *Rhodococcus* sp. species (YHY01, 1918, and 19938) grown using these carbon sources [13].

Odd-chain fatty acids (OCFA) are commercially important products due to their antifungal, anti-allergic, and anti-inflammatory properties [13,67,68]. Microbial oil typically comprises very low OCFA content [13,69], while *Rhodococcus* has the ability to accumulate high OCFA content, mainly pentadecanoic acid (C15:0) and heptadecanoic acid (C17:0). In *Rhodococcus* sp. YHY01, a maximum proportion of 85% w/w of all FA were identified as OCFA when cultivated using a mixture of glycerol, propionate, and ammonium chloride [13]. An increased amount of pentadecanoic acid (C15:0) could also be measured in cultures cultivated using sorbitol (2.4%) and glycerol (3.1%). Elevated amounts of heptadecenoic acid (C17:1) were determined in cultures cultivated using lactose (6.4%) and maltose (9.3%) compared to other carbon sources evaluated in this work.

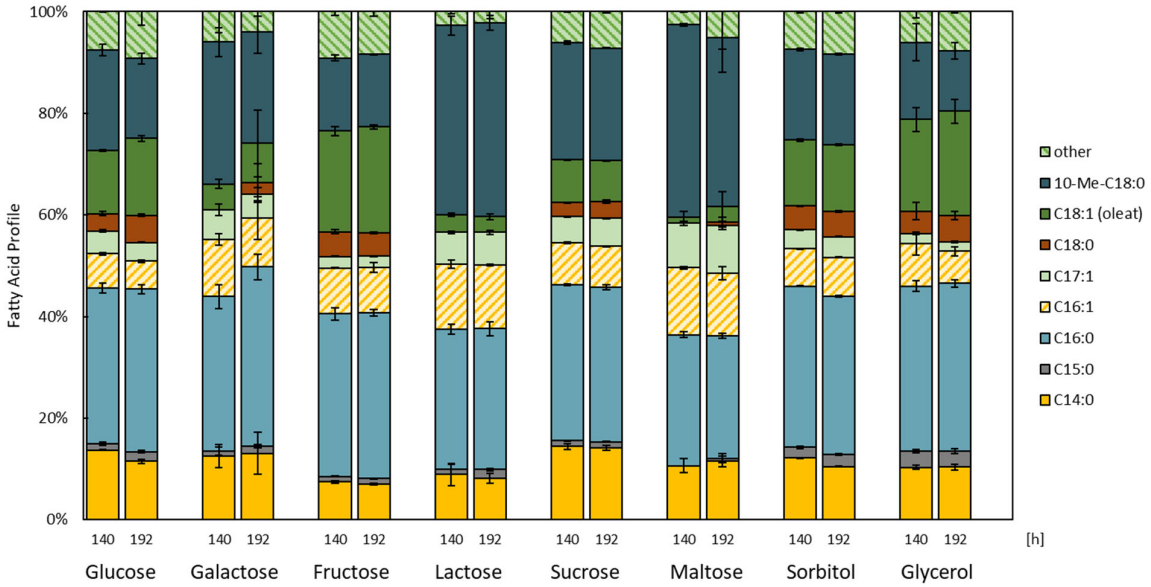

Figure 4. Fatty acid profiles of *R. erythropolis* grown using distinct carbon sources (n = 3, except for Maltose after 192 h, where n = 2, as one sample was excluded as an outlier). "Other" constitutes fatty acids with a total fatty acid content representation of below 3% (w/w) and includes C14:1, C17:0, 14-Methyl-C16:0, C18:3, C20:1, C20:3, C20:5, and C22:1, among others. For each group, the two timepoints—140 h (left) and 192 h (right)—are depicted.

3.4. RSM Model: Effect of Nitrogen and Carbon Concentrations on Biomass, Lipid and Carotenoid Formation of R. erythropolis

As a final step, the effects of a wide range of carbon and nitrogen concentrations on biomass accumulation, as well as lipid and carotenoids production, in *R. erythropolis* was assessed for the first time. To meet this goal, a full central composite design-based DOE (design of experiment) analysis was performed. For the CCD setup, glucose was selected as the carbon source, as the highest biomass was achieved with it (Figure 2). Good growth of *Rhodococcus* strains on glucose is well reported in the literature [70–72]. Ammonium acetate was used as the most promising nitrogen source. A C:N range of 12 to 160 was assessed, with a maximal C:N of 647 being part of the star points. The CCD design matrix, as well as the corresponding response on the dependent factors: biomass, lipid, and carotenoid contents, are illustrated in Table 3.

The fitted regression equations for the CCD model are represented below

$$\text{Biomass-140 h (g L}^{-1}) = -0.145 + 0.076\ \text{C} + 7.195\ \text{N} \quad (2)$$

$$\text{Biomass-192 h (g L}^{-1}) = 1.228 - 0.059\ \text{C} + 5.207\ \text{N} + 0.588\ \text{C} \times \text{N} \quad (3)$$

$$\text{Lipid-140 h (mg g}^{-1}{}_{\text{DCW}}) = 34.867 + 1.608\ \text{C} - 99.460\ \text{N} - 4.281\ \text{C} \times \text{N} + 192.195\ \text{N}^2 \quad (4)$$

$$\text{Lipid-192 h (mg g}^{-1}{}_{\text{DCW}}) = 76.816 + 0.946\ \text{C} - 300.836\ \text{N} + 343.229\ \text{N}^2 \quad (5)$$

$$\text{Carotenoide-140 h (Abs}_{454\text{nm}}\ \text{mg}^{-1}{}_{\text{DCW}}) = 0.019 - 0.0002\ \text{C} - 0.016\ \text{N} + 0.001\ \text{C} \times \text{N} \quad (6)$$

$$\text{Carotenoide-192 h (Abs}_{454\text{nm}}\ \text{mg}^{-1}{}_{\text{DCW}}) = 0.015 - 0.0002\ \text{C} + 0.024\ \text{N} - 0.025\ \text{N}^2 \quad (7)$$

Table 3. Full central composite design for the optimization of carbon and nitrogen concentrations in the cultivation media of *R. erythropolis*. C:N ratio, with C (carbon concentration) and N (nitrogen concentration), as well as the determined biomass, lipid, and carotenoid contents after 140 and 192 h, are listed. Each run was analyzed in two technical replicates. Due to technical complications, results of Run 13 represent one biological sample.

Run	C:N	C $g\ L^{-1}$	N $g\ L^{-1}$	Biomass $g\ L^{-1}$	Lipid Content $mg\ g^{-1}_{DCW}$	Carotenoid Content $Abs_{454nm}\ mg^{-1}_{DCW}$	Biomass $g\ L^{-1}$	Lipid Content $mg\ g^{-1}_{DCW}$	Carotenoid Content $Abs_{454nm}\ mg^{-1}_{DCW}$
				140 h			192 h		
1	60.00	6.000	0.100	1.44	26.90	0.0192	1.72	43.89	0.0159
2	60.00	6.000	0.100	1.23	25.86	0.0175	1.78	40.79	0.0148
3	160.00	16.000	0.100	1.74	41.83	0.0156	1.94	63.19	0.0156
4	160.00	16.000	0.100	1.73	40.09	0.0146	2.12	65.65	0.0133
5	12.00	6.000	0.500	3.21	30.61	0.0124	4.82	22.34	0.0206
6	12.00	6.000	0.500	3.48	30.26	0.0146	4.60	24.36	0.0207
7	32.00	16.000	0.500	4.02	28.18	0.0165	7.43	28.09	0.0186
8	32.00	16.000	0.500	5.12	27.60	0.0156	7.25	25.14	0.0183
9	13.10	3.929	0.300	2.49	27.11	0.0134	3.66	22.01	0.0186
10	13.10	3.929	0.300	2.33	26.76	0.0154	3.45	21.34	0.0202
11	60.24	18.071	0.300	3.19	28.53	0.0238	4.53	29.71	0.0164
12	60.24	18.071	0.300	3.61	26.63	0.0209	5.13	31.30	0.0148
13	647.06	11.000	0.017	0.63	65.72	0.0132	0.50	100.53	0.0138
14	18.87	11.000	0.583	5.37	30.13	0.0173	8.04	22.60	0.0172
15	18.87	11.000	0.583	5.50	27.77	0.0183	7.96	25.68	0.0179
16	36.67	11.000	0.300	2.73	26.96	0.0190	3.96	28.79	0.0196
17	36.67	11.000	0.300	2.83	27.42	0.0173	4.76	29.52	0.0172
18	36.67	11.000	0.300	2.80	26.18	0.0184	4.12	32.76	0.0170
19	36.67	11.000	0.300	2.71	25.23	0.0166	4.05	31.79	0.0183
20	36.67	11.000	0.300	2.77	26.80	0.0189	3.20	33.16	0.0174

C and N represent carbon and nitrogen levels in $g\ L^{-1}$, respectively. Table 4 showcases the ANOVA analysis of the reduced CCD models (insignificant factors excluded). The complete ANOVA analysis of the models after 192 h is listed in Table S8. The regression equations after 192 h translate into the 3D response surface plots depicted in Figure 5.

Table 4. ANOVA of full central composite design (CCD) models for the optimization of carbon and nitrogen concentrations in *R. erythropolis* cultivation media.

Response		Model	*p*-Value Model	*p*-Value Lack of Fit	R^2	Adjusted R^2	Predicted R^2
Biomass	140 h	Linear	<0.0001	0.0318	0.9306	0.9224	0.8976
	192 h	2FI	<0.0001	0.0722	0.9611	0.9538	0.9416
Lipid	140 h	Reduced Quadratic	0.0007	<0.0001	0.7058	0.6273	0.2220
	192 h	Reduced Quadratic	<0.0001	<0.0001	0.8725	0.8486	0.7262
Carotenoids	140 h	2FI	0.1085	0.0004	0.3080	0.1782	−0.1744
	192 h	Reduced Quadratic	<0.0001	0.2525	0.7936	0.7549	0.6715

It can be deduced from the formulated regression Equations (2) and (3) that both of the independent factors, i.e., carbon and nitrogen, greatly affect biomass accumulation. After 192 h, a 2FI model was found to most accurately explain the interactions by exclusively considering significant terms. Carbon (linear) and nitrogen (linear), as well as the interactions between both concentrations, significantly affect the yield of biomass. With increased concentrations of carbon and nitrogen, increased biomass accumulation was determined (Figure 5a). The highest biomass was achieved with 11 $g\ L^{-1}$ of carbon and 0.58 $g\ L^{-1}$ of nitrogen, which corresponds to the highest tested nitrogen concentration, with $8.0 \pm 0.3\ g\ L^{-1}$ being recorded after 192 h.

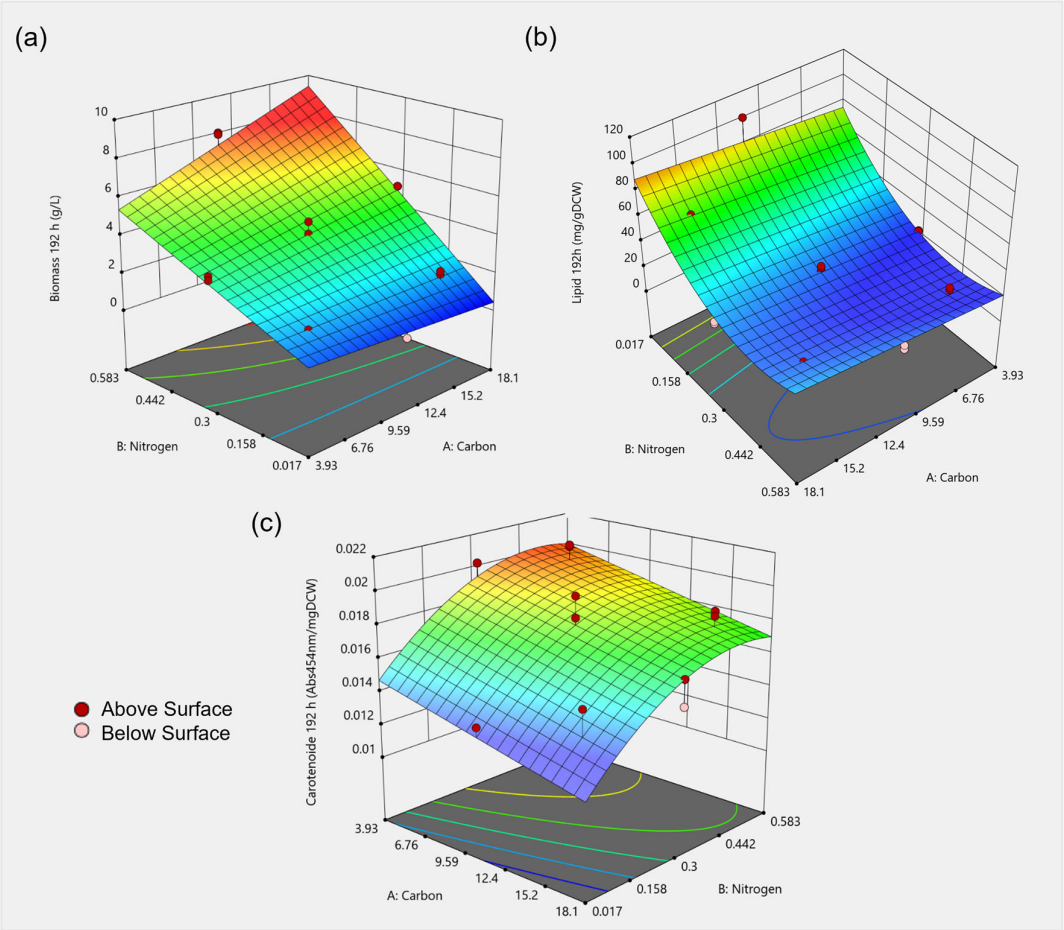

Figure 5. A 3D response surface plot of the combined effect of carbon and nitrogen levels on (**a**) biomass (g L^{-1}), (**b**) lipid content (mg $g^{-1}{}_{DCW}$) and (**c**) carotenoid content ($Abs_{454nm}mg^{-1}{}_{DCW}$) after 192 h. Red points mark the measured points on which the model was built, dark red points were measured above the depicted model surface and light red points were measured below the model surface.

For the lipid content, a reduced quadratic model with carbon (linear) and nitrogen (linear and quadratic) concentrations resulted in the best fitted model after 192 h. An inverse trend regarding biomass accumulation was observed. With decreasing carbon and nitrogen concentration, increasing lipid formation was observed. Nitrogen limitation can lead to high lipid production in oleaginous micro-organisms, but it simultaneously limits the biomass formation, as can be especially observed for Run 13 (Table 3). This observation was shown for a range of micro-organisms, including the oleaginous yeast *Cutaneotrichosporon oleaginosus* [27] and *Rhodotorula glutinis* [73]. Star points (Run 9 to 15) represent extreme low, as well as high, values for each factor of the design. These points are typically applied to estimate the curvature of the model. Run 13 represents minimal nitrogen content in the medium. Here, the lowest biomass (0.5 ± 0.05 g L^{-1}), as well as the highest lipid content (100.5 ± 4.3 mg $g^{-1}{}_{DCW}$), could be determined after 192 h. Due to a drastic decrease in the yield of biomass and increase in lipid formation in the culture compared to other tested media compositions, the model is unable to precisely predict this point, which could explain the significant lack of fit p-value for both lipid titer models (Table 4). Various C:N were tested for *R. opacus* PD630 grown using waste paper hydrolysate. While the biomass accumulation steadily decreased with an increase in C:N of 10 to 80, the lipid content steadily increased. A C:N of 60 yielded a lipid content of 41.6% [2].

The effects of carbon and nitrogen concentration on carotenoid production in *Rhodococcus* were investigated for the first time. When explaining the carotenoid content after 192 h, a reduced quadratic model with carbon (linear) and nitrogen (linear and quadratic) resulted in the best fit. Low carbon and high nitrogen content in the medium resulted in increased carotenoid production (Figure 5c), with a maximal carotenoid content of 0.020 ± 0.001 $Abs_{454nm} mg^{-1}_{DCW}$ (6 g L^{-1} of carbon and 0.5 g L^{-1} of nitrogen). Temperature and pH, as well as initial sugar and nitrogen contents, had effects on the carotenoid production by the yeast *Rhodotorula mucilaginosa.* Increased growth and carotenoid concentration could be observed at higher sugar concentrations [37]. In *Rhodotorula glutinis* CCY20-2-26, the highest pigment accumulation was determined at a C:N of 20, with the content decreasing at a higher C:N ratio [74]. In contrast, the carotenoid content of *Rhodotorula glutinis* increased with an increase in the C:N ratio. Additionally, both high and low concentrations of ammonium had negative effects on carotenoid production [73].

In RSM, low experiment numbers are sufficient to find the optimum parameters, as well as interpret effects among variables. However, this method also has drawbacks [24,29]. Applied quadratic non-linear correlations might not be sufficiently complex to explain non-linear dependencies in biological processes [29]. The CCD of different carbon and nitrogen concentrations presented in this study allows an estimation of the influence on the biomass, lipid, and carotenoid production of *R. erythropolis.* Furthermore, a suitable setup, enabling both biomass and lipid production, could be identified. One possibility is to achieve high-density biomass using high carbon and nitrogen concentrations supplied to the media, followed by nitrogen limitation for lipid accumulation.

4. Conclusions

In this study, a threefold media optimization method was performed for *R. erythropolis* using selected carbon and nitrogen sources. The data generated in this work, together with the CCD, provide a comprehensive source of information for the identification of suitable and cost-efficient feedstocks used in industrial processes. For the first time, the effects of carbon and nitrogen concentrations on the production of lipids and carotenoids in *R. erythropolis* have been assessed via a response surface model. Comparisons between fatty acid profiles when grown on different carbon and nitrogen sources revealed the enhanced production of oleic acid and stearic acid when grown on yeast extract and tryptone/peptone. Higher amounts of odd-chain fatty acids were detected when grown on lactose or maltose. Odd-chain fatty acids have unique pharmacological functions and are positively related to human health; they are, therefore, of high interest [75]. The optimal culture composition developed here could aid future studies that aim to understand de novo lipogenesis in *R. erythropolis*. Further, asymmetric carotenoids are of great industrial interest, as they are very difficult to chemically produce, but they can be produced by a lycopene β-cyclase identified in *R. erythropolis* AN12 [8,18].

Applying a C:N of 100, nine nitrogen and eight carbon sources were investigated. As all other parameters were held constant, new insights about the effects of a wide variety of carbon and nitrogen sources could be concluded. Maximum biomass acquisition was obtained using the nitrogen source ammonium acetate, whereas the complex nitrogen source yeast extract, followed by tryptone/peptone, achieved the highest lipid yield. With respect to different carbon sources, the highest biomasses could be observed using glucose, followed by sucrose. Notably, sugar alcohols, sorbitol and glycerol induced elevated lipid titers. While biomass production increased with the increase in carbon and nitrogen concentrations in the presented CCD, lipid production decreased.

The results of this study facilitate the identification of suitable waste stream substrates for *R. erythropolis* JCM3201^T, as insights into the substrate flexibility and nutrient flow could serve as cultivation references for future studies of this promising organism. Future work could apply more sophisticated modeling solutions, such as machine learning algorithms, i.e. Bayesian optimization, for the optimization of this strain at a larger scale. To this end, additional factors, such as optimal pH, temperature, pO_2, vitamins, and trace elements,

could also be identified in a time- and cost-efficient manner. This current work could also feed into a big data acquisition model, where RSM and other methodologies could be extracted from various works to capture the non-linear behavior of a biological system.

Supplementary Materials: The following supporting information can be downloaded at: https://www.mdpi.com/article/10.3390/microorganisms11092147/s1, Table S1: OD—Nitrogen Sources; Table S2: DCW, Lipid, and Carotenoid Titers of Nitrogen Sources; Table S3: OD—Carbon Sources; Table S4: DCW, Lipid, and Carotenoid Titers of Carbon Sources; Table S5: Onset of stationary phase-Nitrogen and carbon sources; Table S6: FAME profiles of Nitrogen Sources; Table S7: FAME profiles of Carbon Sources; Table S8: Complete ANOVA of central composite design (CCD) models after 192 h.

Author Contributions: Conceptualization, all authors; methodology, S.E.-S.; validation, all authors; writing—original draft preparation, S.E.-S.; writing—review and editing, D.A., T.B. and N.M.; project administration, N.M.; funding acquisition, N.M. All authors have read and agreed to the published version of the manuscript.

Funding: This research was funded by the German Federal Ministry of Education and Research (BMBF), project OleoBuild, grant number: 031B0853A.

Data Availability Statement: Not applicable.

Acknowledgments: The authors gratefully acknowledge the valuable inputs of Nadim Ahmad, Nathanael Arnold, Manfred Ritz, and Felix Melcher.

Conflicts of Interest: The authors declare no conflict of interest.

References

1. Alvarez, H.M.; Steinbuchel, A. Triacylglycerols in prokaryotic microorganisms. *Appl. Microbiol. Biotechnol.* **2002**, *60*, 367–376. [CrossRef]
2. Nair, A.S.; Sivakumar, N. Biodiesel production by oleaginous bacteria *Rhodococcus opacus* PD630 using waste paper hydrolysate. *Biomass Convers. Biorefinery* **2022**. [CrossRef]
3. Ram, S.; Mitra, M.; Shah, F.; Tirkey, S.R.; Mishra, S. Bacteria as an alternate biofactory for carotenoid production: A review of its applications, opportunities and challenges. *J. Funct. Foods* **2020**, *67*, 103867. [CrossRef]
4. Thanapimmetha, A.; Suwaleerat, T.; Saisriyoot, M.; Chisti, Y.; Srinophakun, P. Production of carotenoids and lipids by *Rhodococcus opacus* PD630 in batch and fed-batch culture. *Bioprocess Biosyst. Eng.* **2017**, *40*, 133–143. [CrossRef]
5. Barreiro, C.; Barredo, J.L. Carotenoids Production: A Healthy and Profitable Industry. In *Microbial Carotenoids*; Methods in Molecular Biology; Barreiro, C., Barredo, J.L., Eds.; Humana Press: New York, NY, USA, 2018; Volume 1852, pp. 45–55. [CrossRef]
6. Bell, K.S.; Philp, J.C.; Aw, D.W.; Christofi, N. The genus *Rhodococcus*. *J. Appl. Microbiol.* **1998**, *85*, 195–210. [CrossRef] [PubMed]
7. de Carvalho, C.C.C.R.; da Fonseca, M.M.R. The remarkable *Rhodococcus erythropolis*. *Appl. Microbiol. Biotechnol.* **2005**, *67*, 715–726. [CrossRef]
8. Cappelletti, M.; Presentato, A.; Piacenza, E.; Firrincieli, A.; Turner, R.J.; Zannoni, D. Biotechnology of *Rhodococcus* for the production of valuable compounds. *Appl. Microbiol. Biotechnol.* **2020**, *104*, 8567–8594. [CrossRef] [PubMed]
9. Ochsenreither, K.; Glück, C.; Stressler, T.; Fischer, L.; Syldatk, C. Production Strategies and Applications of Microbial Single Cell Oils. *Front. Microbiol.* **2016**, *7*, 1539. [CrossRef] [PubMed]
10. Tapiero, H.; Townsend, D.M.; Tew, K.D. The role of carotenoids in the prevention of human pathologies. *Biomed. Pharmacother.* **2004**, *58*, 100–110. [CrossRef]
11. Liu, L.; Song, J.; Li, Y.; Li, P.; Wang, H. Robust and cost-saving static solid cultivation method for lipid production using the chlamydospores of Phanerochaete chrysosporium. *Biotechnol. Biofuels* **2019**, *12*, 123. [CrossRef]
12. Pagels, F.; Vasconcelos, V.; Guedes, A.C. Carotenoids from Cyanobacteria: Biotechnological Potential and Optimization Strategies. *Biomolecules* **2021**, *11*, 735. [CrossRef] [PubMed]
13. Bhatia, S.K.; Gurav, R.; Choi, T.-R.; Han, Y.-H.; Park, Y.-L.; Jung, H.-R.; Yang, S.-Y.; Song, H.-S.; Yang, Y.-H. A clean and green approach for odd chain fatty acids production in *Rhodococcus* sp. YHY01 by medium engineering. *Bioresour. Technol.* **2019**, *286*, 121383. [CrossRef]
14. Sangal, V.; Goodfellow, M.; Jones, A.L.; Schwalbe, E.C.; Blom, J.; Hoskisson, P.A.; Sutcliffe, I.C. Next-generation systematics: An innovative approach to resolve the structure of complex prokaryotic taxa. *Sci. Rep.* **2016**, *6*, 38392. [CrossRef] [PubMed]
15. Kitagawa, W.; Hata, M. Development of Efficient Genome-Reduction Tool Based on Cre/loxP System in *Rhodococcus erythropolis*. *Microorganisms* **2023**, *11*, 268. [CrossRef] [PubMed]
16. Herrero, O.M.; Moncalián, G.; Alvarez, H.M. Physiological and genetic differences amongst *Rhodococcus* species for using glycerol as a source for growth and triacylglycerol production. *Microbiology* **2016**, *162*, 384–397. [CrossRef]

17. Alvarez, H.M. Relationship between β-oxidation pathway and the hydrocarbon-degrading profile in actinomycetes bacteria. *Int. Biodeterior. Biodegrad.* **2003**, *52*, 35–42. [CrossRef]
18. Tao, L.; Picataggio, S.; Rouvière, P.E.; Cheng, Q. Asymmetrically acting lycopene β-cyclases (CrtLm) from non-photosynthetic bacteria. *Mol. Genet. Genom.* **2004**, *271*, 180–188. [CrossRef]
19. Tao, L.; Wagner, L.W.; Rouvière, P.E.; Cheng, Q. Metabolic engineering for synthesis of aryl carotenoids in *Rhodococcus*. *Appl. Microbiol. Biotechnol.* **2006**, *70*, 222–228. [CrossRef] [PubMed]
20. Singh, V.; Haque, S.; Niwas, R.; Srivastava, A.; Pasupuleti, M.; Tripathi, C.K.M. Strategies for Fermentation Medium Optimization: An In-Depth Review. *Front. Microbiol.* **2016**, *7*, 2087. [CrossRef]
21. Bao, W.; Li, Z.; Wang, X.; Gao, R.; Zhou, X.; Cheng, S.; Men, Y.; Zheng, L. Approaches to improve the lipid synthesis of oleaginous yeast Yarrowia lipolytica: A review. *Renew. Sustain. Energy Rev.* **2021**, *149*, 111386. [CrossRef]
22. Madani, M.; Enshaeieh, M.; Abdoli, A. Single cell oil and its application for biodiesel production. *Process Saf. Environ. Prot.* **2017**, *111*, 747–756. [CrossRef]
23. Papanikolaou, S.; Aggelis, G. Lipids of oleaginous yeasts. Part I: Biochemistry of single cell oil production. *Eur. J. Lipid Sci. Technol.* **2011**, *113*, 1031–1051. [CrossRef]
24. Sahu, R.; Meghavarnam, A.K.; Janakiraman, S. Response surface methodology: An effective optimization strategy for enhanced production of nitrile hydratase (NHase) by *Rhodococcus rhodochrous* (RS-6). *Heliyon* **2020**, *6*, e05111. [CrossRef]
25. Box, G.E.P.; Wilson, K.B. On the Experimental Attainment of Optimum Conditions. *J. R. Stat. Soc. Ser. B (Methodol.)* **1951**, *13*, 1–38. [CrossRef]
26. Kong, Q.; Zhai, C.; Guan, B.; Li, C.; Shan, S.; Yu, J. Mathematic modeling for optimum conditions on aflatoxin B_1 degradation by the aerobic bacterium *Rhodococcus erythropolis*. *Toxins* **2012**, *4*, 1181–1195. [CrossRef] [PubMed]
27. Awad, D.; Bohnen, F.; Mehlmer, N.; Brueck, T. Multi-Factorial-Guided Media Optimization for Enhanced Biomass and Lipid Formation by the Oleaginous Yeast Cutaneotrichosporon oleaginosus. *Front. Bioeng. Biotechnol.* **2019**, *7*, 54. [CrossRef] [PubMed]
28. Huang, L.; Ma, T.; Li, D.; Liang, F.-L.; Liu, R.-L.; Li, G.-Q. Optimization of nutrient component for diesel oil degradation by *Rhodococcus erythropolis*. *Mar. Pollut. Bull.* **2008**, *56*, 1714–1718. [CrossRef]
29. Mutalik, S.R.; Vaidya, B.K.; Joshi, R.M.; Desai, K.M.; Nene, S.N. Use of response surface optimization for the production of biosurfactant from *Rhodococcus* spp. MTCC 2574. *Bioresour. Technol.* **2008**, *99*, 7875–7880. [CrossRef]
30. Koblitz, J.; Halama, P.; Spring, S.; Thiel, V.; Baschien, C.; Hahnke, R.L.; Pester, M.; Overmann, J.; Reimer, L.C. MediaDive: The expert-curated cultivation media database. *Nucleic Acids Res.* **2023**, *51*, D1531–D1538. [CrossRef] [PubMed]
31. Engelhart-Straub, S.; Cavelius, P.; Hölzl, F.; Haack, M.; Awad, D.; Brueck, T.; Mehlmer, N. Effects of Light on Growth and Metabolism of *Rhodococcus erythropolis*. *Microorganisms* **2022**, *10*, 1680. [CrossRef] [PubMed]
32. Kolekar, P.D.; Phugare, S.S.; Jadhav, J.P. Biodegradation of atrazine by *Rhodococcus* sp. BCH2 to N-isopropylammelide with subsequent assessment of toxicity of biodegraded metabolites. *Environ. Sci. Pollut. Res.* **2014**, *21*, 2334–2345. [CrossRef]
33. Kövilein, A.; Zadravec, L.; Hohmann, S.; Umpfenbach, J.; Ochsenreither, K. Effect of process mode, nitrogen source and temperature on L-malic acid production with Aspergillus oryzae DSM 1863 using acetate as carbon source. *Front. Bioeng. Biotechnol.* **2022**, *10*, 1033777. [CrossRef]
34. Elfeky, N.; Elmahmoudy, M.; Zhang, Y.; Guo, J.; Bao, Y. Lipid and Carotenoid Production by *Rhodotorula glutinis* with a Combined Cultivation Mode of Nitrogen, Sulfur, and Aluminium Stress. *Appl. Sci.* **2019**, *9*, 2444. [CrossRef]
35. Evans, C.T.; Ratledge, C. Effect of Nitrogen Source on Lipid Accumulation in Oleaginous Yeasts. *Microbiology* **1984**, *130*, 1693–1704. [CrossRef]
36. Zhao, Y.; Guo, L.; Xia, Y.; Zhuang, X.; Chu, W. Isolation, Identification of Carotenoid-Producing *Rhodotorula* sp. from Marine Environment and Optimization for Carotenoid Production. *Mar. Drugs* **2019**, *17*, 161. [CrossRef] [PubMed]
37. Aksu, Z.; Eren, A.T. Carotenoids production by the yeast *Rhodotorula mucilaginosa*: Use of agricultural wastes as a carbon source. *Process Biochem.* **2005**, *40*, 2985–2991. [CrossRef]
38. Liu, M.; Yang, Y.; Li, L.; Ma, Y.; Huang, J.; Ye, J. Engineering Sphingobium sp. to Accumulate Various Carotenoids Using Agro-Industrial Byproducts. *Front. Bioeng. Biotechnol.* **2021**, *9*, 784559. [CrossRef] [PubMed]
39. Kizilay, H.K.; Küçükçetin, A.; Demir, M. Optimization of carotenoid production by Umbelopsis ramanniana. *Biotechnol. Prog.* **2023**, e3369. [CrossRef]
40. Bhosale, P.; Bernstein, P.S. β-carotene production by Flavobacterium multivorum in the presence of inorganic salts and urea. *J. Ind. Microbiol. Biotechnol.* **2004**, *31*, 565–571. [CrossRef]
41. Ojha, S.; Kapoor, S.; Mishra, S. Carotenoid Production by a Novel Isolate of Microbacterium paraoxydans. *Indian J. Microbiol.* **2018**, *58*, 118–122. [CrossRef] [PubMed]
42. Alvarez, H.M.; Hernández, M.A.; Lanfranconi, M.P.; Silva, R.A.; Villalba, M.S. *Rhodococcus* as Biofactories for Microbial Oil Production. *Molecules* **2021**, *26*, 4871. [CrossRef] [PubMed]
43. Kurosawa, K.; Plassmeier, J.; Kalinowski, J.; Rückert, C.; Sinskey, A.J. Engineering L-arabinose metabolism in triacylglycerol-producing *Rhodococcus opacus* for lignocellulosic fuel production. *Metab. Eng.* **2015**, *30*, 89–95. [CrossRef]
44. Kurosawa, K.; Wewetzer, S.J.; Sinskey, A.J. Engineering xylose metabolism in triacylglycerol-producing *Rhodococcus opacus* for lignocellulosic fuel production. *Biotechnol. Biofuels* **2013**, *6*, 134. [CrossRef] [PubMed]
45. Xiong, X.; Wang, X.; Chen, S. Engineering of a xylose metabolic pathway in *Rhodococcus* strains. *Appl. Environ. Microbiol.* **2012**, *78*, 5483–5491. [CrossRef] [PubMed]

46. Xiong, X.; Wang, X.; Chen, S. Engineering of an L-arabinose metabolic pathway in *Rhodococcus jostii* RHA1 for biofuel production. *J. Ind. Microbiol. Biotechnol.* **2016**, *43*, 1017–1025. [CrossRef] [PubMed]
47. Donini, E.; Firrincieli, A.; Cappelletti, M. Systems biology and metabolic engineering of *Rhodococcus* for bioconversion and biosynthesis processes. *Folia Microbiol.* **2021**, *66*, 701–713. [CrossRef] [PubMed]
48. Mischko, W.; Hirte, M.; Roehrer, S.; Engelhardt, H.; Mehlmer, N.; Minceva, M.; Brück, T. Modular biomanufacturing for a sustainable production of terpenoid-based insect deterrents. *Green Chem.* **2018**, *20*, 2637–2650. [CrossRef]
49. Kurosawa, K.; Wewetzer, R.J.; Sinskey, A.J. Triacylglycerol Production from Corn Stover Using a Xylose-Fermenting *Rhodococcus* opacus Strain for Lignocellulosic Biofuels. *J. Microb. Biochem. Technol.* **2014**, *6*, 254–259. [CrossRef]
50. Herrero, O.M.; Alvarez, H.M. Whey as a renewable source for lipid production by *Rhodococcus* strains: Physiology and genomics of lactose and galactose utilization. *Eur. J. Lipid Sci. Technol.* **2015**, *118*, 262–272. [CrossRef]
51. Hernández, M.A.; Alvarez, H.M. Glycogen formation by *Rhodococcus* species and the effect of inhibition of lipid biosynthesis on glycogen accumulation in *Rhodococcus* opacus PD630. *FEMS Microbiol. Lett.* **2010**, *312*, 93–99. [CrossRef] [PubMed]
52. Jin, L.-Q.; Li, Y.-F.; Liu, Z.-Q.; Zheng, Y.-G.; Shen, Y.-C. Characterization of a newly isolated strain *Rhodococcus erythropolis* ZJB-09149 transforming 2-chloro-3-cyanopyridine to 2-chloronicotinic acid. *New Biotechnol.* **2011**, *28*, 610–615. [CrossRef]
53. Li, Y.; Xing, J.; Li, W.; Xiong, X.; Li, X.; Liu, H. Medium optimization of *Rhodococcus erythropolis* LSSE8-1 by Taguchi methodology for petroleum biodesulfurization. *Korean J. Chem. Eng.* **2007**, *24*, 781–786. [CrossRef]
54. Cortes, M.A.L.R.M.; de Carvalho, C.C.C.R. Effect of carbon sources on lipid accumulation in *Rhodococcus* cells. *Biochem. Eng. J.* **2015**, *94*, 100–105. [CrossRef]
55. Sriwongchai, S.; Pokethitiyook, P.; Pugkaew, W.; Kruatrachue, M.; Lee, H. Optimization of lipid production in the oleaginous bacterium *Rhodococcus erythropolis* growing on glycerol as the sole carbon source. *Afr. J. Biotechnol.* **2012**, *11*, 14440–14447. [CrossRef]
56. Vázquez, M.; Santos, V.; Parajó, J.C. Effect of the carbon source on the carotenoid profiles of *Phaffia rhodozyma* strains. *J. Ind. Microbiol. Biotechnol.* **1997**, *19*, 263–268. [CrossRef]
57. Sampath, H.; Ntambi, J.M. Polyunsaturated Fatty Acid Regulation of Genes of Lipid Metabolism. *Annu. Rev. Nutr.* **2005**, *25*, 317–340. [CrossRef] [PubMed]
58. Heipieper, H.J.; Weber, F.J.; Sikkema, J.; Keweloh, H.; de Bont, J.A.M. Mechanisms of Resistance of Whole Cells to Toxic Organic-Solvents. *Trends Biotechnol.* **1994**, *12*, 409–415. [CrossRef]
59. Weber, F.J.; de Bont, J.A. Adaptation mechanisms of microorganisms to the toxic effects of organic solvents on membranes. *Biochim. Biophys. Acta* **1996**, *1286*, 225–245. [CrossRef]
60. Wältermann, M.; Hinz, A.; Robenek, H.; Troyer, D.; Reichelt, R.; Malkus, U.; Galla, H.J.; Kalscheuer, R.; Stöveken, T.; von Landenberg, P.; et al. Mechanism of lipid-body formation in prokaryotes: How bacteria fatten up. *Mol. Microbiol.* **2005**, *55*, 750–763. [CrossRef]
61. Blitzblau, H.G.; Consiglio, A.L.; Teixeira, P.; Crabtree, D.V.; Chen, S.; Konzock, O.; Chifamba, G.; Su, A.; Kamineni, A.; MacEwen, K.; et al. Production of 10-methyl branched fatty acids in yeast. *Biotechnol. Biofuels* **2021**, *14*, 12. [CrossRef]
62. McNabb, A.; Shuttleworth, R.; Behme, R.; Colby, W.D. Fatty acid characterization of rapidly growing pathogenic aerobic actinomycetes as a means of identification. *J. Clin. Microbiol.* **1997**, *35*, 1361–1368. [CrossRef] [PubMed]
63. Peng, F.; Liu, Z.; Wang, L.; Shao, Z. An oil-degrading bacterium: *Rhodococcus erythropolis* strain 3C-9 and its biosurfactants. *J. Appl. Microbiol.* **2007**, *102*, 1603–1611. [CrossRef] [PubMed]
64. Machida, S.; Bakku, R.K.; Suzuki, I. Expression of Genes for a Flavin Adenine Dinucleotide-Binding Oxidoreductase and a Methyltransferase from Mycobacterium chlorophenolicum Is Necessary for Biosynthesis of 10-Methyl Stearic Acid from Oleic Acid in Escherichia coli. *Front. Microbiol.* **2017**, *8*, 2061. [CrossRef] [PubMed]
65. Koch, C.; Klatte, S.; Schumann, P.; Burghardt, J.; Kroppenstedt, R.M.; Stackebrandt, E. Transfer of *Arthrobacter picolinophilus* Tate and Ensign 1974 to *Rhodococcus erythropolis*. *Int. J. Syst. Bacteriol.* **1995**, *45*, 576–577. [CrossRef]
66. Tsitko, I.V.; Zaitsev, G.M.; Lobanok, A.G.; Salkinoja-Salonen, M.S. Effect of aromatic compounds on cellular fatty acid composition of *Rhodococcus opacus*. *Appl. Environ. Microbiol.* **1999**, *65*, 853–855. [CrossRef] [PubMed]
67. Avis, T.J.; Belanger, R.R. Specificity and mode of action of the antifungal fatty acid cis-9-heptadecenoic acid produced by *Pseudozyma flocculosa*. *Appl. Environ. Microbiol.* **2001**, *67*, 956–960. [CrossRef]
68. MubarakAli, D.; Praveenkumar, R.; Shenbagavalli, T.; Mari Nivetha, T.; Parveez Ahamed, A.; Al-Dhabi, N.A.; Thajuddin, N. New reports on anti-bacterial and anti-candidal activities of fatty acid methyl esters (FAME) obtained from *Scenedesmus bijugatus* var. *bicellularis biomass. RSC Adv.* **2012**, *2*, 11552–11556. [CrossRef]
69. Park, Y.-K.; Dulermo, T.; Ledesma-Amaro, R.; Nicaud, J.-M. Optimization of odd chain fatty acid production by *Yarrowia lipolytica*. *Biotechnol. Biofuels* **2018**, *11*, 158. [CrossRef]
70. Kurosawa, K.; Boccazzi, P.; de Almeida, N.M.; Sinskey, A.J. High-cell-density batch fermentation of *Rhodococcus opacus* PD630 using a high glucose concentration for triacylglycerol production. *J. Biotechnol.* **2010**, *147*, 212–218. [CrossRef]
71. Shields-Menard, S.A.; Amirsadeghi, M.; Sukhbaatar, B.; Revellame, E.; Hernandez, R.; Donaldson, J.R.; French, W.T. Lipid accumulation by *Rhodococcus rhodochrous* grown on glucose. *J. Ind. Microbiol. Biotechnol.* **2015**, *42*, 693–699. [CrossRef]
72. Kurane, R.; Toeda, K.; Takeda, K.; Suzuki, T. Culture Conditions for Production of Microbial Flocculant by *Rhodococcus erythropolis*. *Agric. Biol. Chem.* **2014**, *50*, 2309–2313. [CrossRef]

73. Braunwald, T.; Schwemmlein, L.; Graeff-Hönninger, S.; French, W.T.; Hernandez, R.; Holmes, W.E.; Claupein, W. Effect of different C/N ratios on carotenoid and lipid production by *Rhodotorula glutinis*. *Appl. Microbiol. Biotechnol.* **2013**, *97*, 6581–6588. [CrossRef] [PubMed]
74. Tkáčová, J.; Klempová, T.; Čertík, M. Kinetic study of growth, lipid and carotenoid formation in β-carotene producing *Rhodotorula glutinis*. *Chem. Pap.* **2017**, *72*, 1193–1203. [CrossRef]
75. Zhang, L.-S.; Liang, S.; Zong, M.-H.; Yang, J.-G.; Lou, W.-Y. Microbial synthesis of functional odd-chain fatty acids: A review. *World J. Microbiol. Biotechnol.* **2020**, *36*, 35. [CrossRef] [PubMed]

Effects of Light on Growth and Metabolism of *Rhodococcus erythropolis*

microorganisms

MDPI

Article

Effects of Light on Growth and Metabolism of *Rhodococcus erythropolis*

Selina Engelhart-Straub †, Philipp Cavelius †, Fabian Hölzl, Martina Haack, Dania Awad, Thomas Brueck * and Norbert Mehlmer *

Werner Siemens-Chair of Synthetic Biotechnology, Department of Chemistry, Technical University of Munich (TUM), 85748 Garching, Germany

* Correspondence: brueck@tum.de (T.B.); norbert.mehlmer@tum.de (N.M.)

† These authors contributed equally to this work.

Abstract: *Rhodococcus erythropolis* is resilient to various stressors. However, the response of *R. erythropolis* towards light has not been evaluated. In this study, *R. erythropolis* was exposed to different wavelengths of light. Compared to non-illuminated controls, carotenoid levels were significantly increased in white (standard warm white), green (510 nm) and blue light (470 nm) illuminated cultures. Notably, blue light (455, 425 nm) exhibited anti-microbial effects. Interestingly, cellular lipid composition shifted under light stress, increasing odd chain fatty acids (C15:0, C17:1) cultured under white (standard warm white) and green (510 nm) light. When exposed to blue light (470, 455, 425 nm), fatty acid profiles shifted to more saturated fatty acids (C16:1 to C16:0). Time-resolved proteomics analysis revealed several oxidative stress-related proteins to be upregulated under light illumination.

Keywords: *Rhodococcus*; photo-oxidative stress; stress response; antimicrobial blue light; carotenoids; fatty acids; time-resolved proteomics

Citation: Engelhart-Straub, S.; Cavelius, P.; Hölzl, F.; Haack, M.; Awad, D.; Brueck, T.; Mehlmer, N. Effects of Light on Growth and Metabolism of *Rhodococcus erythropolis*. *Microorganisms* **2022**, *10*, 1680. https://doi.org/10.3390/microorganisms10081680

Academic Editors: Carla C. C. R. de Carvalho, Miroslav Pátek, Martina Cappelletti and Héctor M. Alvarez

Received: 29 July 2022
Accepted: 17 August 2022
Published: 20 August 2022

1. Introduction

The genus *Rhodococcus* comprises a cluster of aerobic, non-sporulating, Gram-positive and non-motile bacteria [1,2]. They are ideal candidates for efficient production of a wide range of compounds such as biosurfactants, carotenoids, triacylglycerols or antimicrobials [3]. Furthermore, the genus harbors great potential for finding novel bioactive natural products [4]. The oleaginous *Rhodococcus erythropolis* is known for its high stress tolerance, the ability to metabolize various substrates and the synthesis of carotenoids, resulting in its characteristic coloration [5]. However, little is known about carotenoid function in *R. erythropolis*.

All aerobic organisms, including *R. erythropolis*, cope with oxidative stress, more specifically, the formation of reactive oxygen species (ROS), including singlet oxygen, superoxide radicals, hydroxyl radicals and hydrogen peroxide. Exposure to visible light and UV irradiation results in higher levels of oxidative stress (photo-oxidative stress). One mechanism of increased ROS formation under light is mediated by intracellular photosensitizers, which absorb incoming light-energy at certain wavelengths and by transfer of excitation energy onto molecular oxygen to generate singlet oxygen [6–8]. Some photosensitizers also react by transferring electrons onto oxygen, forming superoxide radicals, hydrogen peroxide and hydroxyl radicals. These, in turn, may trigger damage of cellular components, such as proteins and lipids [9]. Notably, not only UV-light but also blue light exhibits anti-microbial effects against several bacterial species [7,10]. Especially, the wavelengths of 405 nm [11,12], 425 nm [13] and 470 nm [11,12] have been evaluated in previous studies. Here, porphyrins and riboflavins are hypothesized to act as endogenous photosensitizers for blue light [7,10–14].

Cellular detoxification from ROS is mainly performed by oxidoreductases, specifically catalases and peroxidases, which are able to degrade reactive peroxides. Furthermore,

highly reactive radicals can be directly deactivated by molecular acceptors, which include different groups of non-protein compounds [6–8]. Among these groups, carotenoids can be found in almost all photosynthetic-, as well as various species of non-photosynthetic organisms such as *R. erythropolis*. So far, most studies focused on their function in light harvesting, where they help to efficiently utilize incoming light via absorption of the blue-green light spectrum followed by singlet-singlet energy transfer onto chlorophyll. They are also known for their antioxidant properties. Carotenoids act as quenchers for certain photosensitizers (e.g., triplet chlorophyll) and can directly inactivate different ROS [6]. Similarly, in non-photosynthetic carotenoid-producing organisms, carotenoids serve as protectors against photo-oxidative stress. To that end, photodynamic damaging effects are reduced due to their ability to absorb green and blue light, to react with light-excited photosensitizers, thus preventing increased ROS formation, and their ability to minimize singlet oxygen and radical damage [6,8,15,16].

Enhanced stress resistance can also be conferred through modification of membrane properties, by shifting the ratio between saturated, unsaturated and branched fatty acids (FAs) [17–19]. *Rhodococcus opacus*, a close relative of *R. erythropolis*, accumulates high amounts of polyunsaturated fatty acids in response to various stressors, such as salt or ROS [20–22]. When *R. erythropolis* was subjected to non-optimal conditions of pH and temperatures, increased FA saturation could be detected [17]. A previously reported stress-related shift in lipid composition is catalyzed by the cyclopropane-fatty acid-acyl phospholipid synthase in *E. coli* and other bacteria, which enables direct modification of membrane lipids by adding cyclopropane moieties to unsaturated FA bonds. These changes are known to influence the physiochemical properties of the membrane (e.g., permeability and fluidity), affecting the cell's resistance to different stress conditions, including osmotic and oxidative stress, high pressure and temperature change [18,19].

In this study, the photo-oxidative stress response of *R. erythropolis* was investigated by exposure to a selected set of wavelengths of light under aerobic growth conditions. In order to unravel the extensive light stress adaptations, alterations in growth characteristics, carotenoid accumulation and FA profile were monitored. Additionally, quantitative time-resolved proteomics enabled identification of differential levels of proteins and altered regulation of metabolic pathways under light-induced conditions.

2. Materials and Methods

2.1. Bacterial Strain and Culture Conditions

R. erythropolis JCM3201 (DSM No. 43066, German Collection of Microorganisms and Cell Cultures GmbH) was maintained on Luria-Bertani (LB) agar plates (10 g L^{-1} peptone, 5 g L^{-1} yeast extract, 10 g L^{-1} sodium chloride, 14 g L^{-1} agar). For seed cultures, single colonies were initially cultured in 500 mL baffled shaking flasks holding 100 mL LB liquid medium (10 g L^{-1} peptone, 5 g L^{-1} yeast extract, 10 g L^{-1} sodium chloride) in a rotary incubator (New Brunswick InnovaTM 44, Eppendorf, Hamburg, Germany) for 48 h. All cultivations were performed in 500 mL baffled shaking flasks holding 100 mL LB. Biological triplicates were inoculated to OD_{600nm} 0.5 and cultivated at 28 °C and 120 rpm.

2.2. Cultivation of R. erythropolis under Light of Different Wavelenths

To determine growth as well as lipid and carotenoid accumulation, experiments were conducted with different wavelengths of light (LED): blue (425, 455 and 470 nm), green (510 nm), red (680 nm) as well as standard warm white (SWW) light. Control samples were collected from cultures incubated in the dark. Each setting was adjusted to an equal energy output of 236 W m^{-2}. Light spectra for each experimental setup are depicted in Figure S1 (Supplementary Materials). The light cultivation setup was a customized shaker unit, with individual, bottom-up LED illumination of flasks as described by Paper et al. [23]. Cross-illumination was prevented by shading individual flasks with black paper (Figure S2, Supplementary Materials). The cultivation setup for control samples was a separate shaker (New Brunswick InnovaTM 44, Eppendorf, Hamburg, Germany) lacking the light system.

To ensure light-free conditions, the flasks were also shaded with black paper, and the glass door of the shaker was covered with aluminum foil. Experiments were performed in 500 mL baffled shaking flasks with Duran GL32 Membrane Vented Screw caps (DWK Life Science, Wertheim, Germany). Sampling for OD_{600nm} was performed twice a day. Samples for dry cell weight (DCW), carotenoid titers and FA profile were collected after 40 h and once after 122 h and 94 h.

2.3. Cultivation of R. erythropolis under LED Light for Proteomic Analysis

To determine growth and carotenoid titers and to conduct proteomics analysis, cultures of *R. erythropolis* were exposed to white LEDs. Setup consisted of a LED Mini- Matrices (Spectral color of 6500 K, max. 750 µmol m^{-2} s^{-1}, 504 LEDs, 27 × 42 cm, 24V; LUMITRONIX® LED-Technik GmbH, Hechingen, Germany) installed in a rotary shaker (New Brunswick InnovaTM 42, Eppendorf, Hamburg, Germany) at a height of 30 cm over the incubator platform. Control samples were collected from cultures incubated in the dark and samples from all cultures were collected after 40 h and 122 h.

2.4. Growth Analysis

Optical density was measured at 600 nm in a photometer (Nano Photometer NP80, IMPLEN, Munich, Germany) in standard semi-micro cuvettes made of polystyrene holding sample volumes of 1 mL.

DCW analysis, 25 mL culture was collected. Subsequently, cultures were centrifuged (3500× *g*, 10 min), and cells were washed and lyophilized (−80 °C, ≥ 72 h). Gravimetric measurements were carried out, and the weight of empty vessels was subtracted from weight of vessels containing lyophilized samples.

A light microscope (Motic BA310E) equipped with a Moticam 5.0 MP (Moticeurope, Barcelona, Spain) was used to evaluate cell morphology and contamination.

2.5. Pigment Extraction

For pigment extraction from dry biomass, 15 mg of lyophilized biomass was transferred into a reaction tube and mixed with glass beads (0.5 mm) and 1 mL of HPLC-grade acetone. Samples were vortexed horizontally for 10 min and centrifuged at 8000× *g* for 5 min. A volume of 700 µL of the supernatant was carefully transferred into a glass tube and tightly closed. Reaction tubes and glass tubes were wrapped in aluminum foil to avoid light exposure. Carotenoid levels were measured at an absorbance of 454 nm (Nano Photometer NP80, IMPLEN, Munich, Germany), using a solvent-stable cuvette.

For pigment extraction from wet biomass used in proteomic analysis, a volume of 7.5 mL cell suspension was centrifuged and washed with ddH_2O. Glass beads (0.5 mm) and 1.5 mL hexane: acetone: ethanol (2:1:1—*v*/*v*/*v*) were added to the cell pellet. The suspension was vortexed horizontally for 30 min to lyse the cells. The liquid phases were separated by centrifugation at 20,000× *g* for 10 min. The hexane phase was collected and carotenoids levels were directly measured in a solvent-stable cuvette in a photometer at 454 nm (UV/Vis spectrophotometer Hewlett Packard 8453, HP, Palo Alto, CA, USA).

2.6. Fatty Acid Profile

Lipids extracted from lyophilized biomass were converted into fatty acid methyl ester (FAME) and then analyzed by gas chromatography. In detail, lyophilized biomass (5 mg) was transferred into 10 mL glass vials, crimped with bimetallic lid including a septum (Macherey-Nagel, Düren, Germany). The MultiPurposeSampler MPS robotic (Gerstel, Linthicum Heights, MD, USA), equipped with QuickMix, CF200, Agitator/Stirrer was used for methyl esterification of the intracellular triacylglycerides (TAGs). For quantification, an internal standard of 10 g L^{-1} glyceryl tridodecanoate (C12:0; Sigma-Aldrich, St. Louis, MO, USA) solved in toluol as stock solution was prepared and a volume of 490 µL toluol and 10 µL internal standard were added to the biomass and mixed for 1 min at 1000 rpm. Then, 1 mL of 0.5 M sodium methoxide in methanol was added and the vial was vortexed

at 750 rpm and 80 °C for 20 min. The solution was cooled at 5 °C for 5 min, then 1 mL of 5% HCl in methanol (Supleco 17935 solution, Merck AG, Darmstadt, Germany) was added, and the mixture was vortexed at 750 rpm and 80 °C for 20 min. Subsequently, the mixture was cooled at 5 °C for 5 min. A volume of 400 µL ddH_2O was added and the mixture was vortexed at 1000 rpm for 30 s, then 1 mL hexane was added. FAMEs were extracted by three equal intervals of intermittent shaking for 12 s at 2000 rpm. Then, the vial was centrifuged at 1000 rpm for 3 min. After the vial was cooled at 5 °C for 1 min, 200 µL of the organic phase was transferred to micro vials (Macherey-Nagel, Düren, Germany).

A GC-2025 coupled to AOC-20i Auto injector and AOC-20s Auto sampler (Shimadzu, Duisburg, Germany) and a flame ionization detector (FID) was used for the ana-lysis and quantification of the FAMEs [24,25]. The injection temperature was 240 °C with a split ratio of 10 and a purge flow of 3 mL min^{-1} helium. Injection volume for all samples was 1 µL. A Zebron ZB-wax column (Phenomenex, Aschaffenburg, Germany) (30 m × 0.32 mm, film thickness 0.25 µm) was used for separation with an initial oven temperature of 150 °C. This temperature was held for 1 min before increasing at a rate of 5 °C min^{-1} up to a final temperature of 240 °C, which was held for 6 min. As carrier gas, hydrogen with a constant flow rate of 3 mL min^{-1} was used. FID was measured at 245 °C with a hydrogen flow of 40 mL min^{-1}, synthetic air flow of 400 mL min^{-1} and nitrogen as make-up gas at 30 mL min^{-1}. Identification was confirmed with Marine Oil FAME mix (20 components from C14:0 to C24:1; Restek GmbH, Bad Homburg, Germany) and FAME #12 mix (C13:0, C15:0, C17:0, C19:0, C21:0; Restek GmbH, Bad Homburg, Germany) as standards. Normalization was based on the internal methyl laurate (C12; Restek GmbH, Bad Homburg, Germany) standard. Calibration measurements with marine oil mix were performed with 20, 5, 1, 0.5, 0.1 mg mL^{-1}. For calibration with FAME #12 5, 2.5, 1.25, 0.5, 0.25, 0.05, 0.01 mg mL^{-1} were used, with methyl laurate 2, 1, 0.2, 0.05, 0.01, 0.002 mg mL^{-1} were used. This allowed comparative quantitation. FA profiles were calculated as percent of total FA content (w/w).

2.7. Proteomics

2.7.1. Protein Extraction and Precipitation

After cell harvest, samples were strictly kept on ice or at 4 °C in the centrifuge. Bacterial cells from 25 mL cultures were pelleted and washed twice with ddH_2O and centrifugation at 8000× g for 10 min. Lysis and extraction were aided by Protein Extraction Reagent Type 4 (Sigma-Aldrich, St. Louis, MO, USA) (1:3, v/v) and glass beads. Samples were vigorously vortexed for 30 min, then incubated in an ultrasonic bath for 60 min (Ultrasonic Cleaner UCD—THD, VWR, Radnor US). After centrifugation at 13,750× g for 30 min, protein precipitation was achieved by mixing the supernatant 1:1 (v/v) with 20% trichloric acid (v/v) in HPLC-grade acetone (v/v) supplemented with 10 mM dithiothreitol (DTT). The mixture was then vortexed and incubated for 1 h, at −20 °C. After centrifugation at 13,750× g for 10 min, the protein pellet was washed twice with 1 mL of acetone supplemented with 10 mM DTT. The pellet was air-dried and then dissolved in 8 M urea solution supplemented with 10 mM DTT. Three biological and two technical replicates were prepared for every condition.

2.7.2. Protein Quantification and SDS-PAGE

Protein concentration was determined using a Nanophotometer (NanoPhotometer NP80, Implen GmbH, München, Germany) at 280 nm absorbance. To visually assess the qualitative variances in protein levels, protein extracts were separated on a 12% one-dimensional SDS polyacrylamide gel, according to Awad et al. [26].

2.7.3. In-Gel Digestion of Protein Samples and LC-MS/MS Analysis

In-gel digestion of protein samples and LC–MS/MS analysis, using a timsTOF Pro mass spectrometer equipped with a NanoElute LC System (Bruker Daltonik GmbH, Bremen, Germany) on a Aurora column (250 × 0.075 mm, 1.6 µm; IonOpticks, Hanover St.,

Australia), was carried out according to the method of Fuchs et al. [27] with the following modifications: Short 12% SDS polyacrylamide gel was used instead of 10% Criterion™ Tris–HCl Protein Gel. The mobile phase comprised two mixtures for reverse-phase separation: 0.1% (*v*/*v*) formic acid—2% (*v*/*v*) acetonitrile—water mixture (A) and a 0.1% (*v*/*v*) formic acid—acetonitrile mixture (B), which was added as a binary gradient at a flow rate of 0.4 µL min^{-1}. A separation cycle of 120 min (linearly: 2–17% B in 60 min, 17–25% B in 30 min, 25–37% B in 10 min, 37–95% B in 10 min, maintaining B at 95% for 10 min) was performed. To allow measurement normalization, three QC samples, prepared by mixing 1 µL of each sample, were analyzed at equal intervals between samples (first, mid and last).

2.7.4. Bioinformatics Analysis

PEAKS Studio software 10.6 (Bioinformatics Solutions Inc., Waterloo, ON, Canada) [28–30] was used for peptide and subsequent protein identification. *R. erythropolis* JCM3201 protein (fasta) database based on genome assembly was obtained from NCBI (https://www.ncbi.nlm.nih.gov/genome/?term=txid1833[orgn], accessed on 10 May 2022, 5954 proteins). Search parameters included a precursor mass of 25 ppm using monoisotopic mass and fragment ion of 0.05 Da. Trypsin was selected as digestion enzyme, and a maximum two missed cleavages per peptide were allowed. FDR was set to 1.0%, and search was limited to at least 1 unique peptide per identified protein. The different groups were compared using the Quantification tool PEAKSQ, with a mass error tolerance of 20.0 ppm, Ion Mobility Tolerance of 0.05 Da and a Retention Time Shift Tolerance of 6 min (Auto Detect). Fold change and significance were set to 2 and all proteins were exported.

KOALA (KEGG Orthology And Links Annotation, https://www.kegg.jp/blastkoala/, accessed on 4 July 2022) was used for functional characterization of exported protein sequences [31]. Additionally, annotations were further manually validated with NCBI and Uniprot databases.

3. Results

3.1. Influence of Light Quality on Growth Characteristics and Carotenoid Accumulation

Throughout the cultivation period, distinct differential growth patterns amongst the various samples were apparent. Controls grown in dark condition as well as red-light-illuminated (680 nm) samples peaked at 24 h with an OD_{600nm} of 9. In contrast, cultures grown under SWW and green light (510 nm) illumination and to a higher extent blue light (455 nm) illumination exhibited notable reduction in growth compared to the former two sample groups (Figure 1a). The same effect could be observed during early stationary phase (40 h). Controls and red-light-illuminated samples reached an OD_{600nm} of 8.4 and 8.3, respectively, while cultures illuminated with different wavelengths stagnated at an OD_{600nm} of 5.7 and 6.3 for white and green light, respectively and an OD_{600nm} of 4.5 for blue light. At late stationary phase (122 h), all samples exhibited a slight but proportional decline in growth, with OD_{600nm} of 6.3 for controls and red-light-illuminated samples, 5.3 and 4.8 for cultures grown under white and green light, respectively, and 4.1 under blue light illumination.

DCW was determined after 40 and 122 h cultivation. No significant change in biomass formation was observed between control, white- and red-light-illuminated samples, with the latter reaching the highest DCW amongst all three samples at both time points (1.8 and 2.1 g L^{-1}, respectively). Samples grown under green light conditions exhibited a slightly lower biomass formation (1.4 and 1.5 g L^{-1}, at 40 and 122 h, respectively). Blue-light-illuminated samples formed the lowest DCW of 1.0 g L^{-1} following 122 h of cultivation (Figure 1c).

Carotenoid levels also varied between 40 and 122 h. Cultures illuminated with green light exhibited a significant increase in carotenoid levels after 40 h (0.0145 $Abs_{454nm}mg^{-1}{}_{DCW}$) compared to control samples grown under dark condition and samples illuminated with red light (0.0097 $Abs_{454nm}mg^{-1}{}_{DCW}$ and 0.0093 $Abs_{454nm}mg^{-1}{}_{DCW}$, respectively). Blue light illuminated samples deviated slightly from controls after 40 h of cultivation

(0.0081 $Abs_{454nm}mg^{-1}{}_{DCW}$). After 122 h, carotenoid level of samples under blue light illumination (0.0054 $Abs_{454nm}mg^{-1}{}_{DCW}$) were significantly lower when compared to the control (0.0127 $Abs_{454nm}mg^{-1}{}_{DCW}$). While carotenoid levels in samples illuminated with blue light decreased, an increase was observed in the control. This increase was also detected in red-light-illuminated samples, reaching comparable carotenoid levels to samples illuminated with white light. Samples under white light illumination exhibited only minor deviation from 40 h to 122 h. Notably, samples grown under green light had decreased carotenoid levels, reaching comparable values as dark, red and white light illuminated samples.

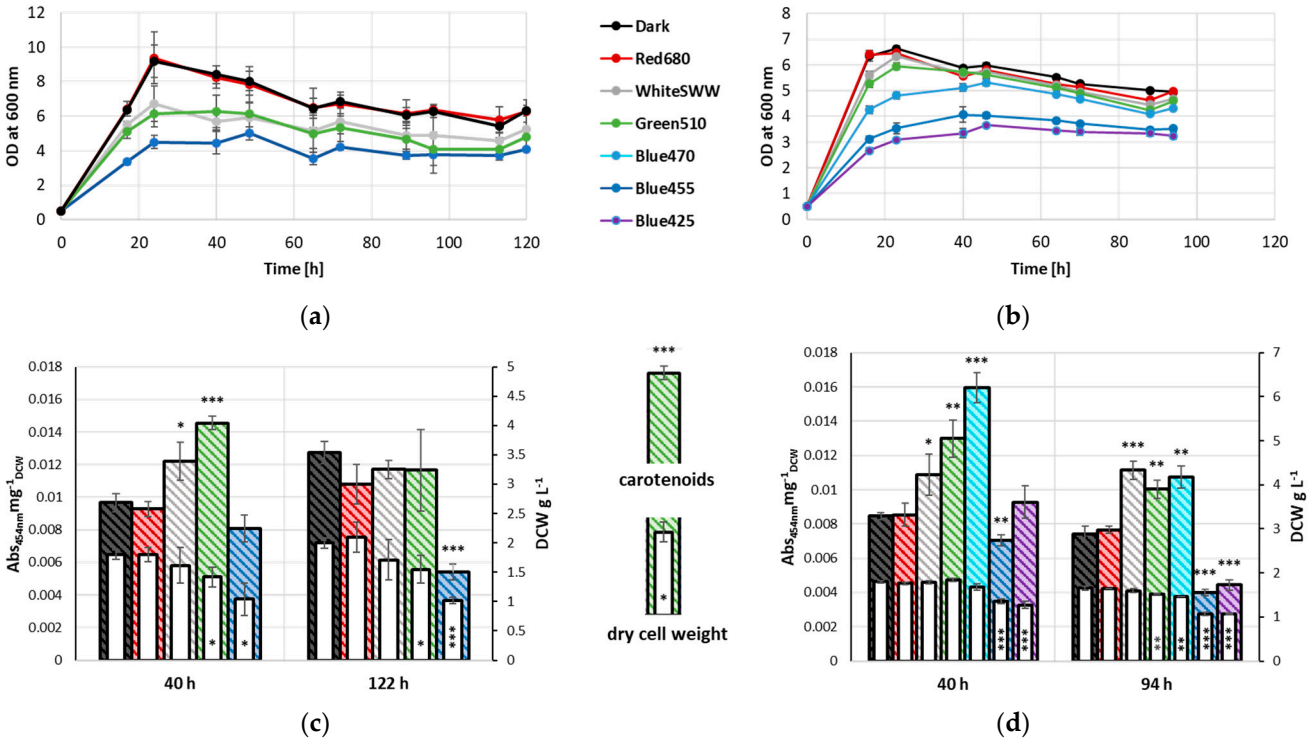

Figure 1. Growth of *R. erythropolis* measured as OD at 600 nm at 236 W s^{-2} illumination with white (standard warm white), blue (455 nm), green (510 nm) and red (680 nm) light as well as control cultivated under exclusion of light, n = 3. (**a**) Growth for 122 h. (**b**) Growth for 94 h with two additional wavelengths (425, 470 nm) of blue light; biomass formation (dry cell weight) and carotenoid accumulation (normalized to dry cell weight) of *R. erythropolis* at 236 W s^{-2} illumination with white (SWW), blue (455 nm), green (510 nm) and red (680 nm) light as well as a control, * $p < 0.05$, ** $p < 0.01$, *** $p < 0.001$ (t-tests evaluated against respective non-illuminated control), n = 3. (**c**) Biomass formation and carotenoid accumulation of *R. erythropolis* at 40 h and 122 h. (**d**) Biomass formation and carotenoid accumulation of *R. erythropolis* at 40 h and 94 h with two additional wavelengths (425, 470 nm) of blue light.

To further investigate the effect of blue light on growth and pigment formation in *R. erythropolis*, two additional wavelengths of blue light (425 and 470 nm) were evaluated. Since carotenoids reached similar levels in the late stationary phase (122 h), samples were collected at 94 h, to narrow the time frame during which these changes take place. Cells cultivated under 425 nm illumination exhibited severely reduced growth (OD_{600nm} 3.4 and 3.2, after 40 and 94 h, respectively) when compared to controls (OD_{600nm} 5.9 and 5.0 after 40 h and 94 h, respectively), and also exhibiting more growth impediment than samples under green light conditions (OD_{600nm} 4.1 and 3.5 after 40 h and 94 h, respectively). Illumination with 470 nm wavelength light led to intermediate effects on growth when compared to green and the 455 nm light, and allowed the formation of biomass at levels comparable to non-illuminated samples at 40 h. Interestingly, carotenoid accumulation after 40 h was

highly increased in the 470 nm illuminated cultures (0.0160 $Abs_{454nm}mg^{-1}{}_{DCW}$), while biomass formation was slightly reduced. In comparison, green-light-illuminated samples exhibited slightly lower carotenoid level (0.0130 $Abs_{454nm}mg^{-1}{}_{DCW}$), while the control reached carotenoid level of merely 0.0085 $Abs_{454nm}mg^{-1}{}_{DCW}$ (Figure 1b). When compared to the non-illuminated controls, illumination with 425 nm light did not exhibit differential carotenoid level in early stationary phase. After 94 h of cultivation, a significant decrease in carotenoid level was observed (0.0045 $Abs_{454nm}mg^{-1}{}_{DCW}$). Interestingly, carotenoid levels of samples illuminated with green light or 470 nm light dropped to comparable levels as white light after 94 h (Figure 1d).

Microscopy of all the *Rhodococcus* cultures showed agglomeration of cells under blue light conditions. While agglomeration was enhanced at 455 nm light illumination, only dense cellular aggregates could be detected in samples illuminated at 425 nm (Figure 2).

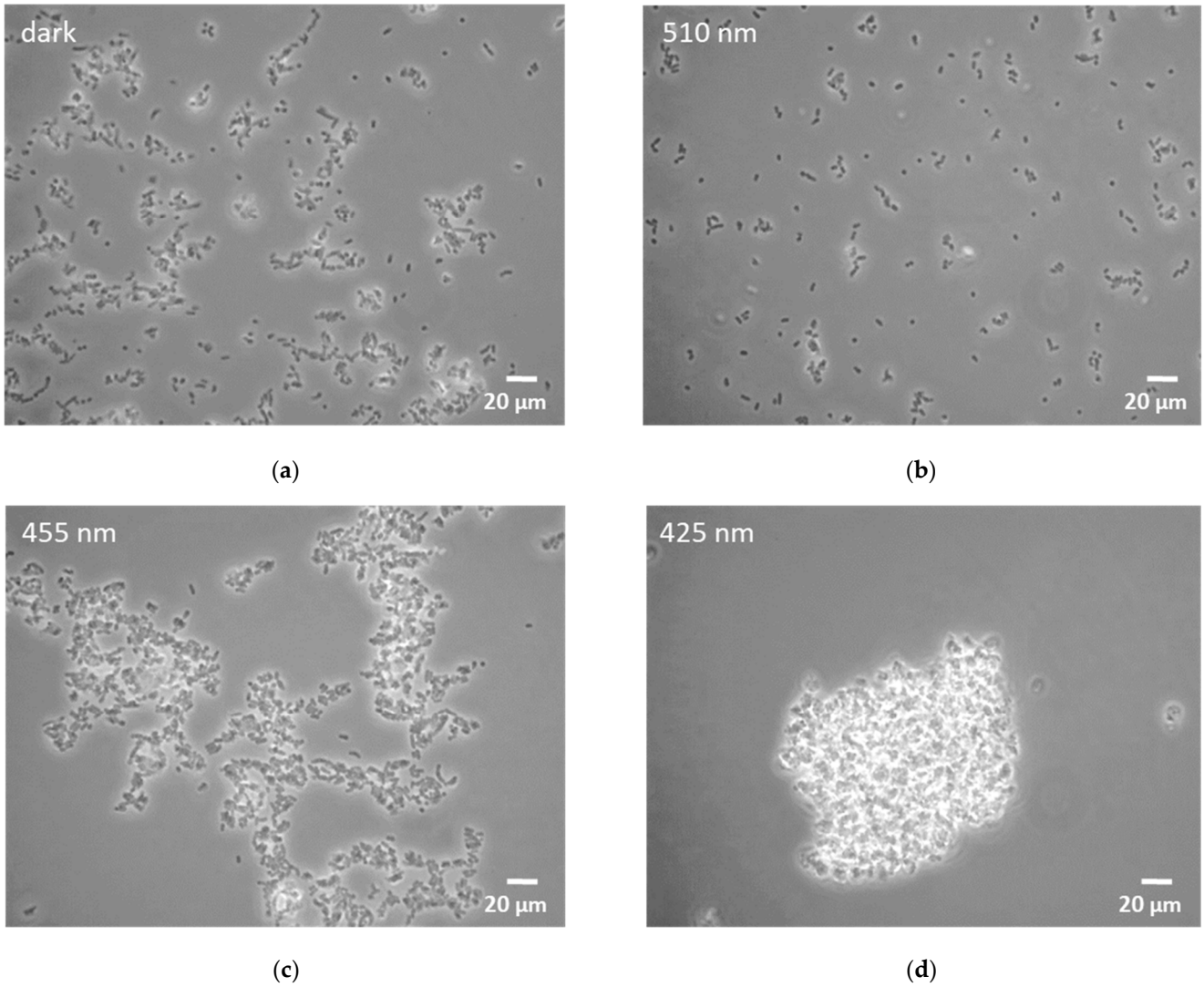

Figure 2. Microscopy images of *R. erythropolis* exposed to selected light conditions for 46 h. (**a**) Non-illuminated control; (**b**) green light (510 nm); (**c**) blue light (455 nm); (**d**) blue light (425 nm). Scale bar indicates a length of 20 µm.

3.2. Influence of Light Quality on Fatty Acid Composition

The influence of light on the FA profiles were assessed by FAME analysis. The FA content of *R. erythropolis* ranged between 45.6 and 59.4 µg $mg^{-1}{}_{DCW}$ for all cultures. Relative quantification of FAs are depicted as percentage of total FAs (*w*/*w*). Vaccenic acid (C18:1),

palmitic acid (C16:0) and palmitoleic acid (C16:1) remained the major FA components. Although the FA profile shifts induced by light stress only slightly diverged over time, the profile shift is most apparent in the increase in odd chain fatty acids (OCFAs; Figure 3). This shift in distribution can be observed as an increase in pentadecanoic acid (C15:0) as well as heptadecenoic acid (C17:1) in cells stressed under white and green light compared to non-illuminated control. After 40 h, OCFAs in cells treated with white light increased to 7.1% (C15:0) and 5.4% (C17:1). OCFAs in cells treated with green light increased to 8.1% (C15:0) and 5.6% (C17:1) compared to the control (2.7% C15:0 and 3.7% C17:1) (Figure 3a). These observations were recorded at all time points; over time, the concentration of OCFAs in the cultures remained nearly constant (Figure 3). Red light showed no significant effect on the FA profile compared to the control. For blue light wavelengths, a shift from C16:1 to C16:0 was detected. Illumination at 425, 455 and 470 nm wavelength resulted in C16:0 content of 24.8%, 25.5% and 24.2% as well as C16:1 content of 12.4%, 12.2% and 12.9%, respectively. In comparison, the control contained 17% of C16:0 and 16.6% of C16:1 at 40 h (Figure 3c). This measurement was consistent with samples collected at 94 h (Figure 3d).

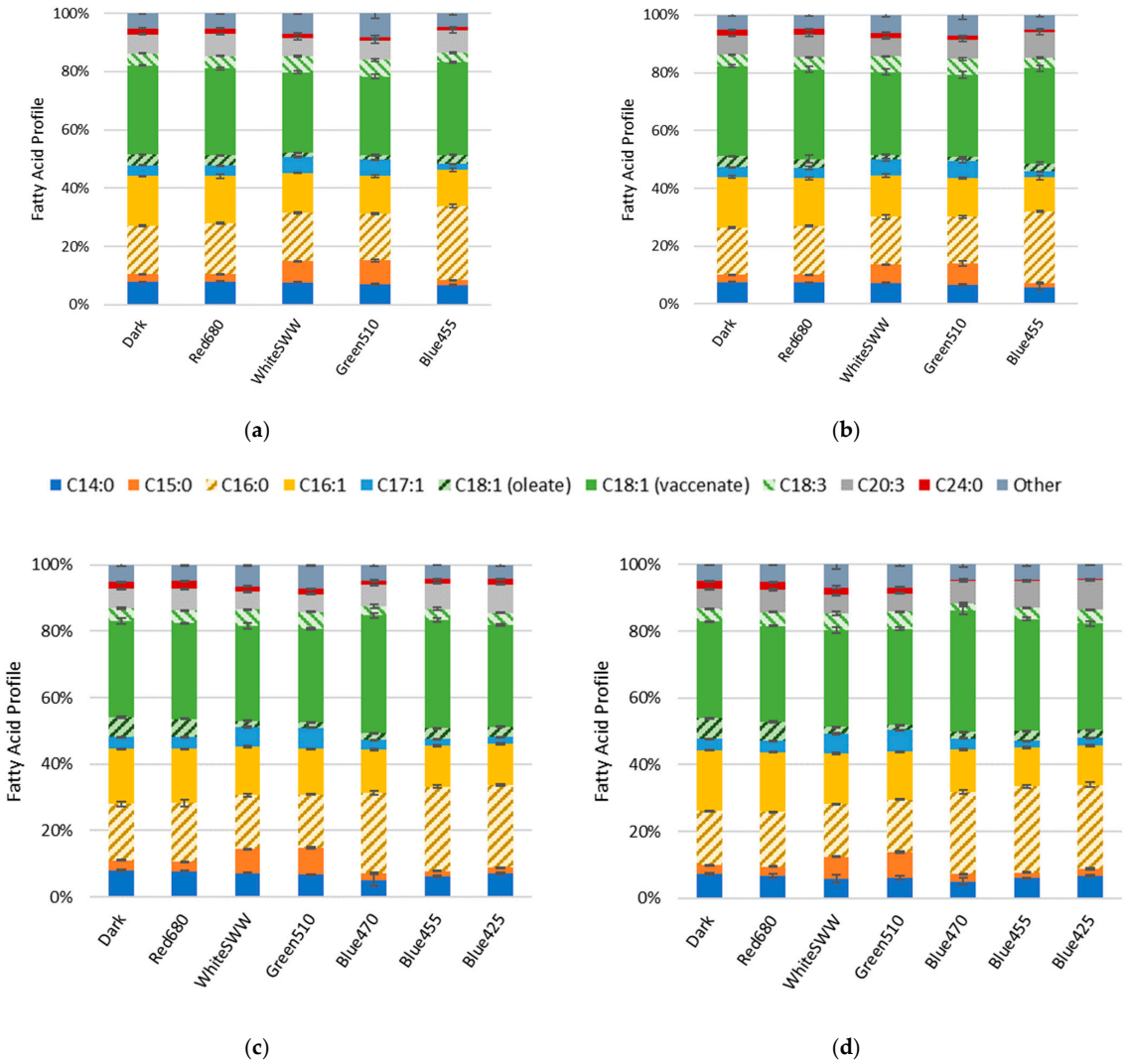

Figure 3. Fatty acid profiles of *R. erythropolis* at 236 W s^{-2} illumination with white (standard warm white), blue (425, 455 and 470 nm), green (510 nm) and red (680 nm) light as well as a control (n = 3). "Other" constitutes fatty acids with a representation below 2% of total fatty acid content (*w*/*w*), and include C14:1, C17:0, C18:0, C20:1, C20:5, C22:1. (**a**) Fatty acid profile collected at 40 h, (**b**) at 122 h, (**c**) at 40 h, (**d**) and at 94 h.

3.3. Effect of Light on Protein Levels

To elucidate the response of *R. erythropolis* to light stress, a time-resolved proteomics approach was implemented. As we were interested in the physiologically relevant stress response to natural light conditions, a daylight LED (6500 K) was chosen for further testing. Carotenoid titers are shown in Figure S3 (Supplementary Materials). A total of 3565 proteins of 5954 annotated proteins in the database were identified with at least one unique peptide, corresponding to a coverage of 60%. Time-resolved proteomics revealed 355 proteins (significance ≥ 2, fold change ≥ 2, detected in at least one sample per group, based on LFQ by PEAKS Studio; see Table S1, Supplementary Materials) as differentially regulated after 40 h under light stress. This set of proteins comprises 141 upregulated and 214 downregulated proteins compared to control (Figure 4a). After 122 h, 704 proteins were differentially regulated, of which 287 proteins were upregulated and 417 proteins downregulated compared to control (Figure 4b). In contrast to the phenotypic observations of increased carotenoid accumulation at 40 h, *R. erythropolis* exhibited a strong response on the proteomic level at 122 h; twice the number of proteins were differentially regulated by light stress, in comparison to 40 h.

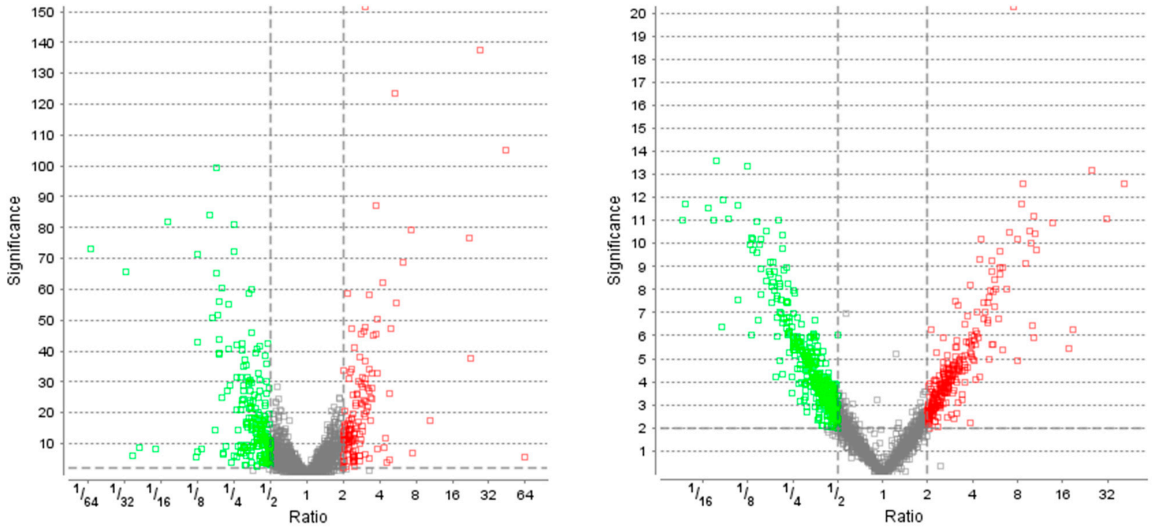

(**a**) (**b**)

Figure 4. Volcano plots of proteins extracted from cultures grown under LED light compared to the control. Analysis was performed based on label-free quantification (LFQ). The significance is plotted against the fold change ratio. The non-axial vertical lines denote fold change thresholds of 2 (upregulated ≥ 2 in red and downregulated ≤ 0.5 in green), the non-axial horizontal lines denote a significance threshold of 2. Figure compiled by PEAKS Studio Xpro. (**a**) Volcano plot after 40 h. (**b**) Volcano plot after 122 h.

Differentially regulated proteins (fold change and significance ≥ 2) were annotated to molecular functions by KEGG; orthologs may be assigned with the same KEGG Object (KO) identifier. At 40 h, 53.3% of down- and 44.7% of upregulated proteins were matched to KO identifiers. At 122 h, 53.5% of down- and 50.5% of upregulated protein were matched. Fold changes above 1 represent upregulation, while downregulation is illustrated by fold changes below 1.

Table 1 highlights proteins related to the stress response of *R. erythropolis* under light conditions with different abundance compared to the control at 40 and 122 h. Distinctly, four different transcription factors involved in oxidative stress response were identified: WP_020906739.1 (40 h 2.38-fold), WP_019747469.1 (40 h 2.38-fold; 122 h 3.88-fold), WP_060939090.1 (122 h 3.29-fold) and WP_020906601.1 (122 h 4.51-fold).

Additionally, several enzymes involved in inactivation of ROS were identified: WP_003940303.1 (40 h 3.06-fold; 122 h 2.80-fold), WP_021346030.1 (40 h 2.60-fold) and WP_003942119.1 (40 h 2.35-fold; 122 h 2.16-fold). However, a bifunctional catalase/peroxidase was identified in a cluster of downregulated genes (WP_060938296.1; 40 h 0.45-fold). A second protein, that exhibited a decreased level is WP_019749140.1 (122 h 0.49-fold). Two more stress-related proteins were upregulated: WP_019747464.1 (122 h 2.0-fold), WP_019749386.1 (40 h 2.39-fold). The regulation of WP_003942530.1 inverted during cultivation, displaying downregulation after 40 h and upregulation after 122 h (40 h 0.43-fold, 122 h 2.86-fold).

The shift in FA profile of *R. erythropolis* under light stress towards OCFAs could be connected to differentially regulated proteins involved in the propanoate pathway. At 40 h, 2-oxoisovalerate dehydrogenase E1 component alpha subunit (WP_060938994.1, K00166) and beta subunit (WP_060938993.1, K00167) as well as 2-oxoisovalerate dehydrogenase E2 component (WP_020970089.1, K09699) synthesizing propanoyl-CoA from 2-oxobutanoate were upregulated 3.82-, 2.63- and 3.05-fold, respectively. Dihydrolipoamide dehydrogenase (WP_174531767.1, K00382), which facilitates the reaction of dihydrolipoamide-E to lipoamide-E was downregulated by 0.41-fold. This enzymatic step branches off the propanoyl-CoA production pathway from 2-oxobutanoate. Furthermore, the acetyl-CoA synthetase (WP_019745948.1, K01895) facilitating the reaction from propanoyl-CoA to propanoate is downregulated by 0.46-fold (Figure 5).

At 122 h, the following enzymes remained upregulated (K00166, K00167, K09699): WP_060938994.1, 2.73-fold; WP_060938993.1, 2.62-fold; WP_020970089.1, 3.10-fold. In contrast to this, proteins matched to the same activity and therefore the same KO identifiers were downregulated: WP_060938768.1, WP_060938769.1 and WP_060938770.1 with a 0.42-, 0.23-, 0.35-fold change, respectively. The enzyme bccA (WP_060939079.1) synthesizing malonyl-CoA from acetyl-CoA was upregulated at both time points (40 h 3.28-fold; 122 h 3.92-fold).

Additionally, two enzymes of the cyclopropane-fatty-acyl-phospholipid synthase family were significantly upregulated. After 40 and 122 h, levels of WP_060938639.1 increased 22.02- and 18.92-fold. The level of WP_060938640.1 increased 43.79- and 31.54-fold, respectively (Table 2).

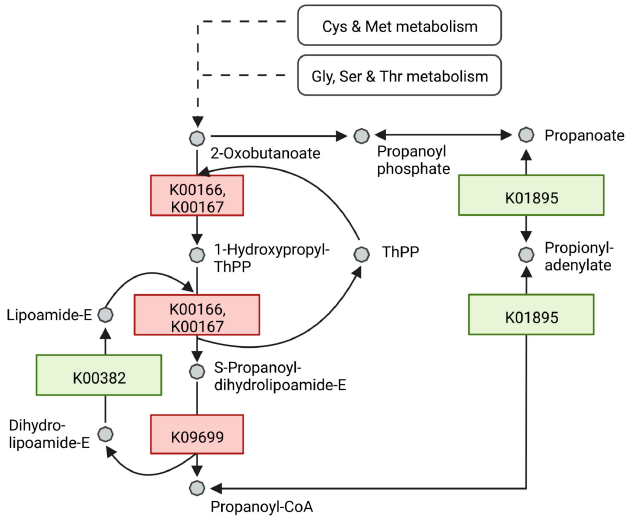

Figure 5. Schematic illustration of an excerpt from the propanoate metabolism in *R. erythropolis*. After 40 h of growth, proteins which are at least 2-fold upregulated by light stimulation are depicted in red, proteins downregulated at least 2-fold are depicted in green. Each enzyme is represented with its respective KO identifier. Cys = Cysteine, Met = Methionine, Gly = Glycine, Ser = Serine, Thr = Threonine. Adapted from KEGG pathway 00640 Propanoate metabolism. Created with BioRender.com.

Table 1. Selected proteins involved in oxidative stress discussed here. Protein abundance and fold change in samples grown under white light were compared to non-illuminated control. NCBI accession numbers as well as matched KO identifiers are listed. Further identified unique peptides, significance and fold change at 40 h and 122 h of samples are stated. Fractions below 1 depict downregulation. n.d. = not detected.

Transcription Factors Involved in Oxidative Stress								
			40 h			122 h		
Accession Number	**Description**	**KO-ID**	**Identified Unique Peptides**	**Significance**	**Fold Change**	**Identified Unique Peptides**	**Significance**	**Fold Change**
WP_019747469.1	SigB; RNA polymerase sigma-B factor	K03090	1	3.8	2.38	1	2.2	3.88
WP_020906601.1	hspR; MerR family transcriptional regulator, heat shock protein hspR	K13640	2	2.36	1.38	1	4.19	4.51
WP_020906739.1	MULTISPECIES: RNA polymerase sigma factor SigF [*Rhodococcus*]	K03090	1	4.35	2.38	n.d.	n.d.	n.d.
WP_060939090.1	hspR; MerR family transcriptional regulator, heat shock protein hspR	K13640	5	4.07	1.39	4	4.52	3.29
Catalases and Peroxidases								
WP_019749140.1	BCP, PRXQ, DOT5; thioredoxin-dependent peroxiredoxin [EC:1.11.1.24]	K03564	8	0.11	0.99	8	3.13	0.49
WP_021346030.1	katE, CAT, catB, srpA; catalase [EC:1.11.1.6]	K03781	14	26.31	2.6	14	0.19	1.06
WP_003940303.1	SOD; superoxide dismutase, Fe-Mn family [EC:1.15.1.1]	K04564	5	47.57	3.06	3	4.34	2.8
WP_003942119.1	ahpC; lipoyl-dependent peroxiredoxin subunit C [EC:1.11.1.28]	K24126	16	47.31	2.35	16	3.56	2.16
WP_060938296.1	katG; catalase-peroxidase [EC:1.11.1.21]	K03782	27	23.13	0.45	24	1.78	0.63
Other Stress-Related Proteins								
WP_003942530.1	trxA; thioredoxin	K03671	2	9.59	0.43	3	4.05	2.86
WP_019747464.1	dps; starvation-inducible DNA-binding protein	K04047	14	0.32	0.98	14	2.98	2.0
WP_019749386.1	dnaJ; molecular chaperone DnaJ	K03686	12	5.42	2.39	13	0.78	1.28

Table 2. Selected proteins involved in propanoate metabolism and cyclopropane-fatty-acyl-phospholipid synthesis discussed here. Protein abundance and fold change in samples grown under white light were compared to non-illuminated control. NCBI Accession numbers as well as matched KO identifiers are listed. Further identified unique peptides, significance and fold change at 40 h and 122 h of samples are stated. Fractions below 1 depict downregulation. n.d. = not detected.

Propanoate Pathway								
			40 h			122 h		
Accession Number	Description	KO-ID	Identified Unique Peptides	Significance	Fold Change	Identified Unique Peptides	Significance	Fold Change
WP_019745948.1	acs; acetyl-CoA synthetase [EC:6.2.1.1]	K01895	20	26.37	0.46	15	13.6	0.08
WP_020970089.1	bkdB; 2-oxoisovalerate dehydrogenase E2 component (dihydrolipoyl transacylase) [EC:2.3.1.168]	K09699	7	29.17	3.05	7	4.78	3.1
WP_060938768.1	bkdA1; 2-oxoisovalerate dehydrogenase E1 component alpha subunit [EC:1.2.4.4]	K00166	22	20.92	0.59	19	4.81	0.42
WP_060938769.1	bkdA2; 2-oxoisovalerate dehydrogenase E1 component beta subunit [EC:1.2.4.4]	K00167	11	28.47	0.57	11	8.94	0.23
WP_060938770.1	bkdB; 2-oxoisovalerate dehydrogenase E2 component (dihydrolipoyl transacylase) [EC:2.3.1.168]	K09699	21	23.64	0.55	18	5.08	0.35
WP_060938993.1	bkdA2; 2-oxoisovalerate dehydrogenase E1 component beta subunit [EC:1.2.4.4]	K00167	11	30.2	2.63	12	4.09	2.62
WP_060938994.1	bkdA1; 2-oxoisovalerate dehydrogenase E1 component alpha subunit [EC:1.2.4.4]	K00166	12	50.3	3.82	13	4.41	2.73

Table 2. *Cont.*

Propanoate Pathway								
			40 h			122 h		
Accession Number	**Description**	**KO-ID**	**Identified Unique Peptides**	**Significance**	**Fold Change**	**Identified Unique Peptides**	**Significance**	**Fold Change**
WP_060939079.1	bccA, pccA; acetyl-CoA/propionyl-CoA carboxylase, biotin carboxylase, biotin carboxyl carrier protein [EC:6.4.1.2 6.4.1.3 6.3.4.14]	K11263	31	58.35	3.28	34	5.63	3.92
WP_060939587.1	acs; acetyl-CoA synthetase [EC:6.2.1.1]	K01895	23	33.08	2.28	20	4.29	2.39
WP_174531767.1	DLD, lpd, pdhD; dihydrolipoamide dehydrogenase [EC:1.8.1.4]	K00382	22	30.59	0.41	16	8.77	0.19
Cyclopropane-Fatty-Acyl-Phospholipid Synthase Family								
WP_060938639.1	cfa; cyclopropane-fatty-acyl-phospholipid synthase [EC:2.1.1.79]	K00574	2	76.43	22.02	1	6.24	18.92
WP_060938640.1	cfa; cyclopropane-fatty-acyl-phospholipid synthase [EC:2.1.1.79]	K00574	3	105.03	43.79	4	11.05	31.54

4. Discussion

4.1. Effects of Light Illumination on Growth

In accordance with previous studies [7,10–14], blue light exhibits antimicrobial activity on *R. erythropolis*. Spectrophotometric (OD_{600nm}) data and DCW consistently revealed a significant decrease in bacterial growth when illuminated with 425 or 455 nm blue light. To a lesser extent, cells illuminated by 470 nm light also exhibited reduced growth, with OD_{600nm} values between 455 nm and green light illumination. Wang et al. [11] reported similar results when comparing the effects of 405 nm to 470 nm light illumination on the human pathogen *Neisseria gonorrhoeae*, the causative agent of Gonorrhoeae. Furthermore, Mathews and Sistrom [32] reported that carotenoid-deficient mutants of the pigment-producing non-phototrophic organism *Sarcina lutea* were highly susceptible to sunlight. However, lethal effects could only be observed under aerobic conditions, while wild-type cells were not affected by either condition (light anaerobic condition, light aerobic condition). They concluded that photo-oxidative conditions were required to exhibit antimicrobial effects on *S. lutea*, as stand-alone light stress was not sufficient to cause lethal effects. Furthermore, they stated, that carotenoids can protect cells against photo-oxidative damage, as wild-type was not susceptible to sunlight treatment [32]. This cumulative data suggests that the antimicrobial effect of blue light could, in part, be propagated by endogenous photosensitizer present in *R. erythropolis*. These photosensitizers would absorb light-energy and transfer the excitation energy or electrons onto oxygen, resulting in ROS among other reaction products [6–8].

White light and green light also had distinct effects on cell growth. Here, cultures exhibited slightly decreased growth compared to the control for around 24 h from inoculation. After that, differences in growth slowly decreased. This is likely correlated to the induction of intracellular adaptation mechanisms such as increasing carotenoid content, which, following initial adaptation period, enabled growth more similar to those of control samples. Red light did not have an effect on culture growth and carotenoid accumulation.

4.2. Changes in Carotenoid Content

Spectrometric analysis of sample extracts after 40 h growth revealed a drastic increase in carotenoid level, particularly when cells were illuminated with blue (470 nm) and green (510 nm) light and to a lesser extend with white light. This observation suggests that carotenoids in *R. erythropolis* serve as protectors against photo-oxidative damage. As carotenoids themselves generally absorb light in the range of 400 to 550 nm, they can protect endogenous photosensitizers from exciting light of that wavelength. Available models describe the reaction of carotenoids with reactive oxygen species (e.g., singlet oxygen), where the former drain the excitation energy from the singlet oxygen and subsequently dissipate the captured energy via heat formation. They might react similarly with different endogenous excited photosensitizers, preventing the formation of ROS. Other models also predict possible reactions with radicals, generating different mechanisms by which these reactions and the subsequent recovery of reacted carotenoids could occur [6,8,15].

Following 122 h of cultivation, 425 nm blue light led to a significant decrease in carotenoid content, consistent with the severe decrease in biomass formation. Growth under dark conditions and red light illumination led to comparable carotenoid levels to those of cultures grown under white or green light. Here, carotenoid levels under dark conditions and red light illumination increased, while samples under green light conditions exhibited decreased carotenoid accumulation. Nutrient limitation, especially nitrogen limitation, can trigger carotenoid accumulation in *Rhodococcus*, this could explain the increase in carotenoids in control and red-light-illuminated samples [33,34]. As nitrogen limitation often occurs simultaneously with oxidative stress, carotenoid accumulation could present as an adaptation response mechanism [35]. This is in line with the 2.0-fold increase in Dps, a starvation-inducible DNA-binding protein, after 122 h. Dps is mainly regulated by nutrient deprivation and also acts in oxidative stress response. In our work, no differential regulation of Dps was observed at 40 h [36–38]. As stated earlier, carotenoid

level in cells illuminated with green or blue (470 nm) light significantly increased during the first 40 h of cultivation, but decreased in late stationary phase (94 h and 122 h). This change in accumulation levels could occur due to nutrient deficiency in late stationary phase and the resulting energy demand being too severe to maintain these high amounts of carotenoids. Therefore, expendable amounts of carotenoids were degraded. Comparison between samples taken at 122 h and 94 h revealed that the observed decrease in carotenoids in light treated samples already occurred before 122 h. However, an increase in carotenoid content in non-illuminated controls and red-light-illuminated samples did not occur after 94 h of cultivation.

In summary, the detected increase in carotenoids under white, green and blue (470 nm) light represents an early response (40 h) to light stress, while the later increase in carotenoid levels for control and red illuminated samples (122 h) depicts an adaptive response to nitrogen limitation, which occurs at a later point. In accordance to these findings, Cohen et al. [39] observed an increase in carotenoid content in *Rhodococcus* sp. APG1 isolates when grown under light.

4.3. Transcription Factors

Proteomics analysis allowed identification of several proteins involved in photo-oxidative stress response. Sigma factor sigF (WP_020906739.1) is part of the heat stress and oxidative stress response in *Mycobacterium smegmatis* [40,41]. Within this studies' data, sigF displays a 2.38-fold increase in protein level after 40 h; however, it was not differentially regulated after 122 h of cultivation. In contrast, sigB (WP_019747469.1) a light- and heat-stress-related sigma factor, was significantly up-regulated at 40 h and 122 h (2.38-fold and 3.88-fold, respectively). sigB is well characterized in *Listeria monocytogenes* and *Synechocystis* sp. PCC 6803 and is induced as an essential factor during heat-, oxidative- and light-stress response, especially under blue light [42–46]. Furthermore, Hakkila et al. [45] and Turunen et al. [44] reported similar results in the cyanobacterium *Synechocystis* sp. *PCC 6803*. The former group was able to engineer mutants of *S.* sp. *PCC 6803* with deletion mutations in all group 2 σ factors except sigB. The mutants exhibited high carotenoid accumulation and good growth under singlet oxygen and high light stress [45].

Two more proteins belonging to the hspR MerR transcriptional regulator family (WP_060939090.1 and WP_020906601.1) were upregulated after 122 h (3.29- and 4.51-fold) and were recently reported to be involved in hydrogen peroxide-induced oxidative stress response. Additionally, Lu et al. [47] established, that mutants missing hspR activity exhibited greater sensitivity to hydrogen peroxide. Furthermore, they identified *ahpC*, coding for a lipoyl-dependent peroxiredoxin, to be upregulated by hspR activity.

4.4. Catalases and Peroxidases

Three enzymes involved in ROS-inactivation were identified as additional indicators of photo-oxidative stress after 40 h. A superoxide dismutase (SOD) (WP_003940303.1) was 3.06-fold upregulated, while a monofunctional catalase (WP_021346030.1; katE) was upregulated 2.60-fold under light compared to the control. SOD converts superoxide radicals to hydrogen peroxide, the catalase reduces two hydrogen peroxide molecules to water and molecular oxygen. *katE* is of major interest, as it is reported to be induced by hydrogen peroxide. On the contrary *katG* (WP_060938296.1), a gen coding for a catalase/peroxidase found in a cluster of downregulated proteins after 40 h (0.45-fold), is reported not to be affected by hydrogen peroxide level [20,35,48].

The third enzyme, ahpC (WP_003942119.1), more specifically a subunit of the respective enzyme exhibited a 2.35-fold increase in protein abundance. This enzyme belongs to a group of peroxidases that utilize cysteine residues for reduction in alkyl-peroxides.

After 122 h, SOD and ahpC levels remained upregulated under light conditions (2.80- and 2.16-fold, respectively); however, no other differentially upregulated catalases were confirmed. Interestingly, another peroxidase (thioredoxin-dependent thiol peroxidase; WP_019749140.1) exhibited a 2-fold decrease in protein level after 122 h.

4.5. Other Proteins Related to Stress

Besides proteins specific to certain types of stress response dnaJ a molecular chaperon is part of the overall stress response [20,35]. However, upregulation was only detected after 40 h (WP_019749386.1 2.39-fold). Furthermore, levels of thioredoxin trxA, another part of an antioxidant system [20,35], was downregulated after 40 h of cultivation (0.43-fold), but exhibited elevated levels after 122 h (WP_003942530.1 2.86-fold).

Interestingly, a starvation-inducible DNA-binding protein (Dps) (WP_019747464.1) did not differ in protein abundance after 40 h, but increased 2.0-fold after 122 h, indicating severe nutrient deficiency in samples at late stationary phase. Previous reports presented data linking Dps to nutrient deprivation as well as oxidative stress, where its production is induced as part of the stress response [36–38].

4.6. Influence of Light on Fatty Acid Composition

One aspect of adaptation to various stress conditions takes place at the cell membrane. To maintain biological functions, bacteria adapt their lipid composition to maintain membrane fluidity by changing the level of FA saturation [49–51]. Properties, such as membrane fluidity and permeability, are of major importance for cell survival. Temperature fluctuation, oxidation of cellular lipids and other stressors can threaten cell viability and trigger changes in membrane composition, modulating these properties [18,19].

While oxidative stress led to increased lipid accumulation in the closely related *R. opacus* [52], the FA content remained in a similar range of around 5% (g g^{-1} $_{DCW}$) in all *R. erythropolis* samples subjected to light stress.

After exposure to H_2O_2-induced oxidative stress, a decrease in cell size and the tendency to form multicellular conglomerates was observed in *R. opacus* 1CP [22]. In our study, *R. erythropolis* cells subjected to blue light stress also agglomerated (455 nm)/aggregated (425 nm) (Figure 2). In this manner, inner cells of the agglomerate/aggregate could be shielded from damaging blue light [53,54].

The FA composition of *R. erythropolis* shifts towards saturated FAs, especially C16:0, in contrast to the observation reported by Solyanikova et al. [22] for *R. opacus* 1CP, where upon H_2O_2 exposure, levels in unsaturated FAs increased. The increase in saturated FA detected in our work is in accordance with Wu et. al., whereby methicillin-resistant *S. aureus* (MRSA) displayed decreased levels of unsaturated FAs, namely, C16:1, C20:1 and C20:4, when illuminated with blue light (415 nm) [55]. It is hypothesized that an increase in saturated FAs in the membrane renders the membrane less permeable [20].

The levels of saturated OCFAs, mainly C15:0 and C17:0 (2- to 3-fold), and branched (10-methyl) FAs were reported to be increased in *R. opacus* in the presence of aromatic compounds [56]. In our work, elevated content of OCFAs were detected under green and white light conditions. OCFAs were produced in *Yarrowia lipolytica* and *Rhodococcus* sp. YHY01 when supplemented with propionate as carbon source. Propanoyl-CoA was proposed as primer for OCFA synthesis in *Rhodococcus*, while malonyl-CoA, generated from acetyl-CoA, acts as primer for even chain fatty acid synthesis [57,58]. As a metabolic intermediate, propanoyl-CoA can be synthesized by the degradation of propionate, OCFAs and some amino acids such as cysteine, methionine and threonine. Due to the cellular toxicity of propanoyl-CoA at high concentrations, microorganisms evolved to regulate its accumulation [59,60]. As depicted in Figure 5, 2-oxoisovalerate dehydrogenase E1 component subunits (K00166 and K00167) as well as 2-oxoisovalerate dehydrogenase E2 (K09699), responsible for the synthesis of propanoyl-CoA are upregulated at 40 h and 122 h for cells cultivated under white light. Increased availability of these enzymes could explain the increase in OCFAs, namely, C15:0 and C17:1, in *R. erythropolis* cells. The bidirectional acetyl-CoA synthetase (K01895) could be tightly regulated under feedback mechanisms to limit the adenylation of propanoyl-CoA back to propionate, ensuring ample levels of the building block for OCFA production. The enzyme level is downregulated by 2-fold under light conditions.

Furthermore, time-resolved proteomics revealed a significant increase in cyclopropane-fatty-acyl-phospholipid synthase family proteins. Specifically, levels of two proteins, WP_060938639.1 and WP_060938640.1, exhibited a drastic 22.0-fold and 43.8-fold increase after 40 h under light conditions and an 18.9-fold and 31.5-fold increase after 122 h, respectively. These enzymes are responsible for modification of FA double bonds by adding cyclopropyl moieties, a modification that was found to increase resistance to different stresses in *E. coli* and other bacteria, namely, high pressure, acidity and heat resistance [18,19]. Our work demonstrates that protein production of this group of enzymes is also subject to light stress. The effect of heat or temperature stress, especially in combination with light stress, could be further investigated in *R. erythropolis*.

5. Conclusions

The results obtained in this study provide insight into adaptation mechanisms of *R. erythropolis* when subjected to photo-oxidative stress. To that end, an increase in stress-related sigma factors and other proteins, specifically peroxidases, was detected by time-resolved proteomic analysis. Most proteins discussed here were directly linked to oxidative stress specifically, indicating that light stress in *R. erythropolis* likely acts via endogenous photosensitizers and oxygen. Blue light (425, 455 nm) significantly curbed growth, while green (510) and white (SWW) light led to slightly reduced growth compared to control under dark conditions, further adding to previous studies investigating antimicrobial properties blue light. Blue light of 470 nm wavelength exhibited an intermediate effect between white/green and blue (455, 425 nm) light. Additionally, carotenoid levels were found to be increased in samples illuminated with SWW light and to much higher extent when treated with green (510 nm) and blue (470 nm) light. In regard to previous studies, these results imply carotenoids are synthesized as part of a photo-oxidative stress response. Stress adaptations further involved a shift in FA composition towards OCFAs as well as saturated and branched FAs, likely altering membrane properties.

Supplementary Materials: The following supporting information can be downloaded at: https://www.mdpi.com/article/10.3390/microorganisms10081680/s1, Figure S1: Spectrum of light, Figure S2: Customized shaking incubator, Table S1: Proteomics-Effect of light on RE3201.xlsx, Table S2: OD, Table S3: DCW; Table S4: Carotenoid accumulation, Table S5: Fatty acid profile, Figure S3: Carotenoid accumulation of proteomic samples, Figure S4: Schematic figure of heat map of proteomic analysis, high resolution figures are provided as separate files (Figure S4a.png and Figure S4b.png).

Author Contributions: Conceptualization, all authors; methodology, S.E.-S., P.C., F.H., and M.H.; validation, all authors; writing—original draft preparation, S.E.-S. and P.C.; writing—review and editing, D.A., T.B. and N.M.; project administration, N.M.; funding acquisition, N.M. All authors have read and agreed to the published version of the manuscript.

Funding: This research was funded by the German Federal Ministry of Education and Research (BMBF), project OleoBuild, grant number: 031B0853A.

Data Availability Statement: Not applicable.

Acknowledgments: The authors gratefully acknowledge the valuable input offered by Felix Melcher and Nathanael Arnold with regard to experimental LED setup.

Conflicts of Interest: The authors declare no conflict of interest.

References

1. Bell, K.S.; Philp, J.C.; Aw, D.W.; Christofi, N. The genus *Rhodococcus*. *J. Appl. Microbiol.* **1998**, *85*, 195–210. [CrossRef] [PubMed]
2. Gűrtler, V.; Seviour, R.J. Systematics of Members of the Genus *Rhodococcus* (Zopf 1891) Emend Goodfellow et al. 1998. In *Biology of Rhodococcus*; Microbiology Monographs; Springer: Berlin/Heidelberg, Germany, 2010; pp. 1–28.
3. Cappelletti, M.; Presentato, A.; Piacenza, E.; Firrincieli, A.; Turner, R.J.; Zannoni, D. Biotechnology of *Rhodococcus* for the production of valuable compounds. *Appl. Microbiol. Biotechnol.* **2020**, *104*, 8567–8594. [CrossRef] [PubMed]

4. Ceniceros, A.; Dijkhuizen, L.; Petrusma, M.; Medema, M.H. Genome-based exploration of the specialized metabolic capacities of the genus *Rhodococcus*. *BMC Genom.* **2017**, *18*, 593. [CrossRef] [PubMed]
5. de Carvalho, C.C.; da Fonseca, M.M. The remarkable *Rhodococcus erythropolis*. *Appl. Microbiol. Biotechnol.* **2005**, *67*, 715–726. [CrossRef] [PubMed]
6. Sandmann, G. Antioxidant Protection from UV- and Light-Stress Related to Carotenoid Structures. *Antioxidants* **2019**, *8*, 219. [CrossRef]
7. Dai, T.; Gupta, A.; Murray, C.K.; Vrahas, M.S.; Tegos, G.P.; Hamblin, M.R. Blue light for infectious diseases: *Propionibacterium acnes*, *Helicobacter pylori*, and beyond? *Drug Resist. Updates* **2012**, *15*, 223–236. [CrossRef]
8. Orlandi, V.T.; Bolognese, F.; Chiodaroli, L.; Tolker-Nielsen, T.; Barbieri, P. Pigments influence the tolerance of *Pseudomonas aeruginosa* PAO1 to photodynamically induced oxidative stress. *Microbiology* **2015**, *161*, 2298–2309. [CrossRef]
9. Sharma, P.; Jha, A.B.; Dubey, R.S.; Pessarakli, M. Reactive Oxygen Species, Oxidative Damage, and Antioxidative Defense Mechanism in Plants under Stressful Conditions. *J. Bot.* **2012**, *2012*, 1–26. [CrossRef]
10. Halstead, F.D.; Thwaite, J.E.; Burt, R.; Laws, T.R.; Raguse, M.; Moeller, R.; Webber, M.A.; Oppenheim, B.A. Antibacterial Activity of Blue Light against Nosocomial Wound Pathogens Growing Planktonically and as Mature Biofilms. *Appl. Environ. Microbiol.* **2016**, *82*, 4006–4016. [CrossRef]
11. Wang, Y.; Ferrer-Espada, R.; Baglo, Y.; Gu, Y.; Dai, T. Antimicrobial Blue Light Inactivation of *Neisseria gonorrhoeae*: Roles of Wavelength, Endogenous Photosensitizer, Oxygen, and Reactive Oxygen Species. *Lasers Surg. Med.* **2019**, *51*, 815–823. [CrossRef]
12. Guffey, J.S.; Wilborn, J. In vitro bactericidal effects of 405-nm and 470-nm blue light. *Photomed. Laser Surg.* **2006**, *24*, 684–688. [CrossRef] [PubMed]
13. Kim, S.; Kim, J.; Lim, W.; Jeon, S.; Kim, O.; Koh, J.T.; Kim, C.S.; Choi, H.; Kim, O. In vitro bactericidal effects of 625, 525, and 425 nm wavelength (red, green, and blue) light-emitting diode irradiation. *Photomed. Laser Surg.* **2013**, *31*, 554–562. [CrossRef] [PubMed]
14. Tardu, M.; Bulut, S.; Kavakli, I.H. MerR and ChrR mediate blue light induced photo-oxidative stress response at the transcriptional level in *Vibrio cholerae*. *Sci. Rep.* **2017**, *7*, 40817. [CrossRef] [PubMed]
15. Sumi, S.; Suzuki, Y.; Matsuki, T.; Yamamoto, T.; Tsuruta, Y.; Mise, K.; Kawamura, T.; Ito, Y.; Shimada, Y.; Watanabe, E.; et al. Light-inducible carotenoid production controlled by a MarR-type regulator in *Corynebacterium glutamicum*. *Sci. Rep.* **2019**, *9*, 13136. [CrossRef] [PubMed]
16. Mathews, M.M.; Sistrom, W.R. Intracellular location of carotenoid pigments and some respiratory enzymes in *Sarcina lutea*. *J. Bacteriol.* **1959**, *78*, 778–787. [CrossRef]
17. de Carvalho, C.C. Adaptation of *Rhodococcus erythropolis* cells for growth and bioremediation under extreme conditions. *Res. Microbiol.* **2012**, *163*, 125–136. [CrossRef]
18. Choi, T.R.; Song, H.S.; Han, Y.H.; Park, Y.L.; Park, J.Y.; Yang, S.Y.; Bhatia, S.K.; Gurav, R.; Kim, H.J.; Lee, Y.K.; et al. Enhanced tolerance to inhibitors of *Escherichia coli* by heterologous expression of cyclopropane-fatty acid-acyl-phospholipid synthase (cfa) from *Halomonas socia*. *Bioprocess. Biosyst. Eng.* **2020**, *43*, 909–918. [CrossRef]
19. Hari, S.B.; Grant, R.A.; Sauer, R.T. Structural and Functional Analysis of *E. coli* Cyclopropane Fatty Acid Synthase. *Structure* **2018**, *26*, 1251–1258. [CrossRef]
20. Patek, M.; Grulich, M.; Nesvera, J. Stress response in *Rhodococcus* strains. *Biotechnol. Adv.* **2021**, *53*, 107698. [CrossRef]
21. de Carvalho, C.C.; Marques, M.P.; Hachicho, N.; Heipieper, H.J. Rapid adaptation of *Rhodococcus erythropolis* cells to salt stress by synthesizing polyunsaturated fatty acids. *Appl. Microbiol. Biotechnol.* **2014**, *98*, 5599–5606. [CrossRef]
22. Solyanikova, I.P.; Suzina, N.E.; Emelyanova, E.V.; Polivtseva, V.N.; Pshenichnikova, A.B.; Lobanok, A.G.; Golovleva, L.A. Morphological, Physiological, and Biochemical Characteristics of a Benzoate-Degrading Strain *Rhodococcus opacus* 1CP under Stress Conditions. *Mikrobiologiia* **2017**, *86*, 188–200. [CrossRef] [PubMed]
23. Paper, M.; Glemser, M.; Haack, M.; Lorenzen, J.; Mehlmer, N.; Fuchs, T.; Schenk, G.; Garbe, D.; Weuster-Botz, D.; Eisenreich, W.; et al. Efficient Green Light Acclimation of the Green Algae *Picochlorum* sp. Triggering Geranylgeranylated Chlorophylls. *Front. Bioeng. Biotechnol.* **2022**, *10*, 689. [CrossRef] [PubMed]
24. Woortman, D.V.; Fuchs, T.; Striegel, L.; Fuchs, M.; Weber, N.; Bruck, T.B.; Rychlik, M. Microalgae a Superior Source of Folates: Quantification of Folates in Halophile Microalgae by Stable Isotope Dilution Assay. *Front Bioeng Biotechnol* **2019**, *7*, 481. [CrossRef] [PubMed]
25. Shaigani, P.; Awad, D.; Redai, V.; Fuchs, M.; Haack, M.; Mehlmer, N.; Brueck, T. Oleaginous yeasts- substrate preference and lipid productivity: A view on the performance of microbial lipid producers. *Microb. Cell Factories* **2021**, *20*, 220. [CrossRef]
26. Awad, D.; Brueck, T. Optimization of protein isolation by proteomic qualification from *Cutaneotrichosporon oleaginosus*. *Anal. Bioanal. Chem.* **2020**, *412*, 449–462. [CrossRef]
27. Fuchs, T.; Melcher, F.; Rerop, Z.S.; Lorenzen, J.; Shaigani, P.; Awad, D.; Haack, M.; Prem, S.A.; Masri, M.; Mehlmer, N.; et al. Identifying carbohydrate-active enzymes of *Cutaneotrichosporon oleaginosus* using systems biology. *Microb. Cell Factories* **2021**, *20*, 205. [CrossRef]
28. Tran, N.H.; Qiao, R.; Xin, L.; Chen, X.; Liu, C.; Zhang, X.; Shan, B.; Ghodsi, A.; Li, M. Deep learning enables de novo peptide sequencing from data-independent-acquisition mass spectrometry. *Nat. Methods* **2019**, *16*, 63–66. [CrossRef]
29. Tran, N.H.; Rahman, M.Z.; He, L.; Xin, L.; Shan, B.; Li, M. Complete De Novo Assembly of Monoclonal Antibody Sequences. *Sci Rep* **2016**, *6*, 31730. [CrossRef]

30. Tran, N.H.; Zhang, X.; Xin, L.; Shan, B.; Li, M. De novo peptide sequencing by deep learning. *Proc. Natl. Acad. Sci. USA* **2017**, *114*, 8247–8252. [CrossRef]
31. Kanehisa, M.; Sato, Y.; Morishima, K. BlastKOALA and GhostKOALA: KEGG Tools for Functional Characterization of Genome and Metagenome Sequences. *J Mol Biol* **2016**, *428*, 726–731. [CrossRef]
32. Mathews, M.M.; Sistrom, W.R. The function of the carotenoid pigments of *Sarcina lutea*. *Arch. Mikrobiol.* **1960**, *35*, 139–146. [CrossRef] [PubMed]
33. Thanapimmetha, A.; Suwaleerat, T.; Saisriyoot, M.; Chisti, Y.; Srinophakun, P. Production of carotenoids and lipids by *Rhodococcus opacus* PD630 in batch and fed-batch culture. *Bioprocess Biosyst. Eng.* **2017**, *40*, 133–143. [CrossRef] [PubMed]
34. Ram, S.; Mitra, M.; Shah, F.; Tirkey, S.R.; Mishra, S. Bacteria as an alternate biofactory for carotenoid production: A review of its applications, opportunities and challenges. *J. Funct. Foods* **2020**, *67*, 103867. [CrossRef]
35. Davila Costa, J.S.; Silva, R.A.; Leichert, L.; Alvarez, H.M. Proteome analysis reveals differential expression of proteins involved in triacylglycerol accumulation by *Rhodococcus jostii* RHA1 after addition of methyl viologen. *Microbiology* **2017**, *163*, 343–354. [CrossRef]
36. Wei, X.; Mingjia, H.; Xiufeng, L.; Yang, G.; Qingyu, W. Identification and biochemical properties of Dps (starvation-induced DNA binding protein) from cyanobacterium *Anabaena* sp. PCC 7120. *IUBMB Life* **2007**, *59*, 675–681. [CrossRef]
37. Calhoun, L.N.; Kwon, Y.M. Structure, function and regulation of the DNA-binding protein Dps and its role in acid and oxidative stress resistance in *Escherichia coli:* A review. *J. Appl. Microbiol.* **2011**, *110*, 375–386. [CrossRef]
38. Almiron, M.; Link, A.J.; Furlong, D.; Kolter, R. A novel DNA-binding protein with regulatory and protective roles in starved *Escherichia coli*. *Genes Dev.* **1992**, *6*, 2646–2654. [CrossRef]
39. Cohen, M.; Meziane, T.; Yamasaki, H. A photocarotenogenic *Rhodococcus* sp. isolated from the symbiotic fern Azolla. *Endocytobiosis Cell Res.* **2004**, *15*, 350–355.
40. Gebhard, S.; Humpel, A.; McLellan, A.D.; Cook, G.M. The alternative sigma factor SigF of *Mycobacterium smegmatis* is required for survival of heat shock, acidic pH and oxidative stress. *Microbiology* **2008**, *154*, 2786–2795. [CrossRef]
41. Ondrusch, N.; Kreft, J. Blue and red light modulates SigB-dependent gene transcription, swimming motility and invasiveness in *Listeria monocytogenes*. *PLoS ONE* **2011**, *6*, e16151. [CrossRef]
42. Humpel, A.; Gebhard, S.; Cook, G.M.; Berney, M. The SigF regulon in *Mycobacterium smegmatis* reveals roles in adaptation to stationary phase, heat, and oxidative stress. *J. Bacteriol.* **2010**, *192*, 2491–2502. [CrossRef]
43. O'Donoghue, B.; NicAogain, K.; Bennett, C.; Conneely, A.; Tiensuu, T.; Johansson, J.; O'Byrne, C. Blue-Light Inhibition of *Listeria monocytogenes* Growth Is Mediated by Reactive Oxygen Species and Is Influenced by sigmaB and the Blue-Light Sensor Lmo0799. *Appl. Environ. Microbiol.* **2016**, *82*, 4017–4027. [CrossRef] [PubMed]
44. Turunen, O.; Koskinen, S.; Kurkela, J.; Karhuvaara, O.; Hakkila, K.; Tyystjarvi, T. Roles of Close Homologues SigB and SigD in Heat and High Light Acclimation of the Cyanobacterium *Synechocystis* sp. PCC 6803. *Life* **2022**, *12*, 162. [CrossRef] [PubMed]
45. Hakkila, K.; Valev, D.; Antal, T.; Tyystji Rvi, E.; Tyystji Rvi, T. Group 2 Sigma Factors are Central Regulators of Oxidative Stress Acclimation in Cyanobacteria. *Plant Cell Physiol.* **2019**, *60*, 436–447. [CrossRef] [PubMed]
46. Dorey, A.L.; Lee, B.H.; Rotter, B.; O'Byrne, C.P. Blue Light Sensing in *Listeria monocytogenes* Is Temperature-Dependent and the Transcriptional Response to It Is Predominantly SigB-Dependent. *Front. Microbiol.* **2019**, *10*, 2497. [CrossRef]
47. Lu, X.; Wang, Q.; Yang, M.; Chen, Z.; Li, J.; Wen, Y. Heat Shock Repressor HspR Directly Controls Avermectin Production, Morphological Development, and H2O2 Stress Response in *Streptomyces avermitilis*. *Appl. Environ. Microbiol.* **2021**, *87*, e00473-21. [CrossRef]
48. Loewen, P.C.; Switala, J.; Triggs-Raine, B.L. Catalases HPI and HPII in *Escherichia coli* are induced independently. *Arch Biochem Biophys* **1985**, *243*, 144–149. [CrossRef]
49. Heipieper, H.J.; Weber, F.J.; Sikkema, J.; Keweloh, H.; Debont, J.A.M. Mechanisms of Resistance of Whole Cells to Toxic Organic-Solvents. *Trends Biotechnol.* **1994**, *12*, 409–415. [CrossRef]
50. Weber, F.J.; de Bont, J.A. Adaptation mechanisms of microorganisms to the toxic effects of organic solvents on membranes. *Biochim. Biophys. Acta* **1996**, *1286*, 225–245. [CrossRef]
51. Sinensky, M. Homeoviscous adaptation–a homeostatic process that regulates the viscosity of membrane lipids in *Escherichia coli*. *Proc. Natl. Acad. Sci. USA* **1974**, *71*, 522–525. [CrossRef]
52. Sundararaghavan, A.; Mukherjee, A.; Sahoo, S.; Suraishkumar, G.K. Mechanism of the oxidative stress-mediated increase in lipid accumulation by the bacterium, *R. opacus* PD630: Experimental analysis and genome-scale metabolic modeling. *Biotechnol. Bioeng.* **2020**, *117*, 1779–1788. [CrossRef] [PubMed]
53. Wu, B.; Zhuang, W.Q.; Sahu, M.; Biswas, P.; Tang, Y.J. Cu-doped TiO(2) nanoparticles enhance survival of *Shewanella oneidensis* MR-1 under ultraviolet light (UV) exposure. *Sci. Total Environ.* **2011**, *409*, 4635–4639. [CrossRef] [PubMed]
54. Monier, J.M.; Lindow, S.E. Differential survival of solitary and aggregated bacterial cells promotes aggregate formation on leaf surfaces. *Proc. Natl. Acad. Sci. USA* **2003**, *100*, 15977–15982. [CrossRef] [PubMed]
55. Wu, J.; Chu, Z.; Ruan, Z.; Wang, X.; Dai, T.; Hu, X. Changes of Intracellular Porphyrin, Reactive Oxygen Species, and Fatty Acids Profiles During Inactivation of Methicillin-Resistant Staphylococcus aureus by Antimicrobial Blue Light. *Front. Physiol.* **2018**, *9*, 1658. [CrossRef]
56. Tsitko, I.V.; Zaitsev, G.M.; Lobanok, A.G.; Salkinoja-Salonen, M.S. Effect of aromatic compounds on cellular fatty acid composition of *Rhodococcus opacus*. *Appl. Environ. Microbiol.* **1999**, *65*, 853–855. [CrossRef] [PubMed]

57. Bhatia, S.K.; Gurav, R.; Choi, T.R.; Han, Y.H.; Park, Y.L.; Jung, H.R.; Yang, S.Y.; Song, H.S.; Yang, Y.H. A clean and green approach for odd chain fatty acids production in *Rhodococcus* sp. YHY01 by medium engineering. *Bioresour. Technol.* **2019**, *286*, 121383. [CrossRef]
58. Park, Y.K.; Dulermo, T.; Ledesma-Amaro, R.; Nicaud, J.M. Optimization of odd chain fatty acid production by *Yarrowia lipolytica*. *Biotechnol. Biofuels* **2018**, *11*, 158. [CrossRef]
59. Srirangan, K.; Bruder, M.; Akawi, L.; Miscevic, D.; Kilpatrick, S.; Moo-Young, M.; Chou, C.P. Recent advances in engineering propionyl-CoA metabolism for microbial production of value-added chemicals and biofuels. *Crit. Rev. Biotechnol.* **2017**, *37*, 701–722. [CrossRef]
60. Otzen, C.; Bardl, B.; Jacobsen, I.D.; Nett, M.; Brock, M. *Candida albicans* utilizes a modified beta-oxidation pathway for the degradation of toxic propionyl-CoA. *J. Biol. Chem.* **2014**, *289*, 8151–8169. [CrossRef]

4 Discussion and Outlook

4.1 Medium Optimization of *R. erythropolis* for Efficient Growth and Lipid Formation

One of the most important factors in industrial fermentation processes is the medium composition, as the cost of the growth medium is estimated to be around 60 % of the process costs for microbial lipid production. Glucose is the largest contributor with around 80 % of the cost [158,159]. In the techno-economic analysis of microbial lipid production in *C. oleaginosus* raw materials only accounted for around 18 % of the cost, with capital and operation cost attributing to around 41 % each. In the cost of operation the utilities, mainly power and chilled water, were the biggest factor [15]. As every production strain has unique nutritional requirements, screening of carbon and nitrogen sources as well as their combinations can substantially enhance the microbial biomass and yield of product, thereby increasing the viability of a process [123]. For example, glucose was found to have a repression effect on penicillin production in *Penicillium chrysogenum*, whereas lactose is a slowly assimilating source, with which increased production titres were achieved [160,161]. Microbial lipid production first consists of a phase of growth with sufficient nitrogen, followed by lipid accumulation with an abundance of carbon and a limitation of nitrogen. In a microbial process, the maximum lipid yield depends on the optimum ratio between the growth rate and the lipid biosynthesis rate, as well as progression over time, ensuring that the most carbon is used for lipid production at the end of fermentation [25,162]. For each individual microorganism and fermentation process, the optimal conditions have to be identified. Further, alternatives for expensive components have to be determined to lower the cost [123]. For these reasons, the formulation and optimization of growth medium remains very important in biotechnology. In this study, the nutrient requirements of *R. erythropolis* and the efficiency of uptake and metabolism of commonly available and non-toxic substances including nine nitrogen and eight carbon sources with different chemical compositions were investigated.

To optimize the medium composition, different strategies are used frequently. The classical method is the OFAT approach, which can be grouped into removal experiments, supplementation experiments, and replacement experiments [123]. Due to its simple and convenient design, it is often the preferred choice for screening in the initial stages of medium composition design [123,163]. Its disadvantages include being expensive and time-consuming. Further, OFAT approach can lead to misinterpretation of the results, as it is unable to consider interactions between the factors [164]. For example, the fungus *Umbelopsis ramanniana* exhibited the highest carotenoid production when supplied with diammonium hydrogen

phosphate as nitrogen source and maltose as carbon source, compared with other nitrogen sources, whereas the lowest carotenoid yield was recorded when glucose was used as the carbon source [165]. This insight might be easily overlooked with an OFAT approach and must be taken into account at all times.

Further, statistical methods, also known as Design of Experiment (DOE) can be used for medium optimization. Here the efficiency and reliability of the medium optimization is increased using a reduced number of experiments and time. Furthermore, DOE enables the detection of interaction between the factors [166]. In order to screen for the significant factors from a larger list, designs such as fractional factorial design, Plackett-Burman design and Taguchi design are most commonly used. While in full factorial designs, every combination of the factors is tested, in a fractional factorial design only a few selected combinations are tested. For the optimization of already identified significant factors, RSM is commonly used, with designs such as full factorial design, CCD and Box-Behnken design [123,167,168].

In this work, different carbon and nitrogen sources have been screened with an OFAT approach in a series of replacement experiments. When grown on the five tested inorganic nitrogen sources, an extended lag phase of *R. erythropolis* was observed. The best growth, without a detectable lag phase, could be observed on the complex organic sources yeast extract and tryptone/peptone and the defined organic source ammonium acetate [135]. Complex media, rich in peptides, vitamins and minerals, offer the advantage of lower cost and more robust cell growth [169]. Contrary, a defined medium with a known amount of each component can be used to study the minimal nutritional requirements of a microorganism as well as to carry out a wide variety of physiological and metabolic studies [170]. A synthetic media also offers advantages such as enhanced process consistency and better control and monitoring [169,170]. When investigating the cost for bacterial cellulose production, the major fraction of the medium cost was attributed to yeast extract and peptone. The use of a defined minimal medium was determined as a viable possibility to lower production cost with comparable yields [170].

Since a large part of the cost arises from the carbon source, low-cost feedstock should be used in order to ensure that the process is economically viable. In addition, by utilizing waste streams, a circular economy can be established, preserving the value of the product for as long as possible and avoiding waste. Microorganisms capable of assimilating xylose can efficiently utilize cellulose and hemicellulose degradation products [171] including wheat bran [51], corn stover [172] or unbleached kraft hardwood pulp hydrolysate [43]. The ability to utilize xylose and arabinose has been successfully transferred to *R. opacus* PD630 [43-45]. For xylose utilization, the xylose isomerase *xylA* and xylulokinase *xylB* from the related

Streptomyces lividans or *Streptomyces padanus* have been expressed in the *Rhodococcus* strains *R. jostii* RHA1 and *R. opacus* PD630 [43,44]. In the here presented work, limited to no growth of *R. erythropolis* could be detected on xylose, arabinose, galactose, lactose and maltose [135]. In order to establish *R. erythropolis* as a platform organism, the utilization of xylose could be enabled in a similar manner. In general, the viability of a process can be increased by generating mutants able to utilize cheaper raw materials [123].

4.2 RSM based optimisation of carbon and nitrogen concentration

In this work, carbon and nitrogen concentrations have been optimized with a CCD for increased yield of biomass, lipids and carotenoids. While biomass production was enhanced with increased carbon and nitrogen concentrations, lipid production increased with decreasing nitrogen concentration. The highest carotenoid yield was achieved with a high nitrogen and low carbon concentration.

RSM results in the best model from the fewest observations, enabling a rapid and cheap exploration of the design space [173,174]. In classical experimental design, modelling and optimisation are separated, while newer approaches can incorporate optimisation into the modelling process. One machine learning based approach to experimental design is Bayesian Optimisation (BO). The sample efficient algorithm allows to optimise black-box systems, indicating that the function does not have a closed-form representation and only allows point-wise evaluation [173,175]. Factorial designs assume a linear model and therefore sample at orthogonal corners of the design space. While for classical DOE the sampling pattern is determined before measurements are made and cannot be adapted during the course of the experiment, BO uses adaptive sampling, a sequential process which determines the next sampling point based on two criteria: Exploration for model improvement and exploitation for determination of the optimal parameters [173,176]. It has been claimed that BO can reduce the number of experiments needed for optimal formulation and process parameters in pharmaceutical product development from 25 in DoE to 10 [176]. The optimization of a cell culture media consisting of 14 components for cell agriculture was performed with BO in 38 % less experiments than with DoE methods [177]. While BO is an iterative method reducing experimental time and resources [178], experiments have to be performed successively, increasing the time until the final formulation is available. Plakett-Burman and CCD have been successfully coupled with a Bayesian Network step in order to minimize the number of experiments to optimize the antifungal metabolite expression of *Bacillus amyloliquefaciens*, therefore a coupling of these techniques could also be advantageous [179].

The data generated in shake flasks rarely match the behaviour in fermenters [123,180,181]. Key differences are an uncontrolled pH, poor oxygen transfer, insufficient mixing and

significant evaporation [123]. In order to control the C:N ratio for enhanced lipid production, three different fermentation modes, namely batch, fed-batch and continuous fermentation, are commonly used. As the most reliable mode, fed-batch fermentation offers precise control over nutrient flow rates, thereby providing an efficient and reproducible lipid production process [182,183]. In the future, new parameters could be included in the optimization of the fermentation process of *R. erythropolis*, such as temperature or pH at a larger scale.

4.3 Modulation of Lipid and Carotenoid Production

While lipids are accumulated during the early stationary phase, carotenoids are mainly produced during the late stationary phase of microorganism growth [184], further an appropriate carbon source needs to be available for the production of both compounds [25,185]. To induce lipogenesis, nutrient limitation, particularly nitrogen, is often used [186]. In order to produce lipids and carotenoids in the same process, first a high C/N ratio for lipid production is necessary, than as growth progresses, the ratio shifts and carotenoids, produced at a lower C/N ratio, can be accumulated [184,187,188]. This is in line with the response of *R. erythropolis* at different C:N ratios [135]. Additionally, the choice of nitrogen and carbon source as well as medium composition, such as metal ion supplementation, influences the yield of both products [127,189,190]. Carotenoids are overproduced in microorganisms as part of the stress response. As stressors a wide variety of factors have been investigated such as light, temperature, aeration, metal ions and salts as well as solvents and chemical agents [185,191,192]. The yeast *Rhodotorula glutinis* was subjected to UV irradiation, oxidative stress in form of H_2O_2 supplementation and osmotic stress in form of NaCl supplementation. Each stress stand-alone as well as in combination leads to increased carotenoid production [193]. In *R. toruloides*, concomitant production of lipids and carotenoids was increased through osmotic stress with high salt concentrations [187]. Light stress, on the other hand, only increased carotenoid production, not lipid production in *R. toruloides* [194].

To identify these exogeneous stress factors and apply in a targeted manner would allow regulated overproduction of carotenoids. This strategy can especially be used in situations were the use of genetically modified strains is not preferred [193].

4.4 Regulation of the Light Induced Synthesis of Carotenoids in *R. erythropolis*

Detailed information on cellular stress response and involved metabolic processes of *Rhodococcus* cells enable a knowledge-based increase of product yield in subsequent biotechnological processes. The precursors for all terpenoids, including carotenoids, are IPP and DMAPP, which are produced via die MEP pathway in *Rhodococcus* [111]. Terpenoids, which includes terpenes as well as their functionalized derivatives, are one of the largest and most structurally diverse natural compound groups with applications such as pharmaceutical,

cosmetics, flavouring and agricultural industry [116,195]. In carotenogenic organisms the necessary metabolic pathways are already in operation, which than can be engineered to further increase terpenoid yields [116,196]. Further, carotenoid production can be used as a simple colorimetric readout system for enhanced isoprenoid productivities [197]. The adaptation mechanisms of *R. erythropolis* to photo-oxidative stress was investigated in the second chapter of this study [198]. Here, an increase in carotenoid production in *R. erythropolis* cultures under white (SWW), green (510 nm) and blue (470 nm) light could be detected. The production of carotenoids is a photoprotective mechanisms [99]. Adaptation to light stress was also associated with a shift in the fatty acid composition towards OCFA or saturated and branched fatty acid. By altering the membrane properties, the stress resistance might be increased. The cellular response of stress adaptation to white light was not yet described in literature. In order to investigate the adaptation of *R. erythropolis* to light stress, a time-resolved and quantitative proteomics approach was performed to identify the underlying changes in protein abundancy. While several oxidative stress-related proteins as well as enzymes involved in the synthesis of propanoyl-CoA, a primer for OCFA biosynthesis, could be detected, no proteins in the MEP pathway could be identified as significantly upregulated [198].

Proteomics refers to techniques that yield information on the abundance, interactions and activities of proteins within a given sample [199]. In case of stress, two complementary mechanisms remodel the proteome, on the one hand rewiring of the transcriptome and on the other hand modulating proteolysis [71]. While transcriptomic analysis allows direct insights into gene expression, proteomic analysis illuminates the set of proteins in a given sample at a precise timepoint. There is evidence that in a wide spectrum of organisms, such as *Rhodobacter sphaeroides*, the abundance of RNA does not generally correlate with the abundance of proteins. This difference could be explained by post-transcriptional regulation [200,201]. Additional investigation of the adaptation mechanism with transcriptomics and an increased number of time points could allow a better understanding of the stress adaptation mechanism. In *R. toruloides,* the regulation of carotenoid biosynthesis under light stress has been shown to be controlled at a transcription level [194].

While a general understanding of stress response in bacteria has been achieved, often the inducing signal, all players and their interactions as well as the resulting behaviour are not yet known [71]. The understanding of both the bioregulation of carotenoids and lipids as well as their interaction is important to determine optimal production conditions [194]. Further, process conditions with increased carotenoid yields could enable conditions with increased precursors for production of a range of terpenoids. So are the target products of OleoBuild, ß-ionone and cembratrienol, also produced via the MEP pathway and could therefore potentially be

produced at an increased yield. The identification of proteins which are elevated in abundance via proteomics enables the targeted genetic modification of the terpenoid production pathway.

4.5 Effect of Growth Conditions on the Lipid Composition

Oleaginous microorganisms are promising platforms for the production of lipid-based chemicals [8]. The fatty acid profile plays a decisive role for the industrial application of a SCO. For example, the fatty acid composition of lipids produced by *R. erythropolis* has shown similarities with cocoa butter before [202]. To a certain degree, the desired fatty acid profile for an application can be obtained by careful selection of the cultivation parameters such as the source of nutrients [1]. So did the degree of saturation vary in the fatty acid profile of *C. oleaginosus* depending on the carbon source used [127]. The fatty acid profile of *Y. lipolytica* A101 differed depending on the batch of crude glycerol used as substrate. The different batches were waste products derived from soap, bio-diesel or stearin production and pure glycerol as a control [203]. Variances in the fatty acid profile can strongly influence the quality of a product. For example, the properties of biodiesel varies depending on fatty acid type, chain length as well as number and position of double bonds of the used lipids [204,205].

OCFA are positively related to human health [206] and are produced from odd-chain precursors such as propanoyl-CoA [207]. In microorganisms, the content can be increased through fermentation strategies, although maximum OCFA concentration remained lower than 2 $g\ L^{-1}$ in bacterial cultures, thereby hindering commercial production. Carbon sources including propionate, propionic acid and 1-propanol significantly increased OCFA production, as they can be used to synthesise propanoyl-CoA [206]. *Rhodococcus sp.* YHY01 produced up to 69 % OCFA when grown on propionate [130]. In *R. erythropolis* increased quantities have been detected when grown on lactose or maltose as carbon source [135]. Additionally, higher amounts have been detected when grown under white (SWW) or green (510 nm) light compared to non-illuminated samples, although the quantity of C15:0 as well as C17:1 always remained lower than 10 % of the fatty acid profile [135,198]. In the future, this content could be increased with feeding techniques, by which an increased pool of OCFA precursors are made available, or genetic engineering, where identified bottleneck enzymes could be overexpressed.

Genetic engineering has been employed in various microorganisms to alter the fatty acid profile to mimic a complex product or increase the yield of a specific fatty acid. The fatty acid profile of cocoa butter was mimicked by *Y. lipolytica* by engineering of its desaturases. A palette of different fatty acid profiles while maintaining high lipid strains was achieved [208]. In attempts to increase OCFA the biomass and oil content of engineered strains has been relatively low [206]. In that regard, most attempts focus on the increase of propanoyl-CoA concentration

[157,206,209]. In the oleaginous yeast *Y. lipolytica*, *PHD1* was disrupted and OCFA production significantly increased. This gene, encoding a 2-methylcitrate dehydratase, is part of the in the methyl citrate cycle and converts propanoyl-CoA to 2-methyl aconitate, thereby decreasing the propanoyl-CoA pool [157].

In this work, the fatty acid profile of all tested conditions was examined. The influence of different nitrogen and carbon sources on the lipid yield and fatty acid profile can help determine an appropriate medium composition or the composition of a suitable waste stream for each intended industrial application.

4.6 *R. erythropolis* as a recombinant platform organism

Rhodococci are getting recognition as a rapidly developing platform organism for biocatalysis, biodegradation as well as biosynthesis. While *R. opacus* PD630 and *R. jostii* RHA1 are often used as oleaginous models in the *Rhodococcus* genus due to their high lipid titres [210], *R. erythropolis* generally produces lower amounts of lipids when grown on sugars, organic acids or hydrocarbons [202,211]. As the produced fatty acid composition varies between different *Rhodococcus* strains [202], different strains have to be investigated for different applications. *R. erythropolis* is a highly versatile bacterium due to a wide set of enzymes, which enables various bioconversion and degradation reactions [49]. In order for *Rhodococcus* to become a widely used biotechnological platform organism, the ability for genetic engineering has to be expanded with a wide set of available genetic parts and tools specific to the genus. This includes a variety of vectors, expression control elements, reporter proteins, genome editing methods and also specifically designed laboratory strains (Figure 5). Unfortunately, the majority of tools and genetic parts used for *E. coli* are not compatible in *Rhodococcus*. Thus far, there is a dependency on *E. coli*, as most cloning steps are carried out in *E. coli* cells. Therefore, the use of shuttle vectors is necessary. Due to genetic diversity between different *Rhodococcus* strains, the use of universal vectors for the whole genus is potentially limited. While *Rhodococcus* has been extensively studied in the last few years, there is a lack for multicopy plasmid replicons, cells have a low electro-competence as well as low transformation and recombination efficiencies [19,212].

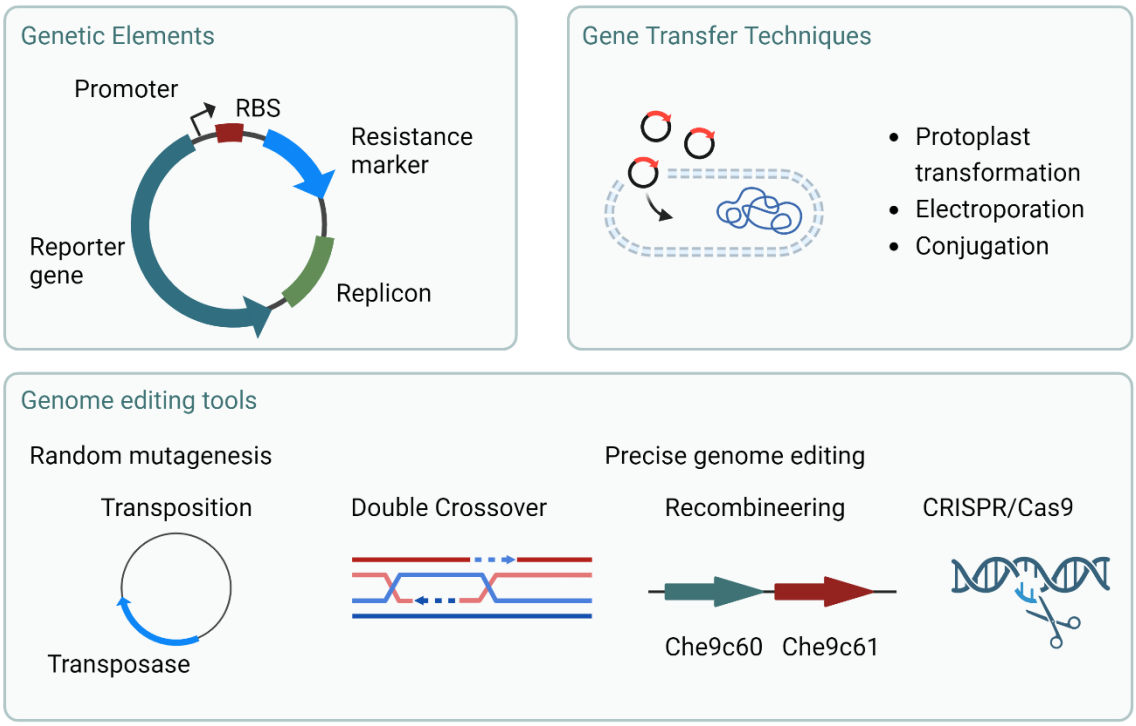

Figure 5. Schematics of genetic elements, gene transfer techniques and genome editing tools developed for Rhodococcus*. Adapted from Liang and Yu (2021) [19]. Created with BioRender.com.*

So far, there is a lack of model strains as well as industrial strains of *Rhodococcus*. The stability of cloning vectors as well as the ability to produce a specific product can be increased by genome reductions, as it has been shown in *E. coli* [213] or *Bacillus subtilis* [214] strains [19]. As *Rhodococcus* strains often have large and complex genomes with highly redundant pathways, this could enable the production of more efficient strains [19,58]. Recently, an effective plasmid curing method has been developed using the *Cre/loxP* system. With this, a genome-structure-stabilized host strain can be developed, lacking unfavourable genes or functions [57].

The use of omics technologies, including genomics, transcriptomics, proteomics and metabolomics, will allow an in-depth understanding of the cellular physiology and metabolic fluxes in *Rhodococcus* cells, thereby enabling an increased production of valuable chemicals [215]. A wide variety of factors such as consumption of intermediates by differing pathways, mRNA and protein abundance and enzyme activity may influence pathway performance. Monitoring pathway intermediates at a metabolic levels is often difficult as pathways might divert, therefore bottlenecks for the final product formation are disguised, some intermediates degrade rapidly or are isomers such as IPP and DMAPP. Efficient pathway optimization is depended on balanced protein production levels [216]. With proteomics, the abundance of a protein in a culture can be identified, among other techniques this can be achieved through “label-free” quantification or selected-reaction monitoring (SRM) mass spectrometry, which

allows the quantification of specific proteins in a sample with increased sensitivity [216-219]. SRM mass spectrometry was used to monitor proteins levels of the MEP pathway in *E. coli,* which was engineered to produce a sesquiterpene. This method allowed the identification of bottlenecks*.* Subsequent protein overexpression resulted in an increased product titre [216]. Selected identified proteins, upregulated under light-stress, can be overexpressed to modify *R. erythropolis* for increased production of compounds such as OCFA or carotenoids. The proteomics analysis also allowed a better understanding of the adaptation of the bacterium to light stress. As good targets for forward-engineering strategies, proteins and pathways which are part of the stress response can be identified and utilized. This strategy was used in the construction of a robust production strain of the cyanobacterium *Synechocystis* PCC6803 for butanol production. By proteomics and transcriptomics analysis, a protein was identified as part of the butanol stress response and the subsequent gene knock-out increased stress resistance of the strain [220,221].

Due to the progress in bioinformatics and the availability of genome sequences, isolation of interesting genes from new natural microorganisms is much more efficient [215]. For example, a new oleate hydratase, producing hydroxy fatty acids, as well as a lycopene β-cyclase, producing asymmetric carotenoids, were identified in *R. erythropolis* [58,115,222]. So far, only six carotenoids are deemed industrially significant, namely astaxanthin, β-carotene, canthaxanthin, lutein, lycopene and zeaxanthin [223]. The identification and characterization of the carotenoids produced in *R. erythropolis* could broaden this spectrum.

To be commercially viable, the yield of lipids and carotenoids has to be increased, while simultaneously utilizing inexpensive waste streams as energy source. This work provided insights into the substrate flexibility and nutrient requirements of *R. erythropolis* to facilitate the identification of suitable waste streams [135]. Further, it investigated the adaptation mechanisms of *R. erythropolis* when subjected to photo-oxidative stress in the form of light. Significantly upregulated proteins involved in the production of propanoyl-CoA, a primer for OCFA synthesis have been identified [198], which can be targeted with genetic engineering for an increased production of the valuable OCFA.

Concluding remarks

The continuously growing world population and the associated demand for sustainable, biobased materials, make the production of valuable oleochemicals such as lipids and carotenoids with the help of microorganisms increasingly interesting and important. In regards to enhanced yields, strain improvement and media optimization are valuable tools [123].

This work can be used as a guide for researchers throughout the development stages of bioprocesses using *R. erythropolis*. The use of statistical modelling for the optimization of carbon and nitrogen concentration for the production of biomass, lipids and carotenoids was demonstrated. A wide range of nitrogen and carbon sources were tested for their effect on *R. erythropolis*. In future work, additional factors, such as optimal pH, temperature and trace elements, could be identified on a larger scale. Commercial effort will likely focus on high-value specialty oleochemicals such as OCFA and monocyclic carotenoids. Finally, adoption of a circular bioeconomy and thereby utilization of low-value feedstocks could enable the commercialization of this sustainable biotechnology.

Further, the adaptation mechanism of *R. erythropolis* to photo-oxidative stress has been investigated. In response to light, enhanced amounts of carotenoids and OCFA were detected. Time-resolved quantitative proteomics were used to detect changes in protein abundance between samples grown in the dark or under light stress. This understanding of stress adaptation allows a deeper understanding of metabolic changes. Moreover, targets for genetic engineering were identified to either increase the resistance of the strain to oxidative-stress or increase production of carotenoids and OCFA without the externally induced light stress.

R. erythropolis is a bacterium with tremendous potential. In order to be established as a platform organism, its genetic engineering toolbox has to be expanded and simplified. Furthermore, its production pathways and regulation mechanisms have to be elucidated. With this knowledge, increased lipid and carotenoid production can be achieved and the bacterium can be used commercially in a wide range of biotechnological processes.

5 List of Publications

Effects of Light on Growth and Metabolism of *Rhodococcus erythropolis*

Selina Engelhart-Straub†, Philipp Cavelius†, Fabian Hölzl, Martina Haack, Dania Awad, Thomas Brueck, Norbert Mehlmer

Microorganisms 2022, 10, 1680. https://doi.org/10.3390/microorganisms10081680

Adaptation of Proteome and Metabolism in Different Haplotypes of *Rhodosporidium toruloides* during Cu(I) and Cu(II) Stress.

Philipp Cavelius†, **Selina Engelhart-Straub**†, Alexander Biewald, Martina Haack, Dania Awad, Thomas Brueck, Norbert Mehlmer

Microorganisms 2023, 11, 553. https://doi.org/10.3390/microorganisms11030553

Optimization of *Rhodococcus erythropolis* JCM3201^T Nutrient Media to Improve Biomass, Lipid, and Carotenoid Yield Using Response Surface Methodology

Selina Engelhart-Straub, Martina Haack, Dania Awad, Thomas Brueck, Norbert Mehlmer

Microorganisms 2023, *11*, 2147. https://doi.org/10.3390/microorganisms11092147

Essay

The potential of biofuels from first to fourth generation.

Philipp Cavelius†, **Selina Engelhart-Straub**†**,** Norbert Mehlmer, Johannes Lercher, Dania Awad, Thomas Brueck

PLOS Biology 2023, 21(3): e3002063. https://doi.org/10.1371/journal.pbio.3002063

Book chapter

Agricultural Biocatalysis: From Waste Stream to Food and Feed Additives

Philipp Cavelius†, **Selina Engelhart-Straub**†**,** Kevin Heieck†, Melania Pilz†, Felix Melcher, Thomas Brueck

In *Agricultural Biocatalysis*; 2022; pp. 133-182. https://doi.org/10.1201/9781003313076-4

† These authors contributed equally to this work.

6 Reprint Permission

Optimization of *Rhodococcus erythropolis* JCM3201^T Nutrient Media to Improve Biomass, Lipid, and Carotenoid Yield Using Response Surface Methodology

Published in MDPI, *Microorganisms* 2023, 11, 2147.

https://doi.org/10.3390/microorganisms11092147

Effects of Light on Growth and Metabolism of *Rhodococcus erythropolis*

Published in MDPI, *Microorganisms* 2022, 10, 1680.

https://doi.org/10.3390/microorganisms10081680

7 Figures & Tables

List of Figures

List of Tables

8 Bibliography

1. Koreti, D.; Kosre, A.; Jadhav, S.K.; Chandrawanshi, N.K. A comprehensive review on oleaginous bacteria: an alternative source for biodiesel production. *Bioresources and Bioprocessing* **2022**, *9*, doi:10.1186/s40643-022-00527-1.
2. Greses, S.; Llamas, M.; Morales-Palomo, S.; González-Fernández, C.; Tomás-Pejó, E. Microbial Production of Oleochemicals. In *Handbook of Biorefinery Research and Technology*; 2023; pp. 1-23.
3. Yan, Q.; Pfleger, B.F. Revisiting metabolic engineering strategies for microbial synthesis of oleochemicals. *Metab Eng* **2020**, *58*, 35-46, doi:10.1016/j.ymben.2019.04.009.
4. Biermann, U.; Bornscheuer, U.; Meier, M.A.; Metzger, J.O.; Schafer, H.J. Oils and fats as renewable raw materials in chemistry. *Angew Chem Int Ed Engl* **2011**, *50*, 3854-3871, doi:10.1002/anie.201002767.
5. Pfleger, B.F.; Gossing, M.; Nielsen, J. Metabolic engineering strategies for microbial synthesis of oleochemicals. *Metab Eng* **2015**, *29*, 1-11, doi:10.1016/j.ymben.2015.01.009.
6. Abdelmoez, W.; Mustafa, A. Oleochemical industry future through biotechnology. *J Oleo Sci* **2014**, *63*, 545-554, doi:10.5650/jos.ess14022.
7. Zhou, Y.J.; Buijs, N.A.; Zhu, Z.; Qin, J.; Siewers, V.; Nielsen, J. Production of fatty acid-derived oleochemicals and biofuels by synthetic yeast cell factories. *Nat Commun* **2016**, *7*, 11709, doi:10.1038/ncomms11709.
8. Adrio, J.L. Oleaginous yeasts: Promising platforms for the production of oleochemicals and biofuels. *Biotechnol Bioeng* **2017**, *114*, 1915-1920, doi:10.1002/bit.26337.
9. Ochsenreither, K.; Gluck, C.; Stressler, T.; Fischer, L.; Syldatk, C. Production Strategies and Applications of Microbial Single Cell Oils. *Front Microbiol* **2016**, *7*, 1539, doi:10.3389/fmicb.2016.01539.
10. Patel, A.; Sarkar, O.; Rova, U.; Christakopoulos, P.; Matsakas, L. Valorization of volatile fatty acids derived from low-cost organic waste for lipogenesis in oleaginous microorganisms-A review. *Bioresour Technol* **2021**, *321*, 124457, doi:10.1016/j.biortech.2020.124457.
11. Thevenieau, F.; Nicaud, J.-M. Microorganisms as sources of oils. *Ocl* **2013**, *20*, doi:10.1051/ocl/2013034.
12. Round, J.W.; Roccor, R.; Eltis, L.D. A biocatalyst for sustainable wax ester production: re-wiring lipid accumulation inRhodococcusto yield high-value oleochemicals. *Green Chemistry* **2019**, *21*, 6468-6482, doi:10.1039/c9gc03228b.
13. Ratledge, C. Fatty acid biosynthesis in microorganisms being used for Single Cell Oil production. *Biochimie* **2004**, *86*, 807-815, doi:10.1016/j.biochi.2004.09.017.
14. Miller, K.K.; Alper, H.S. Yarrowia lipolytica: more than an oleaginous workhorse. *Appl Microbiol Biotechnol* **2019**, *103*, 9251-9262, doi:10.1007/s00253-019-10200-x.
15. Masri, M.A.; Garbe, D.; Mehlmer, N.; Brück, T.B. A sustainable, high-performance process for the economic production of waste-free microbial oils that can replace plant-based equivalents. *Energy & Environmental Science* **2019**, *12*, 2717-2732, doi:10.1039/c9ee00210c.

16. Kassab, E.; Fuchs, M.; Haack, M.; Mehlmer, N.; Brueck, T.B. Engineering Escherichia coli FAB system using synthetic plant genes for the production of long chain fatty acids. *Microb Cell Fact* **2019**, *18*, 163, doi:10.1186/s12934-019-1217-7.

17. Nakashima, N.; Mitani, Y.; Tamura, T. Actinomycetes as host cells for production of recombinant proteins. *Microb Cell Fact* **2005**, *4*, 7, doi:10.1186/1475-2859-4-7.

18. Alper, H.; Stephanopoulos, G. Engineering for biofuels: exploiting innate microbial capacity or importing biosynthetic potential? *Nat Rev Microbiol* **2009**, *7*, 715-723, doi:10.1038/nrmicro2186.

19. Liang, Y.; Yu, H. Genetic toolkits for engineering Rhodococcus species with versatile applications. *Biotechnol Adv* **2021**, *49*, 107748, doi:10.1016/j.biotechadv.2021.107748.

20. Riley, L.A.; Guss, A.M. Approaches to genetic tool development for rapid domestication of non-model microorganisms. *Biotechnol Biofuels* **2021**, *14*, 30, doi:10.1186/s13068-020-01872-z.

21. Kim, H.M.; Chae, T.U.; Choi, S.Y.; Kim, W.J.; Lee, S.Y. Engineering of an oleaginous bacterium for the production of fatty acids and fuels. *Nat Chem Biol* **2019**, *15*, 721-729, doi:10.1038/s41589-019-0295-5.

22. Lee, S.Y.; Kim, H.U.; Park, J.H.; Park, J.M.; Kim, T.Y. Metabolic engineering of microorganisms: general strategies and drug production. *Drug Discov Today* **2009**, *14*, 78-88, doi:10.1016/j.drudis.2008.08.004.

23. Liu, H.; Deutschbauer, A.M. Rapidly moving new bacteria to model-organism status. *Curr Opin Biotechnol* **2018**, *51*, 116-122, doi:10.1016/j.copbio.2017.12.006.

24. Anthony, W.E.; Carr, R.R.; DeLorenzo, D.M.; Campbell, T.P.; Shang, Z.; Foston, M.; Moon, T.S.; Dantas, G. Development of Rhodococcus opacus as a chassis for lignin valorization and bioproduction of high-value compounds. *Biotechnol Biofuels* **2019**, *12*, 192, doi:10.1186/s13068-019-1535-3.

25. Ageitos, J.M.; Vallejo, J.A.; Veiga-Crespo, P.; Villa, T.G. Oily yeasts as oleaginous cell factories. *Appl Microbiol Biotechnol* **2011**, *90*, 1219-1227, doi:10.1007/s00253-011-3200-z.

26. Wang, Y.; Zhang, S.; Zhu, Z.; Shen, H.; Lin, X.; Jin, X.; Jiao, X.; Zhao, Z.K. Systems analysis of phosphate-limitation-induced lipid accumulation by the oleaginous yeast Rhodosporidium toruloides. *Biotechnol Biofuels* **2018**, *11*, 148, doi:10.1186/s13068-018-1134-8.

27. Patel, A.; Karageorgou, D.; Rova, E.; Katapodis, P.; Rova, U.; Christakopoulos, P.; Matsakas, L. An Overview of Potential Oleaginous Microorganisms and Their Role in Biodiesel and Omega-3 Fatty Acid-Based Industries. *Microorganisms* **2020**, *8*, doi:10.3390/microorganisms8030434.

28. Park, Y.K.; Nicaud, J.M.; Ledesma-Amaro, R. The Engineering Potential of Rhodosporidium toruloides as a Workhorse for Biotechnological Applications. *Trends Biotechnol* **2018**, *36*, 304-317, doi:10.1016/j.tibtech.2017.10.013.

29. Freitas, C.; Nobre, B.; Gouveia, L.; Roseiro, J.; Reis, A.; Lopes da Silva, T. New at-line flow cytometric protocols for determining carotenoid content and cell viability during Rhodosporidium toruloides NCYC 921 batch growth. *Process Biochemistry* **2014**, *49*, 554-562, doi:10.1016/j.procbio.2014.01.022.

30. Dias, C.; Silva, C.; Freitas, C.; Reis, A.; da Silva, T.L. Effect of Medium pH on Rhodosporidium toruloides NCYC 921 Carotenoid and Lipid Production Evaluated by Flow Cytometry. *Appl Biochem Biotechnol* **2016**, *179*, 776-787, doi:10.1007/s12010-016-2030-y.

31. Tsai, Y.Y.; Ohashi, T.; Wu, C.C.; Bataa, D.; Misaki, R.; Limtong, S.; Fujiyama, K. Delta-9 fatty acid desaturase overexpression enhanced lipid production and oleic acid content in Rhodosporidium toruloides for preferable yeast lipid production. *J Biosci Bioeng* **2019**, *127*, 430-440, doi:10.1016/j.jbiosc.2018.09.005.

32. Wang, Y.; Zhang, S.; Potter, M.; Sun, W.; Li, L.; Yang, X.; Jiao, X.; Zhao, Z.K. Overexpression of Delta12-Fatty Acid Desaturase in the Oleaginous Yeast Rhodosporidium toruloides for Production of Linoleic Acid-Rich Lipids. *Appl Biochem Biotechnol* **2016**, *180*, 1497-1507, doi:10.1007/s12010-016-2182-9.

33. Fillet, S.; Ronchel, C.; Callejo, C.; Fajardo, M.J.; Moralejo, H.; Adrio, J.L. Engineering Rhodosporidium toruloides for the production of very long-chain monounsaturated fatty acid-rich oils. *Appl Microbiol Biotechnol* **2017**, *101*, 7271-7280, doi:10.1007/s00253-017-8461-8.

34. Fillet, S.; Gibert, J.; Suarez, B.; Lara, A.; Ronchel, C.; Adrio, J.L. Fatty alcohols production by oleaginous yeast. *J Ind Microbiol Biotechnol* **2015**, *42*, 1463-1472, doi:10.1007/s10295-015-1674-x.

35. Soong, Y.V.; Zhao, L.; Liu, N.; Yu, P.; Lopez, C.; Olson, A.; Wong, H.W.; Shao, Z.; Xie, D. Microbial synthesis of wax esters. *Metab Eng* **2021**, *67*, 428-442, doi:10.1016/j.ymben.2021.08.002.

36. Sturtevant, D.; Lu, S.; Zhou, Z.W.; Shen, Y.; Wang, S.; Song, J.M.; Zhong, J.; Burks, D.J.; Yang, Z.Q.; Yang, Q.Y.; et al. The genome of jojoba (Simmondsia chinensis): A taxonomically isolated species that directs wax ester accumulation in its seeds. *Sci Adv* **2020**, *6*, eaay3240, doi:10.1126/sciadv.aay3240.

37. Kalscheuer, R.; Stoveken, T.; Luftmann, H.; Malkus, U.; Reichelt, R.; Steinbuchel, A. Neutral lipid biosynthesis in engineered Escherichia coli: jojoba oil-like wax esters and fatty acid butyl esters. *Appl Environ Microbiol* **2006**, *72*, 1373-1379, doi:10.1128/AEM.72.2.1373-1379.2006.

38. Wenning, L.; Ejsing, C.S.; David, F.; Sprenger, R.R.; Nielsen, J.; Siewers, V. Increasing jojoba-like wax ester production in Saccharomyces cerevisiae by enhancing very long-chain, monounsaturated fatty acid synthesis. *Microb Cell Fact* **2019**, *18*, 49, doi:10.1186/s12934-019-1098-9.

39. Coradini, A.L.V.; Anschau, A.; Vidotti, A.D.S.; Reis, É.M.; da Cunha Abreu Xavier, M.; Coelho, R.S.; Franco, T.T. Microorganism for Bioconversion of Sugar Hydrolysates into Lipids. In *Microorganisms in Biorefineries*; Microbiology Monographs; 2015; pp. 51-78.

40. Rerop, Z.S.; Stellner, N.I.; Graban, P.; Haack, M.; Mehlmer, N.; Masri, M.; Brück, T.B. Bioconversion of a Lignocellulosic Hydrolysate to Single Cell Oil for Biofuel Production in a Cost-Efficient Fermentation Process. *Fermentation* **2023**, *9*, doi:10.3390/fermentation9020189.

41. Abeln, F.; Chuck, C.J. The history, state of the art and future prospects for oleaginous yeast research. *Microb Cell Fact* **2021**, *20*, 221, doi:10.1186/s12934-021-01712-1.

42. Poontawee, R.; Yongmanitchai, W.; Limtong, S. Efficient oleaginous yeasts for lipid production from lignocellulosic sugars and effects of lignocellulose degradation compounds on growth and lipid production. *Process Biochemistry* **2017**, *53*, 44-60, doi:10.1016/j.procbio.2016.11.013.

43. Kurosawa, K.; Wewetzer, S.J.; Sinskey, A.J. Engineering xylose metabolism in triacylglycerol-producing Rhodococcus opacus for lignocellulosic fuel production. *Biotechnol Biofuels* **2013**, *6*, 134, doi:10.1186/1754-6834-6-134.

44. Xiong, X.; Wang, X.; Chen, S. Engineering of a xylose metabolic pathway in Rhodococcus strains. *Appl Environ Microbiol* **2012**, *78*, 5483-5491, doi:10.1128/AEM.08022-11.

45. Kurosawa, K.; Plassmeier, J.; Kalinowski, J.; Ruckert, C.; Sinskey, A.J. Engineering L-arabinose metabolism in triacylglycerol-producing Rhodococcus opacus for lignocellulosic fuel production. *Metab Eng* **2015**, *30*, 89-95, doi:10.1016/j.ymben.2015.04.006.

46. Henson, W.R.; Campbell, T.; DeLorenzo, D.M.; Gao, Y.; Berla, B.; Kim, S.J.; Foston, M.; Moon, T.S.; Dantas, G. Multi-omic elucidation of aromatic catabolism in adaptively evolved Rhodococcus opacus. *Metab Eng* **2018**, *49*, 69-83, doi:10.1016/j.ymben.2018.06.009.

47. Larroude, M.; Celinska, E.; Back, A.; Thomas, S.; Nicaud, J.M.; Ledesma-Amaro, R. A synthetic biology approach to transform Yarrowia lipolytica into a competitive biotechnological producer of beta-carotene. *Biotechnol Bioeng* **2018**, *115*, 464-472, doi:10.1002/bit.26473.

48. Spagnuolo, M.; Yaguchi, A.; Blenner, M. Oleaginous yeast for biofuel and oleochemical production. *Curr Opin Biotechnol* **2019**, *57*, 73-81, doi:10.1016/j.copbio.2019.02.011.

49. de Carvalho, C.C.; da Fonseca, M.M. The remarkable *Rhodococcus erythropolis*. *Appl Microbiol Biotechnol* **2005**, *67*, 715-726, doi:10.1007/s00253-005-1932-3.

50. Wen, Z.; Zhang, S.; Odoh, C.K.; Jin, M.; Zhao, Z.K. Rhodosporidium toruloides - A potential red yeast chassis for lipids and beyond. *FEMS Yeast Res* **2020**, *20*, doi:10.1093/femsyr/foaa038.

51. Mischko, W.; Hirte, M.; Roehrer, S.; Engelhardt, H.; Mehlmer, N.; Minceva, M.; Brück, T. Modular biomanufacturing for a sustainable production of terpenoid-based insect deterrents. *Green Chemistry* **2018**, *20*, 2637-2650, doi:10.1039/c8gc00434j.

52. Chen, S.; Lu, Y.; Wang, W.; Hu, Y.; Wang, J.; Tang, S.; Lin, C.S.K.; Yang, X. Efficient production of the beta-ionone aroma compound from organic waste hydrolysates using an engineered Yarrowia lipolytica strain. *Front Microbiol* **2022**, *13*, 960558, doi:10.3389/fmicb.2022.960558.

53. Lopez, J.; Essus, K.; Kim, I.K.; Pereira, R.; Herzog, J.; Siewers, V.; Nielsen, J.; Agosin, E. Production of beta-ionone by combined expression of carotenogenic and plant CCD1 genes in Saccharomyces cerevisiae. *Microb Cell Fact* **2015**, *14*, 84, doi:10.1186/s12934-015-0273-x.

54. Cavelius, P.; Engelhart-Straub, S.; Heieck, K.; Pilz, M.; Melcher, F.; Brück, T. Agricultural Biocatalysis: From Waste Stream to Food and Feed Additives. In *Agricultural Biocatalysis*; 2022; pp. 133-182.

55. Welte, M.A.; Gould, A.P. Lipid droplet functions beyond energy storage. *Biochim Biophys Acta Mol Cell Biol Lipids* **2017**, *1862*, 1260-1272, doi:10.1016/j.bbalip.2017.07.006.

56. Martinkova, L.; Uhnakova, B.; Patek, M.; Nesvera, J.; Kren, V. Biodegradation potential of the genus Rhodococcus. *Environ Int* **2009**, *35*, 162-177, doi:10.1016/j.envint.2008.07.018.

57. Kitagawa, W.; Hata, M. Development of Efficient Genome-Reduction Tool Based on Cre/loxP System in Rhodococcus erythropolis. *Microorganisms* **2023**, *11*, doi:10.3390/microorganisms11020268.

58. Cappelletti, M.; Presentato, A.; Piacenza, E.; Firrincieli, A.; Turner, R.J.; Zannoni, D. Biotechnology of *Rhodococcus* for the production of valuable compounds. *Appl Microbiol Biotechnol* **2020**, *104*, 8567-8594, doi:10.1007/s00253-020-10861-z.

59. Larkin, M.J.; Kulakov, L.A.; Allen, C.C. Biodegradation and Rhodococcus--masters of catabolic versatility. *Curr Opin Biotechnol* **2005**, *16*, 282-290, doi:10.1016/j.copbio.2005.04.007.

60. Cortes, M.A.L.R.M.; de Carvalho, C.C.C.R. Effect of carbon sources on lipid accumulation in Rhodococcus cells. *Biochemical Engineering Journal* **2015**, *94*, 100-105, doi:10.1016/j.bej.2014.11.017.

61. Kitagawa, W.; Tamura, T. Three Types of Antibiotics Produced from Rhodococcus erythropolis Strains. *Microbes Environ* **2008**, *23*, 167-171, doi:10.1264/jsme2.23.167.

62. Sangal, V.; Goodfellow, M.; Jones, A.L.; Schwalbe, E.C.; Blom, J.; Hoskisson, P.A.; Sutcliffe, I.C. Next-generation systematics: An innovative approach to resolve the structure of complex prokaryotic taxa. *Sci Rep* **2016**, *6*, 38392, doi:10.1038/srep38392.

63. Alvarez, H.M.; Hernandez, M.A.; Lanfranconi, M.P.; Silva, R.A.; Villalba, M.S. Rhodococcus as Biofactories for Microbial Oil Production. *Molecules* **2021**, *26*, doi:10.3390/molecules26164871.

64. Jiang, J.; Liu, L.; Nie, W.; Chen, Y.; Wang, Z. Screening of a high bioflocculant-producing bacterial strain from an intensive fish pond and comparison of the bioflocculation effects withRhodococcus erythropolis. *Aquaculture Research* **2019**, doi:10.1111/are.13977.

65. Nakashima, N.; Tamura, T. A novel system for expressing recombinant proteins over a wide temperature range from 4 to 35 degrees C. *Biotechnol Bioeng* **2004**, *86*, 136-148, doi:10.1002/bit.20024.

66. Nakashima, N.; Tamura, T. Isolation and characterization of a rolling-circle-type plasmid from Rhodococcus erythropolis and application of the plasmid to multiple-recombinant-protein expression. *Appl Environ Microbiol* **2004**, *70*, 5557-5568, doi:10.1128/AEM.70.9.5557-5568.2004.

67. Vallecillo, A.J.; Parada, C.; Morales, P.; Espitia, C. Rhodococcus erythropolis as a host for expression, secretion and glycosylation of Mycobacterium tuberculosis proteins. *Microb Cell Fact* **2017**, *16*, 12, doi:10.1186/s12934-017-0628-6.

68. Saito, Y.; Kitagawa, W.; Kumagai, T.; Tajima, N.; Nishimiya, Y.; Tamano, K.; Yasutake, Y.; Tamura, T.; Kameda, T. Developing a codon optimization method for improved expression of recombinant proteins in actinobacteria. *Sci Rep* **2019**, *9*, 8338, doi:10.1038/s41598-019-44500-z.

69. Mitani, Y.; Meng, X.; Kamagata, Y.; Tamura, T. Characterization of LtsA from Rhodococcus erythropolis, an enzyme with glutamine amidotransferase activity. *J Bacteriol* **2005**, *187*, 2582-2591, doi:10.1128/JB.187.8.2582-2591.2005.

70. Ezraty, B.; Gennaris, A.; Barras, F.; Collet, J.F. Oxidative stress, protein damage and repair in bacteria. *Nat Rev Microbiol* **2017**, *15*, 385-396, doi:10.1038/nrmicro.2017.26.

71. Guo, M.S.; Gross, C.A. Stress-induced remodeling of the bacterial proteome. *Curr Biol* **2014**, *24*, R424-434, doi:10.1016/j.cub.2014.03.023.

72. Scott, M.; Gunderson, C.W.; Mateescu, E.M.; Zhang, Z.; Hwa, T. Interdependence of cell growth and gene expression: origins and consequences. *Science* **2010**, *330*, 1099-1102, doi:10.1126/science.1192588.

73. Patek, M.; Grulich, M.; Nesvera, J. Stress response in *Rhodococcus* strains. *Biotechnol Adv* **2021**, *53*, 107698, doi:10.1016/j.biotechadv.2021.107698.

74. Aggarwal, R.K.; Dawar, C.; Phanindranath, R.; Mutnuri, L.; Dayal, A.M. Draft Genome Sequence of a Versatile Hydrocarbon-Degrading Bacterium, Rhodococcus pyridinivorans Strain KG-16, Collected from Oil Fields in India. *Genome Announc* **2016**, *4*, doi:10.1128/genomeA.01704-15.

75. Kuang, S.; Fan, X.; Peng, R. Quantitative proteomic analysis ofRhodococcus ruberresponsive to organic solvents. *Biotechnology & Biotechnological Equipment* **2018**, *32*, 1418-1430, doi:10.1080/13102818.2018.1533432.

76. Kumari, S.; Debnath, M.; Hari Sonawane, S.; Teja Malkapuram, S.; Mohan Seepana, M. Dye Decolorization by Rhodococcus ruber Strain TES III Isolated from Textile Effluent Wastewater Contaminated Soil. *ChemistrySelect* **2022**, *7*, doi:10.1002/slct.202200421.

77. Willdigg, J.R.; Helmann, J.D. Mini Review: Bacterial Membrane Composition and Its Modulation in Response to Stress. *Front Mol Biosci* **2021**, *8*, 634438, doi:10.3389/fmolb.2021.634438.

78. Alvarez, H.M.; Silva, R.A.; Cesari, A.C.; Zamit, A.L.; Peressutti, S.R.; Reichelt, R.; Keller, U.; Malkus, U.; Rasch, C.; Maskow, T.; et al. Physiological and morphological responses of the soil bacterium Rhodococcus opacus strain PD630 to water stress. *FEMS Microbiol Ecol* **2004**, *50*, 75-86, doi:10.1016/j.femsec.2004.06.002.

79. Alvarez, H.M.; Kalscheuer, R.; Steinbuchel, A. Accumulation and mobilization of storage lipids by Rhodococcus opacus PD630 and Rhodococcus ruber NCIMB 40126. *Appl Microbiol Biotechnol* **2000**, *54*, 218-223, doi:10.1007/s002530000395.

80. Shao, Z.; Dick, W.A.; Behki, R.M. An improved Escherichia coli-Rhodococcus shuttle vector and plasmid transformation in Rhodococcus spp. using electroporation. *Lett Appl Microbiol* **1995**, *21*, 261-266, doi:10.1111/j.1472-765x.1995.tb01056.x.

81. Kagawa, Y.; Mitani, Y.; Yun, H.Y.; Nakashima, N.; Tamura, N.; Tamura, T. Identification of a methanol-inducible promoter from Rhodococcus erythropolis PR4 and its use as an expression vector. *J Biosci Bioeng* **2012**, *113*, 596-603, doi:10.1016/j.jbiosc.2011.12.019.

82. Sallam, K.I.; Mitani, Y.; Tamura, T. Construction of random transposition mutagenesis system in Rhodococcuserythropolis using IS1415. *J Biotechnol* **2006**, *121*, 13-22, doi:10.1016/j.jbiotec.2005.07.007.

83. Geize, R.; Hessels, G.I.; Gerwen, R.; Meijden, P.; Dijkhuizen, L. Unmarked gene deletion mutagenesis of kstD, encoding 3-ketosteroid Î" 1-dehydrogenase, in Rhodococcus erythropolis SQ1 using sacB as counter-selectable marker. *FEMS Microbiology Letters* **2001**, *205*, 197-202, doi:10.1111/j.1574-6968.2001.tb10947.x.

84. Goodfellow, M.; Alderson, G. The actinomycete-genus Rhodococcus: a home for the "rhodochrous" complex. *J Gen Microbiol* **1977**, *100*, 99-122, doi:10.1099/00221287-100-1-99.

85. Yoshida, K.; Kitagawa, W.; Ishiya, K.; Mitani, Y.; Nakashima, N.; Aburatani, S.; Tamura, T. Genome Sequence of Rhodococcus erythropolis Type Strain JCM 3201. *Microbiol Resour Announc* **2019**, *8*, doi:10.1128/MRA.01730-18.

86. Ratledge, C. Regulation of lipid accumulation in oleaginous micro-organisms. *Biochem Soc Trans* **2002**, *30*, 1047-1050, doi:10.1042/bst0301047.

87. Qadeer, S.; Khalid, A.; Mahmood, S.; Anjum, M.; Ahmad, Z. Utilizing oleaginous bacteria and fungi for cleaner energy production. *Journal of Cleaner Production* **2017**, *168*, 917-928, doi:10.1016/j.jclepro.2017.09.093.

88. Waltermann, M.; Hinz, A.; Robenek, H.; Troyer, D.; Reichelt, R.; Malkus, U.; Galla, H.J.; Kalscheuer, R.; Stoveken, T.; von Landenberg, P.; Steinbuchel, A. Mechanism of lipid-body formation in prokaryotes: how bacteria fatten up. *Mol Microbiol* **2005**, *55*, 750-763, doi:10.1111/j.1365-2958.2004.04441.x.

89. Bellou, S.; Triantaphyllidou, I.E.; Aggeli, D.; Elazzazy, A.M.; Baeshen, M.N.; Aggelis, G. Microbial oils as food additives: recent approaches for improving microbial oil production and its polyunsaturated fatty acid content. *Curr Opin Biotechnol* **2016**, *37*, 24-35, doi:10.1016/j.copbio.2015.09.005.

90. Bharti, R.K.; Srivastava, S.; Thakur, I.S. Extraction of extracellular lipids from chemoautotrophic bacteria Serratia sp. ISTD04 for production of biodiesel. *Bioresour Technol* **2014**, *165*, 201-204, doi:10.1016/j.biortech.2014.02.075.

91. Kumar, M.; Rathour, R.; Gupta, J.; Pandey, A.; Gnansounou, E.; Thakur, I.S. Bacterial production of fatty acid and biodiesel: opportunity and challenges. In *Refining Biomass Residues for Sustainable Energy and Bioproducts*; 2020; pp. 21-49.

92. Kennedy, E.P. Biosynthesis of complex lipids. *Fed Proc* **1961**, *20*, 934-940.

93. Amara, S.; Seghezzi, N.; Otani, H.; Diaz-Salazar, C.; Liu, J.; Eltis, L.D. Characterization of key triacylglycerol biosynthesis processes in rhodococci. *Sci Rep* **2016**, *6*, 24985, doi:10.1038/srep24985.

94. Hernandez, M.A.; Comba, S.; Arabolaza, A.; Gramajo, H.; Alvarez, H.M. Overexpression of a phosphatidic acid phosphatase type 2 leads to an increase in triacylglycerol production in oleaginous Rhodococcus strains. *Appl Microbiol Biotechnol* **2015**, *99*, 2191-2207, doi:10.1007/s00253-014-6002-2.

95. Foong, L.C.; Loh, C.W.L.; Ng, H.S.; Lan, J.C. Recent development in the production strategies of microbial carotenoids. *World J Microbiol Biotechnol* **2021**, *37*, 12, doi:10.1007/s11274-020-02967-3.

96. Martínez-Cámara, S.; Ibañez, A.; Rubio, S.; Barreiro, C.; Barredo, J.-L. Main Carotenoids Produced by Microorganisms. *Encyclopedia* **2021**, *1*, 1223-1245, doi:10.3390/encyclopedia1040093.

97. Avalos, J.; Carmen Limon, M. Biological roles of fungal carotenoids. *Curr Genet* **2015**, *61*, 309-324, doi:10.1007/s00294-014-0454-x.

98. Maoka, T. Carotenoids as natural functional pigments. *J Nat Med* **2020**, *74*, 1-16, doi:10.1007/s11418-019-01364-x.

99. Mata-Gomez, L.C.; Montanez, J.C.; Mendez-Zavala, A.; Aguilar, C.N. Biotechnological production of carotenoids by yeasts: an overview. *Microb Cell Fact* **2014**, *13*, 12, doi:10.1186/1475-2859-13-12.

100. Tapiero, H.; Townsend, D.M.; Tew, K.D. The role of carotenoids in the prevention of human pathologies. *Biomed Pharmacother* **2004**, *58*, 100-110, doi:10.1016/j.biopha.2003.12.006.

101. Krinsky, N.I.; Johnson, E.J. Carotenoid actions and their relation to health and disease. *Mol Aspects Med* **2005**, *26*, 459-516, doi:10.1016/j.mam.2005.10.001.

102. Langi, P.; Kiokias, S.; Varzakas, T.; Proestos, C. Carotenoids: From Plants to Food and Feed Industries. In *Microbial Carotenoids: Methods and Protocols*, Barreiro, C., Barredo, J.-L., Eds.; Springer New York: New York, NY, 2018; pp. 57-71.

103. Yabuzaki, J. Carotenoids Database: structures, chemical fingerprints and distribution among organisms. *Database* **2017**, *2017*, doi:10.1093/database/bax004.

104. Saini, R.K.; Keum, Y.S. Microbial platforms to produce commercially vital carotenoids at industrial scale: an updated review of critical issues. *J Ind Microbiol Biotechnol* **2019**, *46*, 657-674, doi:10.1007/s10295-018-2104-7.

105. Grillitsch, K.; Connerth, M.; Kofeler, H.; Arrey, T.N.; Rietschel, B.; Wagner, B.; Karas, M.; Daum, G. Lipid particles/droplets of the yeast Saccharomyces cerevisiae revisited: lipidome meets proteome. *Biochim Biophys Acta* **2011**, *1811*, 1165-1176, doi:10.1016/j.bbalip.2011.07.015.

106. Thiam, A.R.; Beller, M. The why, when and how of lipid droplet diversity. *J Cell Sci* **2017**, *130*, 315-324, doi:10.1242/jcs.192021.

107. Velmurugan, A.; Kodiveri Muthukaliannan, G. Genetic manipulation for carotenoid production in microalgae an overview. *Current Research in Biotechnology* **2022**, *4*, 221-228, doi:10.1016/j.crbiot.2022.03.005.

108. Zhang, X.K.; Wang, D.N.; Chen, J.; Liu, Z.J.; Wei, L.J.; Hua, Q. Metabolic engineering of beta-carotene biosynthesis in Yarrowia lipolytica. *Biotechnol Lett* **2020**, *42*, 945-956, doi:10.1007/s10529-020-02844-x.

109. Guo, Q.; Peng, Q.Q.; Li, Y.W.; Yan, F.; Wang, Y.T.; Ye, C.; Shi, T.Q. Advances in the metabolic engineering of Saccharomyces cerevisiae and Yarrowia lipolytica for the production of beta-carotene. *Crit Rev Biotechnol* **2023**, 1-15, doi:10.1080/07388551.2023.2166809.

110. Schweiggert, R.M.; Carle, R. Carotenoid Production by Bacteria, Microalgae, and Fungi. In *Carotenoids*; 2016; pp. 217-240.

111. Li, C.; Swofford, C.A.; Sinskey, A.J. Modular engineering for microbial production of carotenoids. *Metab Eng Commun* **2020**, *10*, e00118, doi:10.1016/j.mec.2019.e00118.

112. Paniagua-Michel, J.; Olmos-Soto, J.; Ruiz, M.A. Pathways of Carotenoid Biosynthesis in Bacteria and Microalgae. In *Microbial Carotenoids from Bacteria and Microalgae: Methods and Protocols*, Barredo, J.-L., Ed.; Humana Press: Totowa, NJ, 2012; pp. 1-12.

113. Li, M.; Hou, F.; Wu, T.; Jiang, X.; Li, F.; Liu, H.; Xian, M.; Zhang, H. Recent advances of metabolic engineering strategies in natural isoprenoid production using cell factories. *Nat Prod Rep* **2020**, *37*, 80-99, doi:10.1039/c9np00016j.

114. Tao, L.; Wagner, L.W.; Rouviere, P.E.; Cheng, Q. Metabolic engineering for synthesis of aryl carotenoids in Rhodococcus. *Appl Microbiol Biotechnol* **2006**, *70*, 222-228, doi:10.1007/s00253-005-0064-0.

115. Tao, L.; Picataggio, S.; Rouviere, P.E.; Cheng, Q. Asymmetrically acting lycopene beta-cyclases (CrtLm) from non-photosynthetic bacteria. *Mol Genet Genomics* **2004**, *271*, 180-188, doi:10.1007/s00438-003-0969-1.

116. Moser, S.; Pichler, H. Identifying and engineering the ideal microbial terpenoid production host. *Appl Microbiol Biotechnol* **2019**, *103*, 5501-5516, doi:10.1007/s00253-019-09892-y.

117. Gaur, V.K.; Sharma, P.; Gupta, S.; Varjani, S.; Srivastava, J.K.; Wong, J.W.C.; Ngo, H.H. Opportunities and challenges in omics approaches for biosurfactant production and feasibility of site remediation: Strategies and advancements. *Environmental Technology & Innovation* **2022**, *25*, doi:10.1016/j.eti.2021.102132.

118. Kumar, S. *Textbook of microbiology*; JP Medical Ltd: 2012.

119. Bonnet, M.; Lagier, J.C.; Raoult, D.; Khelaifia, S. Bacterial culture through selective and non-selective conditions: the evolution of culture media in clinical microbiology. *New Microbes New Infect* **2020**, *34*, 100622, doi:10.1016/j.nmni.2019.100622.

120. Basu, S.; Bose, C.; Ojha, N.; Das, N.; Das, J.; Pal, M.; Khurana, S. Evolution of bacterial and fungal growth media. *Bioinformation* **2015**, *11*, 182-184, doi:10.6026/97320630011182.

121. Lino, F.S.O.; Basso, T.O.; Sommer, M.O.A. A synthetic medium to simulate sugarcane molasses. *Biotechnol Biofuels* **2018**, *11*, 221, doi:10.1186/s13068-018-1221-x.

122. Sahu, R.; Meghavarnam, A.K.; Janakiraman, S. Response surface methodology: An effective optimization strategy for enhanced production of nitrile hydratase (NHase) by Rhodococcus rhodochrous (RS-6). *Heliyon* **2020**, *6*, e05111, doi:10.1016/j.heliyon.2020.e05111.

123. Singh, V.; Haque, S.; Niwas, R.; Srivastava, A.; Pasupuleti, M.; Tripathi, C.K. Strategies for Fermentation Medium Optimization: An In-Depth Review. *Front Microbiol* **2016**, *7*, 2087, doi:10.3389/fmicb.2016.02087.

124. Box, G.E.P.; Wilson, K.B. On the Experimental Attainment of Optimum Conditions. *Journal of the Royal Statistical Society: Series B (Methodological)* **1951**, *13*, 1-38, doi:10.1111/j.2517-6161.1951.tb00067.x.

125. Khuri, A.I.; Mukhopadhyay, S. Response surface methodology. *WIREs Computational Statistics* **2010**, *2*, 128-149, doi:10.1002/wics.73.

126. Kong, Q.; Zhai, C.; Guan, B.; Li, C.; Shan, S.; Yu, J. Mathematic modeling for optimum conditions on aflatoxin B(1)degradation by the aerobic bacterium Rhodococcus erythropolis. *Toxins* **2012**, *4*, 1181-1195, doi:10.3390/toxins4111181.

127. Awad, D.; Bohnen, F.; Mehlmer, N.; Brueck, T. Multi-Factorial-Guided Media Optimization for Enhanced Biomass and Lipid Formation by the Oleaginous Yeast Cutaneotrichosporon oleaginosus. *Front Bioeng Biotechnol* **2019**, *7*, 54, doi:10.3389/fbioe.2019.00054.

128. Bhattacharya, S. Central Composite Design for Response Surface Methodology and Its Application in Pharmacy. In *Response Surface Methodology in Engineering Science*; 2021.

129. Mutalik, S.R.; Vaidya, B.K.; Joshi, R.M.; Desai, K.M.; Nene, S.N. Use of response surface optimization for the production of biosurfactant from Rhodococcus spp. MTCC 2574. *Bioresour Technol* **2008**, *99*, 7875-7880, doi:10.1016/j.biortech.2008.02.027.

130. Bhatia, S.K.; Gurav, R.; Choi, T.R.; Han, Y.H.; Park, Y.L.; Jung, H.R.; Yang, S.Y.; Song, H.S.; Yang, Y.H. A clean and green approach for odd chain fatty acids production in *Rhodococcus* sp. YHY01 by medium engineering. *Bioresour Technol* **2019**, *286*, 121383, doi:10.1016/j.biortech.2019.121383.

131. Zhang, Z.; Xiaofeng, B. Comparison about the Three Central Composite Designs with Simulation. In Proceedings of the 2009 International Conference on Advanced Computer Control, 2009; pp. 163-167.

132. Myers, R.H.; Montgomery, D.C.; Anderson-Cook, C.M. *Response surface methodology: process and product optimization using designed experiments*; John Wiley & Sons: 2016.

133. Natrella, M. Nist/sematech e-Handbook of statistical methods. Available online: http//www.itl.nist.gov/div898/handbook (accessed on 10.11.2023).

134. Koblitz, J.; Halama, P.; Spring, S.; Thiel, V.; Baschien, C.; Hahnke, R.L.; Pester, M.; Overmann, J.; Reimer, L.C. MediaDive: the expert-curated cultivation media database. *Nucleic Acids Res* **2023**, *51*, D1531-D1538, doi:10.1093/nar/gkac803.

135. Engelhart-Straub, S.; Haack, M.; Awad, D.; Brueck, T.; Mehlmer, N. Optimization of Rhodococcus erythropolis JCM3201(T) Nutrient Media to Improve Biomass, Lipid, and Carotenoid Yield Using Response Surface Methodology. *Microorganisms* **2023**, *11*, doi:10.3390/microorganisms11092147.

136. Paper, M.; Glemser, M.; Haack, M.; Lorenzen, J.; Mehlmer, N.; Fuchs, T.; Schenk, G.; Garbe, D.; Weuster-Botz, D.; Eisenreich, W.; et al. Efficient Green Light Acclimation of the Green Algae *Picochlorum* sp. Triggering Geranylgeranylated Chlorophylls. *Front Bioeng Biotechnol* **2022**, *10*, 885977, doi:10.3389/fbioe.2022.885977.

137. Woortman, D.V.; Fuchs, T.; Striegel, L.; Fuchs, M.; Weber, N.; Bruck, T.B.; Rychlik, M. Microalgae a Superior Source of Folates: Quantification of Folates in Halophile Microalgae by Stable Isotope Dilution Assay. *Front Bioeng Biotechnol* **2019**, *7*, 481, doi:10.3389/fbioe.2019.00481.

138. Shaigani, P.; Awad, D.; Redai, V.; Fuchs, M.; Haack, M.; Mehlmer, N.; Brueck, T. Oleaginous yeasts- substrate preference and lipid productivity: a view on the performance of microbial lipid producers. *Microb Cell Fact* **2021**, *20*, 220, doi:10.1186/s12934-021-01710-3.

139. Awad, D.; Brueck, T. Optimization of protein isolation by proteomic qualification from *Cutaneotrichosporon oleaginosus*. *Anal Bioanal Chem* **2020**, *412*, 449-462, doi:10.1007/s00216-019-02254-7.

140. Fuchs, T.; Melcher, F.; Rerop, Z.S.; Lorenzen, J.; Shaigani, P.; Awad, D.; Haack, M.; Prem, S.A.; Masri, M.; Mehlmer, N.; Brueck, T.B. Identifying carbohydrate-active enzymes of *Cutaneotrichosporon oleaginosus* using systems biology. *Microb Cell Fact* **2021**, *20*, 205, doi:10.1186/s12934-021-01692-2.

141. Shevchenko, A.; Wilm, M.; Vorm, O.; Mann, M. Mass spectrometric sequencing of proteins silver-stained polyacrylamide gels. *Anal Chem* **1996**, *68*, 850-858, doi:10.1021/ac950914h.

142. Granvogl, B.; Gruber, P.; Eichacker, L.A. Standardisation of rapid in-gel digestion by mass spectrometry. *Proteomics* **2007**, *7*, 642-654, doi:10.1002/pmic.200600607.

143. Sandow, J.J.; Infusini, G.; Dagley, L.F.; Larsen, R.; Webb, A.I. Simplified high-throughput methods for deep proteome analysis on the timsTOF Pro. **2021**, doi:10.1101/657908.

144. Meier, F.; Brunner, A.D.; Koch, S.; Koch, H.; Lubeck, M.; Krause, M.; Goedecke, N.; Decker, J.; Kosinski, T.; Park, M.A.; et al. Online Parallel Accumulation-Serial Fragmentation (PASEF) with a Novel Trapped Ion Mobility Mass Spectrometer. *Mol Cell Proteomics* **2018**, *17*, 2534-2545, doi:10.1074/mcp.TIR118.000900.

145. Tran, N.H.; Qiao, R.; Xin, L.; Chen, X.; Liu, C.; Zhang, X.; Shan, B.; Ghodsi, A.; Li, M. Deep learning enables de novo peptide sequencing from data-independent-acquisition mass spectrometry. *Nat Methods* **2019**, *16*, 63-66, doi:10.1038/s41592-018-0260-3.

146. Tran, N.H.; Rahman, M.Z.; He, L.; Xin, L.; Shan, B.; Li, M. Complete De Novo Assembly of Monoclonal Antibody Sequences. *Sci Rep* **2016**, *6*, 31730, doi:10.1038/srep31730.

147. Tran, N.H.; Zhang, X.; Xin, L.; Shan, B.; Li, M. De novo peptide sequencing by deep learning. *Proc Natl Acad Sci U S A* **2017**, *114*, 8247-8252, doi:10.1073/pnas.1705691114.

148. Davila Costa, J.S.; Silva, R.A.; Leichert, L.; Alvarez, H.M. Proteome analysis reveals differential expression of proteins involved in triacylglycerol accumulation by *Rhodococcus jostii* RHA1 after addition of methyl viologen. *Microbiology* **2017**, *163*, 343-354, doi:10.1099/mic.0.000424.

149. Bell, K.S.; Philp, J.C.; Aw, D.W.; Christofi, N. The genus *Rhodococcus*. *J Appl Microbiol* **1998**, *85*, 195-210, doi:10.1046/j.1365-2672.1998.00525.x.

150. Sharma, P.; Jha, A.B.; Dubey, R.S.; Pessarakli, M. Reactive Oxygen Species, Oxidative Damage, and Antioxidative Defense Mechanism in Plants under Stressful Conditions. *Journal of Botany* **2012**, *2012*, 1-26, doi:10.1155/2012/217037.

151. de Carvalho, C.C. Adaptation of *Rhodococcus erythropolis* cells for growth and bioremediation under extreme conditions. *Res Microbiol* **2012**, *163*, 125-136, doi:10.1016/j.resmic.2011.11.003.

152. Hari, S.B.; Grant, R.A.; Sauer, R.T. Structural and Functional Analysis of *E. coli* Cyclopropane Fatty Acid Synthase. *Structure* **2018**, *26*, 1251-1258 e1253, doi:10.1016/j.str.2018.06.008.

153. Choi, T.R.; Song, H.S.; Han, Y.H.; Park, Y.L.; Park, J.Y.; Yang, S.Y.; Bhatia, S.K.; Gurav, R.; Kim, H.J.; Lee, Y.K.; et al. Enhanced tolerance to inhibitors of *Escherichia*

coli by heterologous expression of cyclopropane-fatty acid-acyl-phospholipid synthase (cfa) from *Halomonas socia*. *Bioprocess Biosyst Eng* **2020**, *43*, 909-918, doi:10.1007/s00449-020-02287-8.

154. Sandmann, G. Antioxidant Protection from UV- and Light-Stress Related to Carotenoid Structures. *Antioxidants* **2019**, *8*, doi:10.3390/antiox8070219.

155. Dai, T.; Gupta, A.; Murray, C.K.; Vrahas, M.S.; Tegos, G.P.; Hamblin, M.R. Blue light for infectious diseases: *Propionibacterium acnes*, *Helicobacter pylori*, and beyond? *Drug Resist Updat* **2012**, *15*, 223-236, doi:10.1016/j.drup.2012.07.001.

156. Halstead, F.D.; Thwaite, J.E.; Burt, R.; Laws, T.R.; Raguse, M.; Moeller, R.; Webber, M.A.; Oppenheim, B.A. Antibacterial Activity of Blue Light against Nosocomial Wound Pathogens Growing Planktonically and as Mature Biofilms. *Appl Environ Microbiol* **2016**, *82*, 4006-4016, doi:10.1128/AEM.00756-16.

157. Park, Y.K.; Dulermo, T.; Ledesma-Amaro, R.; Nicaud, J.M. Optimization of odd chain fatty acid production by *Yarrowia lipolytica*. *Biotechnol Biofuels* **2018**, *11*, 158, doi:10.1186/s13068-018-1154-4.

158. Huang, C.; Chen, X.F.; Xiong, L.; Chen, X.D.; Ma, L.L.; Chen, Y. Single cell oil production from low-cost substrates: the possibility and potential of its industrialization. *Biotechnol Adv* **2013**, *31*, 129-139, doi:10.1016/j.biotechadv.2012.08.010.

159. Fei, Q.; Chang, H.N.; Shang, L.; Choi, J.-d.-r. Exploring low-cost carbon sources for microbial lipids production by fed-batch cultivation of Cryptococcus albidus. *Biotechnology and Bioprocess Engineering* **2011**, *16*, 482-487, doi:10.1007/s12257-010-0370-y.

160. Sanchez, S.; Demain, A.L. Metabolic regulation of fermentation processes. *Enzyme and Microbial Technology* **2002**, *31*, 895-906, doi:10.1016/s0141-0229(02)00172-2.

161. Revilla, G.; Lopez-Nieto, M.J.; Luengo, J.M.; Martin, J.F. Carbon catabolite repression of penicillin biosynthesis by Penicillium chrysogenum. *J Antibiot (Tokyo)* **1984**, *37*, 781-789, doi:10.7164/antibiotics.37.781.

162. Nigam, P.S.; Singh, A. Fermentation (Industrial): Production of Oils and Fatty Acids. In *Encyclopedia of Food Microbiology*; 2014; pp. 792-803.

163. Abdel-Hafez, S.M.; Hathout, R.M.; Sammour, O.A. Towards better modeling of chitosan nanoparticles production: screening different factors and comparing two experimental designs. *Int J Biol Macromol* **2014**, *64*, 334-340, doi:10.1016/j.ijbiomac.2013.11.041.

164. Batista, K.A.; Fernandes, K.F. Development and optimization of a new culture media using extruded bean as nitrogen source. *MethodsX* **2015**, *2*, 154-158, doi:10.1016/j.mex.2015.03.001.

165. Kizilay, H.K.; Kucukcetin, A.; Demir, M. Optimization of carotenoid production by Umbelopsis ramanniana. *Biotechnol Prog* **2023**, *39*, e3369, doi:10.1002/btpr.3369.

166. Elibol, M. Optimization of medium composition for actinorhodin production by Streptomyces coelicolor A3(2) with response surface methodology. *Process Biochemistry* **2004**, *39*, 1057-1062, doi:10.1016/s0032-9592(03)00232-2.

167. Keskin Gundogdu, T.; Deniz, I.; Caliskan, G.; Sahin, E.S.; Azbar, N. Experimental design methods for bioengineering applications. *Crit Rev Biotechnol* **2016**, *36*, 368-388, doi:10.3109/07388551.2014.973014.

168. Beg, S.; Swain, S.; Rahman, M.; Hasnain, M.S.; Imam, S.S. Application of Design of Experiments (DoE) in Pharmaceutical Product and Process Optimization. In *Pharmaceutical Quality by Design*; 2019; pp. 43-64.

169. Zhang, J.; Greasham, R. Chemically defined media for commercial fermentations. *Applied Microbiology and Biotechnology* **1999**, *51*, 407-421, doi:10.1007/s002530051411.

170. Sperotto, G.; Stasiak, L.G.; Godoi, J.P.M.G.; Gabiatti, N.C.; De Souza, S.S. A review of culture media for bacterial cellulose production: complex, chemically defined and minimal media modulations. *Cellulose* **2021**, *28*, 2649-2673, doi:10.1007/s10570-021-03754-5.

171. Donini, E.; Firrincieli, A.; Cappelletti, M. Systems biology and metabolic engineering of Rhodococcus for bioconversion and biosynthesis processes. *Folia Microbiol* **2021**, *66*, 701-713, doi:10.1007/s12223-021-00892-y.

172. Kurosawa, K.; Wewetzer, S.J.; Sinskey, A.J. Triacylglycerol Production from Corn Stover Using a Xylose-Fermenting Rhodococcus opacus Strain for Lignocellulosic Biofuels. *Journal of Microbial & Biochemical Technology* **2014**, *06*, doi:10.4172/1948-5948.1000153.

173. Greenhill, S.; Rana, S.; Gupta, S.; Vellanki, P.; Venkatesh, S. Bayesian Optimization for Adaptive Experimental Design: A Review. *IEEE Access* **2020**, *8*, 13937-13948, doi:10.1109/access.2020.2966228.

174. Ariff, A.B.; Mohamad, R.; Hamid, M.; Abbasiliasi, S.; Ajdari, D.; Abdul Manan, M.; Ebrahimpour, A.; Ajdari, Z. Nutrients interaction investigation to improve Monascus purpureus FTC5391 growth rate using Response Surface Methodology and Artificial Neural Network. *Malaysian Journal of Microbiology* **2013**, doi:10.21161/mjm.44912.

175. Jones, D.R.; Schonlau, M.; Welch, W.J. Efficient Global Optimization of Expensive Black-Box Functions. *Journal of Global Optimization* **1998**, *13*, 455-492, doi:10.1023/a:1008306431147.

176. Sano, S.; Kadowaki, T.; Tsuda, K.; Kimura, S. Application of Bayesian Optimization for Pharmaceutical Product Development. *Journal of Pharmaceutical Innovation* **2019**, *15*, 333-343, doi:10.1007/s12247-019-09382-8.

177. Cosenza, Z.; Astudillo, R.; Frazier, P.I.; Baar, K.; Block, D.E. Multi-information source Bayesian optimization of culture media for cellular agriculture. *Biotechnol Bioeng* **2022**, *119*, 2447-2458, doi:10.1002/bit.28132.

178. Rosa, S.S.; Nunes, D.; Antunes, L.; Prazeres, D.M.F.; Marques, M.P.C.; Azevedo, A.M. Maximizing mRNA vaccine production with Bayesian optimization. *Biotechnol Bioeng* **2022**, *119*, 3127-3139, doi:10.1002/bit.28216.

179. Bouchaala, L.; Ben Khedher, S.; Mezghanni, H.l.; Zouari, N.; Tounsi, S. Bayesian network and response surface methodology for prediction and improvement of bacterial metabolite production. *2015 IEEE/ACIS 16th International Conference on Software Engineering, Artificial Intelligence, Networking and Parallel/Distributed Computing (SNPD)* **2015**, 1-6, doi:10.1109/snpd.2015.7176180.

180. O'Kennedy, R.D.; Ward, J.M.; Keshavarz-Moore, E. Effects of fermentation strategy on the characteristics of plasmid DNA production. *Biotechnol Appl Biochem* **2003**, *37*, 83-90, doi:10.1042/ba20020099.

181. Gupta, A.; Rao, G. A study of oxygen transfer in shake flasks using a non-invasive oxygen sensor. *Biotechnol Bioeng* **2003**, *84*, 351-358, doi:10.1002/bit.10740.

182. Beopoulos, A.; Nicaud, J.M.; Gaillardin, C. An overview of lipid metabolism in yeasts and its impact on biotechnological processes. *Appl Microbiol Biotechnol* **2011**, *90*, 1193-1206, doi:10.1007/s00253-011-3212-8.

183. Beopoulos, A.; Cescut, J.; Haddouche, R.; Uribelarrea, J.L.; Molina-Jouve, C.; Nicaud, J.M. Yarrowia lipolytica as a model for bio-oil production. *Prog Lipid Res* **2009**, *48*, 375-387, doi:10.1016/j.plipres.2009.08.005.

184. Somashekar, D.; Joseph, R. Inverse relationship between carotenoid and lipid formation in Rhodotorula gracilis according to the C/N ratio of the growth medium. *World Journal of Microbiology and Biotechnology* **2000**, *16*, 491-493, doi:10.1023/a:1008917612616.

185. Frengova, G.I.; Beshkova, D.M. Carotenoids from Rhodotorula and Phaffia: yeasts of biotechnological importance. *J Ind Microbiol Biotechnol* **2009**, *36*, 163-180, doi:10.1007/s10295-008-0492-9.

186. Ratledge, C.; Wynn, J.P. The biochemistry and molecular biology of lipid accumulation in oleaginous microorganisms. *Adv Appl Microbiol* **2002**, *51*, 1-51, doi:10.1016/s0065-2164(02)51000-5.

187. Singh, G.; Jawed, A.; Paul, D.; Bandyopadhyay, K.K.; Kumari, A.; Haque, S. Concomitant Production of Lipids and Carotenoids in Rhodosporidium toruloides under Osmotic Stress Using Response Surface Methodology. *Front Microbiol* **2016**, *7*, 1686, doi:10.3389/fmicb.2016.01686.

188. Saenge, C.; Cheirsilp, B.; Suksaroge, T.T.; Bourtoom, T. Efficient concomitant production of lipids and carotenoids by oleaginous red yeast Rhodotorula glutinis cultured in palm oil mill effluent and application of lipids for biodiesel production. *Biotechnology and Bioprocess Engineering* **2011**, *16*, 23-33, doi:10.1007/s12257-010-0083-2.

189. Bhosale, P.B.; Gadre, R.V. Production of beta-carotene by a mutant of Rhodotorula glutinis. *Appl Microbiol Biotechnol* **2001**, *55*, 423-427, doi:10.1007/s002530000570.

190. Bhosale, P. Environmental and cultural stimulants in the production of carotenoids from microorganisms. *Appl Microbiol Biotechnol* **2004**, *63*, 351-361, doi:10.1007/s00253-003-1441-1.

191. Bhosale, P.; Gadre, R.V. Manipulation of temperature and illumination conditions for enhanced beta-carotene production by mutant 32 of Rhodotorula glutinis. *Lett Appl Microbiol* **2002**, *34*, 349-353, doi:10.1046/j.1472-765x.2002.01095.x.

192. Mannazzu, I.; Landolfo, S.; Lopes da Silva, T.; Buzzini, P. Red yeasts and carotenoid production: outlining a future for non-conventional yeasts of biotechnological interest. *World J Microbiol Biotechnol* **2015**, *31*, 1665-1673, doi:10.1007/s11274-015-1927-x.

193. Marova, I.; Carnecka, M.; Halienova, A.; Breierova, E.; Koci, R. Production of carotenoid-/ergosterol-supplemented biomass by red yeast Rhodotorula glutinis grown under external stress. *Food Technology and Biotechnology* **2010**, *48*, 56-61.

194. Pham, K.D.; Shida, Y.; Miyata, A.; Takamizawa, T.; Suzuki, Y.; Ara, S.; Yamazaki, H.; Masaki, K.; Mori, K.; Aburatani, S.; et al. Effect of light on carotenoid and lipid production in the oleaginous yeast Rhodosporidium toruloides. *Biosci Biotechnol Biochem* **2020**, *84*, 1501-1512, doi:10.1080/09168451.2020.1740581.

195. Pattanaik, B.; Lindberg, P. Terpenoids and their biosynthesis in cyanobacteria. *Life* **2015**, *5*, 269-293, doi:10.3390/life5010269.

196. Su, A.; Chi, S.; Li, Y.; Tan, S.; Qiang, S.; Chen, Z.; Meng, Y. Metabolic Redesign of Rhodobacter sphaeroides for Lycopene Production. *J Agric Food Chem* **2018**, *66*, 5879-5885, doi:10.1021/acs.jafc.8b00855.

197. Emmerstorfer-Augustin, A.; Moser, S.; Pichler, H. Screening for improved isoprenoid biosynthesis in microorganisms. *J Biotechnol* **2016**, *235*, 112-120, doi:10.1016/j.jbiotec.2016.03.051.

198. Engelhart-Straub, S.; Cavelius, P.; Holzl, F.; Haack, M.; Awad, D.; Brueck, T.; Mehlmer, N. Effects of Light on Growth and Metabolism of Rhodococcus erythropolis. *Microorganisms* **2022**, *10*, doi:10.3390/microorganisms10081680.

199. Page, M.J.; Griffiths, T.A.; Bleackley, M.R.; MacGillivray, R.T. Proteomics: applications relevant to transfusion medicine. *Transfus Med Rev* **2006**, *20*, 63-74, doi:10.1016/j.tmrv.2005.08.006.

200. Vogel, C.; Marcotte, E.M. Insights into the regulation of protein abundance from proteomic and transcriptomic analyses. *Nat Rev Genet* **2012**, *13*, 227-232, doi:10.1038/nrg3185.

201. Bathke, J.; Konzer, A.; Remes, B.; McIntosh, M.; Klug, G. Comparative analyses of the variation of the transcriptome and proteome of Rhodobacter sphaeroides throughout growth. *BMC Genomics* **2019**, *20*, 358, doi:10.1186/s12864-019-5749-3.

202. Herrero, O.M.; Moncalian, G.; Alvarez, H.M. Physiological and genetic differences amongst Rhodococcus species for using glycerol as a source for growth and triacylglycerol production. *Microbiology* **2016**, *162*, 384-397, doi:10.1099/mic.0.000232.

203. Dobrowolski, A.; Mitula, P.; Rymowicz, W.; Mironczuk, A.M. Efficient conversion of crude glycerol from various industrial wastes into single cell oil by yeast Yarrowia lipolytica. *Bioresour Technol* **2016**, *207*, 237-243, doi:10.1016/j.biortech.2016.02.039.

204. Patel, A.; Arora, N.; Mehtani, J.; Pruthi, V.; Pruthi, P.A. Assessment of fuel properties on the basis of fatty acid profiles of oleaginous yeast for potential biodiesel production. *Renewable and Sustainable Energy Reviews* **2017**, *77*, 604-616, doi:10.1016/j.rser.2017.04.016.

205. Sajjadi, B.; Raman, A.A.A.; Arandiyan, H. A comprehensive review on properties of edible and non-edible vegetable oil-based biodiesel: Composition, specifications and prediction models. *Renewable and Sustainable Energy Reviews* **2016**, *63*, 62-92, doi:10.1016/j.rser.2016.05.035.

206. Zhang, L.S.; Liang, S.; Zong, M.H.; Yang, J.G.; Lou, W.Y. Microbial synthesis of functional odd-chain fatty acids: a review. *World J Microbiol Biotechnol* **2020**, *36*, 35, doi:10.1007/s11274-020-02814-5.

207. Arai, K.; Kawaguchi, A.; Saito, Y.; Koike, N.; Seyama, Y.; Yamakawa, T.; Okuda, S. Propionyl-Coa induced synthesis of even-chain-length fatty acids by fatty acid synthetase from Brevibacterium ammoniagenes. *J Biochem* **1982**, *91*, 11-18, doi:10.1093/oxfordjournals.jbchem.a133667.

208. Konzock, O.; Matsushita, Y.; Zaghen, S.; Sako, A.; Norbeck, J. Altering the fatty acid profile of Yarrowia lipolytica to mimic cocoa butter by genetic engineering of desaturases. *Microb Cell Fact* **2022**, *21*, 25, doi:10.1186/s12934-022-01748-x.

209. Wu, H.; San, K.Y. Engineering Escherichia coli for odd straight medium chain free fatty acid production. *Appl Microbiol Biotechnol* **2014**, *98*, 8145-8154, doi:10.1007/s00253-014-5882-5.

210. Alvarez, H.M.; Herrero, O.M.; Silva, R.A.; Hernandez, M.A.; Lanfranconi, M.P.; Villalba, M.S. Insights into the Metabolism of Oleaginous Rhodococcus spp. *Appl Environ Microbiol* **2019**, *85*, doi:10.1128/AEM.00498-19.

211. Alvarez, H.M. Relationship between β-oxidation pathway and the hydrocarbon-degrading profile in actinomycetes bacteria. *International Biodeterioration & Biodegradation* **2003**, *52*, 35-42, doi:10.1016/s0964-8305(02)00120-8.

212. Grechishnikova, E.G.; Shemyakina, A.O.; Novikov, A.D.; Lavrov, K.V.; Yanenko, A.S. Rhodococcus: sequences of genetic parts, analysis of their functionality, and

development prospects as a molecular biology platform. *Crit Rev Biotechnol* **2023**, *43*, 835-850, doi:10.1080/07388551.2022.2091976.

213. Posfai, G.; Plunkett, G., 3rd; Feher, T.; Frisch, D.; Keil, G.M.; Umenhoffer, K.; Kolisnychenko, V.; Stahl, B.; Sharma, S.S.; de Arruda, M.; et al. Emergent properties of reduced-genome Escherichia coli. *Science* **2006**, *312*, 1044-1046, doi:10.1126/science.1126439.

214. Aguilar Suarez, R.; Stulke, J.; van Dijl, J.M. Less Is More: Toward a Genome-Reduced Bacillus Cell Factory for "Difficult Proteins". *ACS Synth Biol* **2019**, *8*, 99-108, doi:10.1021/acssynbio.8b00342.

215. Kirk, O.; Borchert, T.V.; Fuglsang, C.C. Industrial enzyme applications. *Curr Opin Biotechnol* **2002**, *13*, 345-351, doi:10.1016/s0958-1669(02)00328-2.

216. Redding-Johanson, A.M.; Batth, T.S.; Chan, R.; Krupa, R.; Szmidt, H.L.; Adams, P.D.; Keasling, J.D.; Lee, T.S.; Mukhopadhyay, A.; Petzold, C.J. Targeted proteomics for metabolic pathway optimization: application to terpene production. *Metab Eng* **2011**, *13*, 194-203, doi:10.1016/j.ymben.2010.12.005.

217. Gallien, S.; Duriez, E.; Domon, B. Selected reaction monitoring applied to proteomics. *J Mass Spectrom* **2011**, *46*, 298-312, doi:10.1002/jms.1895.

218. Bubis, J.A.; Levitsky, L.I.; Ivanov, M.V.; Tarasova, I.A.; Gorshkov, M.V. Comparative evaluation of label-free quantification methods for shotgun proteomics. *Rapid Commun Mass Spectrom* **2017**, *31*, 606-612, doi:10.1002/rcm.7829.

219. Picotti, P.; Bodenmiller, B.; Mueller, L.N.; Domon, B.; Aebersold, R. Full dynamic range proteome analysis of S. cerevisiae by targeted proteomics. *Cell* **2009**, *138*, 795-806, doi:10.1016/j.cell.2009.05.051.

220. Landels, A.; Evans, C.; Noirel, J.; Wright, P.C. Advances in proteomics for production strain analysis. *Curr Opin Biotechnol* **2015**, *35*, 111-117, doi:10.1016/j.copbio.2015.05.001.

221. Chen, L.; Wu, L.; Wang, J.; Zhang, W. Butanol tolerance regulated by a two-component response regulator Slr1037 in photosynthetic Synechocystis sp. PCC 6803. *Biotechnol Biofuels* **2014**, *7*, 89, doi:10.1186/1754-6834-7-89.

222. Lorenzen, J.; Driller, R.; Waldow, A.; Qoura, F.; Loll, B.; Brück, T. Rhodococcus erythropolis Oleate Hydratase: a New Member in the Oleate Hydratase Family Tree—Biochemical and Structural Studies. *ChemCatChem* **2017**, *10*, 407-414, doi:10.1002/cctc.201701350.

223. Barreiro, C.; Barredo, J.L. Carotenoids Production: A Healthy and Profitable Industry. *Methods Mol Biol* **2018**, *1852*, 45-55, doi:10.1007/978-1-4939-8742-9_2.